Mémoire d'Habilitation à Diriger des Recherches

Spécialité : Mathématiques

Smooth manifolds and their knots

Finite type invariants
Trisections and multisections
Ribbon-slice questions

Thèse présentée par **Delphine Moussard**

préparée au sein de l'*Institut de Mathématiques de Marseille*,
Aix–Marseille Université

soutenue publiquement le **12 janvier 2023** devant le jury composé de

Anna Beliakova
Professeur, Universität Zürich, *Rapporteur*
David Gay
Professeur, University of Georgia, *Rapporteur*
Peter Teichner
Professeur, MPIM Bonn, *Rapporteur*
Stéphane Baseilhac
Professeur, Université de Montpellier
Christian Blanchet
Professeur, Université Paris Cité
Michel Boileau
Professeur, Université Aix–Marseille
Luisa Paoluzzi
Professeur, Université Aix–Marseille

Acknowledgments

I am very grateful to Anna Beliakova, David Gay and Peter Teichner who accepted to act as referees of this thesis. My thanks also go to Stéphane Baseilhac, Christian Blanchet, Michel Boileau and Luisa Paoluzzi for their participation to the jury. Further, I would like to thank Anne Pichon who was my mentor for the preparation of this habilitation.

Since my PhD thesis, I have had the occasion to work in different institutes in Pisa, Dijon, Kyoto and Marseille. It has been a real pleasure to meet many different people and discuss maths with them. I won't try to write a nominative list which would necessarily contain omissions. Nevertheless, I would like to express my sincere gratitude to all these people.

I am grateful to the *Institut de Mathématiques de Marseille* for having hired me. The working conditions are sometimes difficult, but this is countervailed by the energy and enthousiasm of many colleagues which make the institute a lively place; a special thought goes to the frumamians.

Working on a research project is certainly more pleasant with collaborators. I am thankful to Gaël, Benjamin, Manu, Vincent, Gwénaël, Trent, Sylvain, Marco, Fathi, Jean-Paul for the good moments spent working together.

Highlights of the research life are workshops and thematic schools. I would like to thank in particular JB, Manu, Paolo and Vincent for the organization of Winterbraids, Thomas for the school of Matemale, Jules, Léo, Loulou and Marco for the nice experience Between The Waves, Alex, Dave and Jeff for the trisectors meetings, Anthony and Marco for Le Croisic, and all the participants of these events.

Last, but not least, thanks Airelle for your inexhaustible support and simply for your presence.

Cette thèse présente une part substantielle des travaux de recherche que j'ai menés jusqu'à maintenant. Ma recherche se situe dans le domaine de la topologie géométrique, qui est l'étude des variétés et de leurs plongements d'un point de vue topologique, et elle est liée à la topologie quantique, un domaine de la topologie qui a des racines dans la mécanique quantique. Je me suis principalement intéressée à la topologie en petites dimensions, mais aussi aux généralisations de concepts et de résultats des petites dimensions aux dimensions supérieures. Ce manuscrit contient trois parties. La première est dédiée à la notion d'invariants de type fini, la deuxième traite des trisections et multisections et la troisième concerne des questions autour du problème ribbon-slice. Cette thèse se focalise sur des travaux qui contribuent à mes projets de recherche à long terme. Certains des articles de ma liste de publication n'y sont pas mentionnés; en particulier une collaboration avec Gaël Cousin portant sur une étude des orbites finies d'une action de groupes de tresses sur des sphères épointées, et une collaboration avec Gwénaël Massuyeau établissant une formule de "splicing" pour l'invariant LMO.

Mes travaux sur les invariants de type fini remontent à ma thèse de doctorat, dans laquelle j'ai décrit l'espace des invariants de type fini des sphères d'homologie rationnelle de dimension trois et j'ai commencé l'étude des invariants de type fini des nœuds dans les sphères d'homologie. Depuis lors, j'ai poursuivi l'objectif de décrire complètement l'espace des invariants de type fini des nœuds dans les sphères d'homologie, dans le but de démontrer une conjecture de Lescop, qui dit que l'invariant de Kricker et l'invariant de Lescop sont équivalents. Le premier objectif a été atteint, principalement à travers des résultats de [8], qui étudie en profondeur la structure de l'espace gradué associé aux invariants de type fini des nœuds dans les sphères d'homologie, et d'une collaboration avec Benjamin Audoux [15], qui donne la construction d'un invariant de type fini universel obtenu en raffinant l'invariant de Kricker. Ces résultats constituent un grand pas en direction d'une preuve de la conjecture de Lescop. Ces travaux et projets sont l'objet de la première partie du manuscrit.

Au début des années 2010, David Gay et Robion Kirby ont introduit la notion de trisections, des décompositions des variétés lisses de dimension quatre qui généralisent les scindements de Heegaard des variétés de dimension trois. Ils ont montré que toute variété de dimension 4 admet une trisection, unique à stabilisation près. Une variété trisectée peut être représentée par un diagramme défini par une famille de courbes sur une surface compacte. Avec Vincent Florens [11] et Trenton Schirmer [14], j'ai étudié comment des invariants d'homotopie peuvent être lus sur un diagramme de trisection. De plus, j'ai lancé le projet ANR SyTriQ sur les multisections des variétés lisses, des décompositions qui généralisent les scindements de Heegaard et les trisections aux variétés de dimension supérieure. L'objectif principal est de montrer l'existence de telles décompositions pour toute variété lisse et d'étudier leur unicité. Avec les autres membres, à savoir Benjamin Audoux, Sylvain Courte, Fathi Ben Aribi, Marco Golla et Jean-Paul Mohsen, nous avons déjà obtenu des résultats prometteurs. La deuxième partie de ce manuscrit décrit les travaux et projets associés.

À partir d'un premier travail avec Emmanuel Wagner sur des surfaces plongées dans la sphère de dimension 4, j'ai développé un intérêt pour le problème ribbon-slice et ses généralisations, pour les nœuds usuels et pour les nœuds en dimension supérieure. Dans [13], j'ai étudié le T–genre, ses liens avec le genre slice, et les versions rubans de ces invariants. En dimension supérieure, la réponse à la question ribbon-slice est a priori connue : il y a des nœuds slice qui ne sont pas rubans. Cependant, des questions naturelles apparaissent quand on interroge les définitions de nœuds slice et rubans en dimension supérieure : l'étude d'un problème ribbon-slice généralisé est un projet en cours. Ces travaux et projets sont décrits dans la troisième partie du manuscrit.

This thesis presents a substantial part of the research work I have achieved up to now. My research mainly sits in the domain of geometric topology, namely the study of manifolds and their embeddings from a topological viewpoint, and it is related to quantum topology, a topological field which has roots in quantum mechanics. I have been mainly interested in low-dimensional topology, but also in generalizations of low-dimensional concepts and results to higher dimensions. The manuscript contains three parts. The first part is devoted to the notion of finite type invariants, the second part deals with trisections and multisections and the last part concerns questions around the ribbon-slice problem. This thesis is focused on works that contribute to my long-term research programs. Some articles appear in my publication list that are not mentioned here; in particular a collaboration with Gaël Cousin on a study of finite orbits of some braid group action on punctured spheres, and a collaboration with Gwénaël Massuyeau establishing a splicing formula for the LMO invariant.

My work on finite type invariants dates back to my phD thesis, where I described the space of finite type invariants of rational homology 3–spheres and I started the study of finite type invariants of knots in homology 3–spheres. Since then, I purshued the objective of fully describing the space of finite type invariants of knots in homology 3–spheres, in order to prove a conjecture of Lescop, which asserts that the Kricker invariant and the Lescop invariant are equivalent. The first objective has been reached, mainly via results from [8], which deeply studies the structure of the graded space associated with finite type invariants of knots in homology 3–spheres, and from a collaboration with Benjamin Audoux [15], which gives the construction of a universal finite type invariant obtained as a refinement of the Kricker invariant. These results constitute a great step toward a proof of Lescop's conjecture. The first part of this manuscript first recalls previous works of several authors on finite type invariants of knots and of homology 3–spheres, and then focuses on finite type invariants of knots in homology 3–spheres.

In the early 2010's, David Gay and Robion Kirby introduced the notion of trisections, namely decompositions of smooth 4–manifolds generalizing Heegaard splittings of 3–manifolds. They proved that any smooth 4–manifold admits a trisection, unique up to some stabilization move. A trisected 4–manifold can be represented by a diagram defined by a family of curves on a compact surface. With Vincent Florens [11] and Trenton Schirmer [14], I studied how homotopy invariants of 4–manifolds can be read on a trisection diagram. Further, I launched the ANR project SyTriQ on multisections of smooth manifolds, decompositions that generalize Heegaard splittings and trisections to higher-dimensional manifolds. The main goal is to prove the existence of such decompositions for any smooth manifold and to study their uniqueness. With the other members, namely Benjamin Audoux, Sylain Courte, Fathi Ben Aribi, Marco Golla and Jean-Paul Mohsen, we have obtained promising results and we continue to investigate this topic. The second part of this manuscript describes the related works and projects.

From a first work with Emmanuel Wagner on embedded surfaces in the 4–sphere [10], I developed an interest for the ribbon-slice problem and its generalizations, for standard knots and for higher-dimensional knots. In [13], I studied the T–genus, its relation with the slice genus, and the ribbon counterparts of these invariants. In higher dimensions, the ribbon-slice question has apparently been answered: there are slice knots that are not ribbon. Nevertheless, natural questions appear when we query the definitions of ribbon and slice higher-dimensional knots. The study of a generalized ribbon-slice problem is an ongoing project, for which my work with Emmanuel Wagner might be useful. These works and projects are described in the third part of this manuscript.

Contents

First part: Finite type invariants of 3–manifolds and their knots

1 Introduction

The notion of finite type invariants was first introduced by Goussarov and Vassiliev independently, for the study of invariants of knots in the 3–sphere S^3. In general, the finite type invariants of a set of objects are defined by their polynomial behavior with respect to some elementary move. For knots, the finite type invariants, also called "Vassiliev invariants", are defined by their polynomial behavior with respect to crossing changes on the knots. The discovery of the Kontsevich integral revealed that this class of invariants is highly structured and prolific. It is known, for instance, that it dominates all Witten–Reshetikhin–Turaev's quantum invariants.

The generalization of finite type invariants to the setting of 3–manifolds is due to Ohtsuki, who constructed the first examples for $\mathbb{Z}$–homology 3–spheres. This has been widely developed and generalized since then. In particular, Goussarov and Habiro independently developed a theory which involves all 3–manifolds —and their knots— and which contains the Ohtsuki theory for $\mathbb{Z}$–homology 3–spheres. The elementary move in this case is a certain kind of surgery called borromean surgery, which preserves the $\mathbb{Z}$–homology.

In any theory of finite type invariants, one knows how to define a graded vector space whose dual space naturally identifies with the space of finite type invariants, graded by the degree. One of the main goals in the study of such a theory is to give a combinatorial description of this graded space by identifying it, for instance, with a space of Feynman diagrams. The determination of this graded space is important since it provides a tool for comparing invariants and measuring their power. Technically, the determination of the graded space associated with a theory of finite type invariants contains two main steps. From the one hand, one has to construct a graded space of diagrams adapted to the studied situation, and to define an onto map from this space to the graded space associated with the theory. From the other hand, an invariant has to be constructed which is "universal" for this theory, meaning that it realizes the inverse of the mentioned onto map; this shows that the description of the graded space is complete. In particular, it is important to understand precisely the behavior of this universal invariant with respect to the elementary move which defines the theory.

In Goussarov–Vassiliev's theory for knots and links in the 3–sphere, the graded space has been described by Bar-Natan, using the Kontsevich integral as universal finite type invariant. The Kontsevich integral is constructed combinatorially from a Drinfeld associator by representing the knots and links by diagrams. In the Goussarov–Habiro theory for $\mathbb{Z}$–homology 3–spheres, the graded space has been described by Le [Le97] with the Le–Murakami–Ohtsuki invariant as universal finite type invariant. This LMO invariant is constructed by formal Gaussian integration methods applied to the Kontsevich integral when the 3–manifolds are given by surgery presentations on links in the 3–sphere [LMO98, BGRT04]. The LMO invariant has an extrinsic and slightly geometric definition, but, thanks to its combinatorial nature, it is computable and easily comparable with other invariants, quantum invariants as Witten–Reshetikhin–Turaev's ones, or classical invariants as Casson invariant and Massey products. There exists another universal finite type invariant for $\mathbb{Z}$–homology 3–spheres: the Kontsevich–Kuperberg–Thurston invariant [Kon93, KT99]. The definition of this KKT invariant is intrinsic and uses integrals in configuration spaces, but it is very difficult to compute. These invariants both arise in some sense from the Kontsevich integral. The construction of the LMO invariant directly applies the Kontsevich integral to surgery presentations of 3–manifolds, while the KKT invariant adapts the idea of integrals in configuration spaces to the setting of $\mathbb{Z}$–homology 3–spheres (and more generally of $\mathbb{Q}$–homology 3–spheres). One may expect these two invariants to be deeply related, but there is no known explicit relation between them. The finite type invariants theory of Goussarov–Habiro fills a gap by giving a way to compare these two invariants: since they are both universal finite type invariants of $\mathbb{Z}$–homology 3–spheres, they are equivalent for such manifolds, meaning that two $\mathbb{Z}$–homology 3–spheres are separated by the LMO invariant if and only if they are separated by the KKT invariant.

In [GR04], Garoufalidis and Rozansky introduced a finite type invariants theory for knots in $\mathbb{Z}$–homology 3–spheres. The elementary move in this case is the null-borromean surgery, where "null" stands for a homological condition relative to the knot. In this theory, there are two candidates to be universal invariants: the Kricker lift of the Kontsevich integral [Kri00, GK04] and the invariant constructed by Lescop by means of integrals in configuration spaces [Les11]. They can be understood as equivariant versions of the LMO invariant and the KKT invariant respectively. Once again, both arise from the Kontsevich integral, the Kricker invariant explicitly, with an extrinsic construction directly applying the Kontsevich integral, and the Lescop invariant in that it adapts the idea of the Kontsevich integral in an intrinsic construction. And once again, there is no known explicit relation between them, while we expect them to be equivalent, as was conjectured by Lescop [Les13]. This equivalence has been reached by Kricker, Garoufalidis and Rozansky [Kri00, GK04, GR04] for knots in $\mathbb{Z}$–homology 3–spheres with a trivial Alexander polynomial, by proving that these two invariants are both universal finite type invariants. This was generalized in [8] to null-homologous knots in $\mathbb{Q}$–homology 3–spheres with a trivial Alexander polynomial. For general knots however, these invariants are not universal. The work of [8] provides a graded space of diagrams describing the graded space associated with this theory, while in [15], in collaboration with Benjamin Audoux, we construct a refinement of the Kricker invariant which is a universal finite type invariant for knots in $\mathbb{Z}$–homology 3–spheres, and for null-homologous knots in $\mathbb{Q}$–homology 3–spheres. This constitutes a great step toward a proof of Lescop's conjecture in general.

In Section 2, we review the general framework of a finite type invariant theory, the Goussarov–Vassiliev theory for knots in the 3–sphere and the Goussarov–Habiro theory for $\mathbb{Z}$–homology 3–spheres; we also briefly describe the work of [2] on finite type invariants of $\mathbb{Q}$–spheres. In Section 3, we turn to finite type invariants of knots in homology 3–spheres, we introduce the associated graded space of diagrams and we describe the work of [8, 9], mentioning also [1, 3]. Section 4 is devoted to the refinement of the Kricker invariant constructed in [15], which leads to a complete description of the graded space associated with finite type invariants of knots in homology 3–spheres. Finally, Section 5 presents some perspectives.

Notations. For $\mathbb{K} = \mathbb{Z}, \mathbb{Q}$, a $\mathbb{K}$*–sphere* (resp. $\mathbb{K}$*–ball*, $\mathbb{K}$*–torus*, *genus–g* $\mathbb{K}$*–handlebody*) is a compact connected oriented 3–manifold with the same homology with coefficients in $\mathbb{K}$ as the standard 3–sphere (resp. 3–ball, solid torus, genus–g standard handlebody).
The homology class of a curve γ is denoted by $[\gamma]$.
If A and B are transverse submanifolds of a manifold M such that $\dim A + \dim B = \dim M$, the algebraic intersection number of A and B is denoted $\langle A, B\rangle$.

2 First examples

2.1 The general framework

Consider a set X of topological objects, for instance knots in S^3, 3–dimensional manifolds, knots in some 3–manifolds. Such objects are usually defined up to some equivalence, as isotopy for knots or homeomorphism for manifolds. We want to study the set of *rational* *invariants* of the elements in X, namely the $\mathbb{Q}$–valued maps on our objects, well-defined up to the considered equivalence. We consider some set $\mathcal{O}(X)$ of operations on the elements of X, as crossing changes for knots or some surgeries for manifolds, and we focus on the behavior of the invariants with respect to this operation. A family of operations in $\mathcal{O}(X)$ will be said *independent* if they can be performed simultaneously, for instance surgeries on a manifold with disjoint support. We introduce some formalism as follows. Let $\mathcal{F}_0(X)$ be the rational vector space generated by all elements in X. Given an element $x \in X$ and a family $o_1, \dots, o_n \in \mathcal{O}(X)$ of operations acting on x, we define a *bracket of order n*

$$[x; o_1, \dots, o_n] = \sum_{I \subset \{1,\dots,n\}} (-1)^{|I|} x\big((o_i)_{i\in I}\big) \in \mathcal{F}_0(X),$$

where $x\big((o_i)_{i\in I}\big)$ is the object obtained from x after performing the operations o_i for $i \in I$. We denote $\mathcal{F}_n(X)$ the subspace of $\mathcal{F}_0(X)$ generated by all brackets of order n. Since a bracket of order $n+1$ is easily written as the difference of two brackets of order n, this provides a filtration of $\mathcal{F}_0(X)$.

Definition 2.1. A map $\lambda : X \to \mathbb{Q}$ is a *finite type invariant of degree at most n* if its $\mathbb{Q}$–linear extension to $\mathcal{F}_0(X)$ vanishes on $\mathcal{F}_{n+1}(X)$. The *degree* of a finite type invariant λ is the smaller n such that λ is of degree at most n.

As an elementary example, consider the set $X = \mathbb{Z}^d$ and the operations that add ± 1 to one coordinate. In this case, the evaluation of a map on a bracket of order n is a partial derivative of order n, and the finite type invariants are the polynomial maps in the coordinates.

In the following, given X and $\mathcal{O}(X)$, the goal will be to give a combinatorial description of the graded space $\mathcal{G}(X) = \oplus_{n\in\mathbb{N}} \mathcal{G}_n(X)$ defined by $\mathcal{G}_n(X) = \mathcal{F}_n(X) / \mathcal{F}_{n+1}(X)$. Such a description provides a good understanding of the theory of finite type invariants under consideration in that the dual of $\mathcal{G}(X)$ naturally identifies with the space of finite type invariants, graded by the degree. The standard pattern consists in defining a graded space of diagrams $\mathcal{A}(X)$ together with an onto map $\varphi : \mathcal{A}(X) \to \mathcal{G}(X)$ and producing an invariant that induces the inverse of φ. Such an invariant will be called a *universal finite type invariant.*

2.2 Knots in the 3–sphere

The first notion of finite type invariants was introduced independently by Goussarov and Vassiliev and deals with the set $\mathcal{K}$ of knots in the 3–sphere S^3. The idea was to consider the set of knots as a subset of the set of *singular knots*, namely immersed circles. An invariant of knots can be extended to singular knots and one can study the invariants that vanish on singular knots with a given number of double points. In our formalism, this is recovered by associating to each singular knot a bracket whose order is the number of double points, see Figure 1.

To a singular knot K, we associate a *chord diagram* $\Gamma(K)$ as follows: on the preimage of K represented by a dashed oriented circle, we join by a chord any two points that are sent on the same point of K, see Figure 2. It is not hard to see that the value of a finite type invariant of degree at most n on a singular knot with n double points is not affected by crossing changes performed far from the double points. As a consequence, there is a well-defined onto $\mathbb{Q}$–linear map

$$\varphi_n : \mathcal{D}_n \to \mathcal{G}_n(\mathcal{K}),$$

where $\mathcal{D}_n$ is the $\mathbb{Q}$–vector space generated by chord diagram with n chords. Further, the map φ_n satisfies the relations (1T) and (4T) below, so that it factorizes through $\mathcal{D}_n^T =$

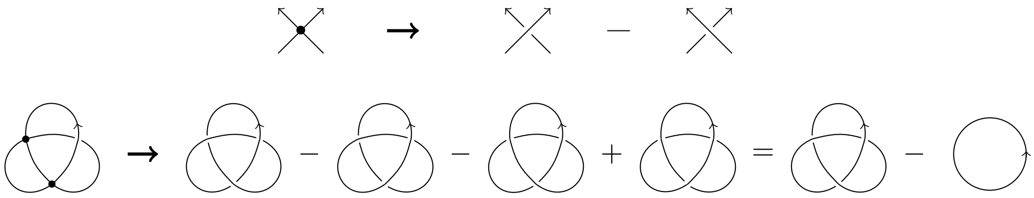

Figure 1: Associating a bracket to a singular knot

$\mathcal{D}_n\big/_{(1T),(4T)}$. The following strong result of Bar-Natan and Kontsevich establishes that the Kontsevich integral is a universal finite type invariant of knots in S^3 [Bar95].

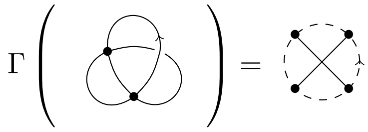

Figure 2: Chord diagram associated to a singular knot

 $= 0$ (1T)

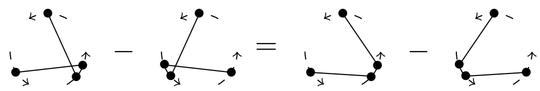 (4T)

Theorem 2.2 (Bar-Natan, Kontsevich)**.** *The Kontsevich integral defines $\mathbb{Q}$–linear maps $Z_n^K : \mathcal{F}_0(\mathcal{K}) \to \mathcal{D}_n^T$ such that $Z_n^K\big(\mathcal{F}_{n+1}(\mathcal{K})\big) = 0$ and Z_n^K induces the inverse of $\varphi_n : \mathcal{D}_n^T \to \mathcal{G}_n(\mathcal{K})$.*

2.3 Surgeries on 3–manifolds

We now introduce the operations on 3–manifolds underlying the finite type invariants theories we will consider in the sequel. We denote by $\mathcal{M}$ the set of closed oriented 3–manifolds up to homeomorphism.

The *standard Y–graph* is the graph $\Gamma_0 \subset \mathbb{R}^2$ represented in Figure 3. The looped edges of Γ_0 are the *leaves.* The vertex incident to three different edges is the *internal vertex.* With Γ_0 is associated a regular neighborhood $\Sigma(\Gamma_0)$ of Γ_0 in the plane. The surface $\Sigma(\Gamma_0)$ is oriented with the usual convention. This induces an orientation of the leaves and an *orientation of the internal vertex, ie* a cyclic order of the three edges. Consider a 3–manifold M and an embedding $h : \Sigma(\Gamma_0) \to M$. The image Γ of Γ_0 is a *Y–graph,* endowed with its *associated surface* $\Sigma(\Gamma) = h(\Sigma(\Gamma_0))$. The Y–graph Γ is equipped with the framing induced by $\Sigma(\Gamma)$. A *Y–link* in a 3–manifold is a collection of disjoint Y–graphs.

Let Γ be a Y–graph in a 3–manifold M. Let $\Sigma(\Gamma)$ be its associated surface. In $\Sigma \times [-1, 1]$, associate with Γ the six components link L represented in Figure 4. The *borromean surgery on* Γ is the surgery along the framed link L. The surgered manifold is denoted $M(\Gamma)$. Borromean surgeries were introduced and studied by Matveev in [Mat87]. He proved

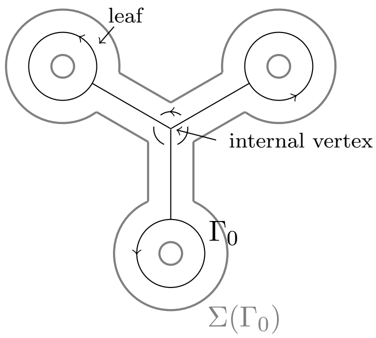

Figure 3: The standard Y–graph

in particular that two closed oriented 3–manifolds are related by a sequence of borromean surgeries if and only if they have isomorphic first homology group and linking pairing.

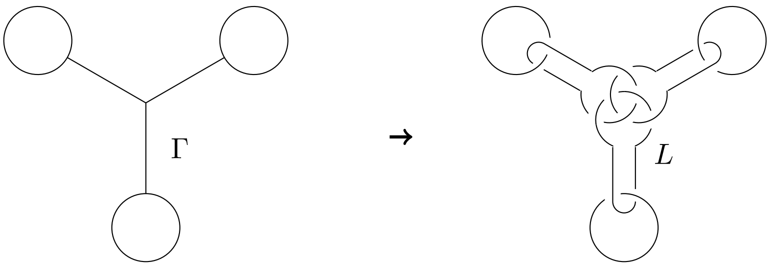

Figure 4: Y–graph and associated surgery link

We now define $\mathbb{K}$LP–surgeries for $\mathbb{K} = \mathbb{Z}, \mathbb{Q}$. Note that the boundary of a genus–g $\mathbb{K}$–handlebody is homeomorphic to the standard genus–g surface. The *Lagrangian* $\mathcal{L}_A$ of a $\mathbb{K}$–handlebody A is the kernel of the map $i_* : H_1(\partial A; \mathbb{K}) \to H_1(A; \mathbb{K})$ induced by the inclusion; it is indeed a Lagrangian subspace of $H_1(\partial A; \mathbb{K})$ with respect to the intersection form. Two $\mathbb{K}$–handlebodies A and B have *LP–identified* boundaries if (A, B) is equipped with a homeomorphism $h : \partial A \to \partial B$ such that $h_*(\mathcal{L}_A) = \mathcal{L}_B$. Now let M be a $\mathbb{K}$–sphere, $A \subset M$ a $\mathbb{K}$–handlebody and B a $\mathbb{K}$–handlebody whose boundary is LP–identified with ∂A (LP stands for Lagrangian-preserving). Set $M\left(\frac{B}{A}\right) = (M \setminus Int(A)) \cup_{\partial A \cong \partial B} B$. We say that the $\mathbb{K}$–sphere $M\left(\frac{B}{A}\right)$ is obtained from M by $\mathbb{K}$*LP–surgery*.

As proved by Matveev in [Mat87], a borromean surgery can be realized by cutting a genus 3 handlebody (a regular neighborhood of the Y–graph) and regluing it in another way, which preserves the Lagrangian. It follows that borromean surgeries are specific $\mathbb{Z}$LP–surgeries, which, in turn, are $\mathbb{Q}$LP–surgeries.

Habegger [Hab00, Theorem 2.5] and Auclair–Lescop [AL05, Lemma 4.11] proved that two $\mathbb{Z}$–handlebodies whose boundaries are LP–identified can be obtained from one another by a finite sequence of borromean surgeries. Therefore, the filtration defined on $\mathcal{F}_0(\mathcal{M})$ by $\mathbb{Z}$LP–surgeries is the same as the filtration defined by borromean surgeries.

2.4 Finite type invariants of $\mathbb{Z}$–spheres

We now review the description of the graded space associated to the Goussarov–Habiro theory of finite type invariants, for the set $\mathcal{M}_{\mathbb{Z}}$ of $\mathbb{Z}$–spheres up to homeomorphism, with respect to borromean surgeries.

A *Jacobi diagram* is a trivalent graph with oriented vertices. An *orientation* of a trivalent vertex is a cyclic order of the three half-edges that meet at this vertex. In the pictures, this orientation is induced by the cyclic order  . The *degree* of a Jacobi diagram is the number of its vertices[1]. Let $\mathcal{A}_n$ denote the rational vector space generated by all degree n Jacobi diagrams, quotiented out by the AS (anti-symmetry) and IHX relations (Figure 5). The space $\mathcal{A}_0$ is generated by the empty diagram. Since any trivalent graph has an even number of vertices, the space $\mathcal{A}_n$ is trivial when n is odd.

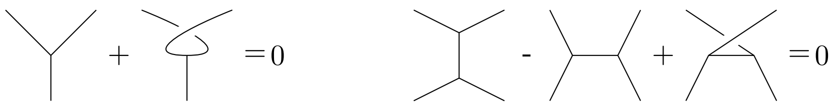

Figure 5: AS and IHX relations

Let Γ be a Jacobi diagram of degree n. Let $h : \Gamma \hookrightarrow \mathbb{R}^3$ be an embedding such that the orthogonal projection on $\mathbb{R}^2 \times \{0\}$ of $h(\Gamma)$ is regular, and hence induces a framing of $h(\Gamma)$. Now associate a Y–link $\tilde{\Gamma}$ in S^3 with Γ by replacing all edges of $h(\Gamma)$ as indicated in Figure 6. The Y–link $\tilde{\Gamma}$ defines a family of n borromean surgeries with disjoint support in S^3. Garoufalidis–Goussarov–Polyak proved in [GGP01] that the associated bracket in $\mathcal{G}_n(\mathcal{M}_{\mathbb{Z}})$ only depends on the class of Γ in $\mathcal{A}_n$. We denote $[S^3;\Gamma] \in \mathcal{G}_n(\mathcal{M}_{\mathbb{Z}})$ this bracket. It provides the following well-defined map, that they also proved to be onto.

$$\begin{array}{rccc} \varphi_n : & \mathcal{A}_n & \to & \mathcal{G}_n(\mathcal{M}_{\mathbb{Z}}) \\ & \Gamma & \mapsto & [S^3;\Gamma] \end{array}$$

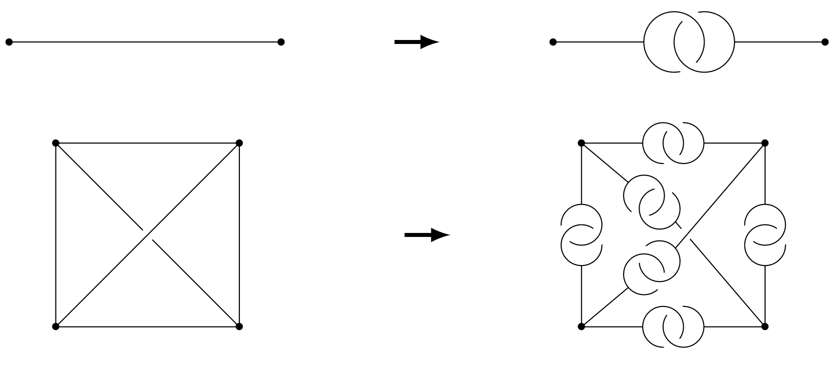

Figure 6: Associating a Y–link to a Jacobi diagram

To prove that the map φ_n is well-defined and surjective, a key ingredient is the understanding of the effect of "sliding an edge" and "cutting a leaf" of a Y–link, see Figures 7 and 8.

[1]It is usual to define the degree of a Jacobi diagram as half the number of its vertices, which is an integer. However, it is more coherent with the other finite type invariant theories that we will consider in the sequel to use this definition.

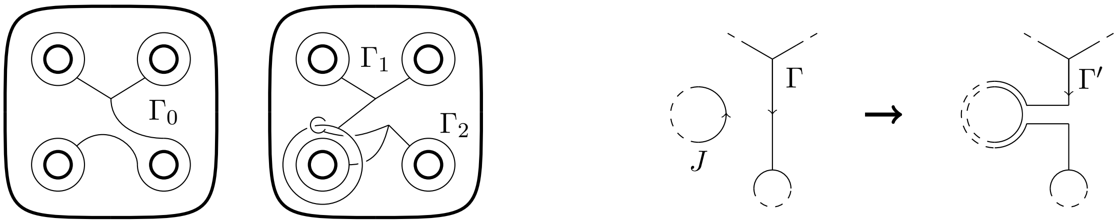

Figure 7: Sliding an edge

Surgeries on Γ_0 and on $\Gamma_1 \cup \Gamma_2$ produce homeomorphic results. A consequence is that the Y–links Γ and Γ', which differ only by the sliding of an edge along any knot J, define equivalent brackets up to a bracket of higher order.

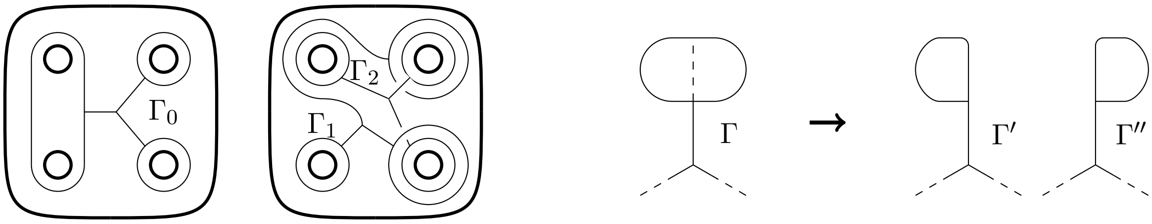

Figure 8: Cutting a leaf

Once again, surgeries on Γ_0 and on $\Gamma_1 \cup \Gamma_2$ are topologically equivalent and it follows that the bracket defined by Γ is equivalent to the sum of the brackets defined by Γ' and Γ'' in the corresponding quotient $\mathcal{G}_n(\mathcal{M}_\mathbb{Z})$.

Le–Murakami–Ohtsuki defined in [LMO98] an invariant Z^{LMO} of 3–manifolds with values in $\mathcal{A} = \oplus_{n\in\mathbb{N}}\mathcal{A}_n$. Le proved in [Le97] that the degree n part of this invariant induces the inverse of the map φ_n.

Theorem 2.3 (Garoufalidis–Goussarov–Polyak, Le)**.** *For all $n \geq 0$, the map $\varphi_n : \mathcal{A}_n \to \mathcal{G}_n(\mathcal{M}_\mathbb{Z})$ is an isomorphism whose inverse is induced by the LMO invariant.*

Remark 2.4. The graded spaces $\mathcal{A}$ and $\mathcal{G}(\mathcal{M}_\mathbb{Z})$ have a natural graded algebra structure. For diagrams, the product is simply the disjoint union. The product of two brackets is defined by the connected sum of the 3–manifolds and the concatenation of the families of surgeries. For these products, the map $\varphi : \mathcal{A} \to \mathcal{G}(\mathcal{M}_\mathbb{Z})$ is a graded algebra isomorphism. Similar products are defined on the graded spaces that appear in the sequel, while we deal with trivalent diagrams.

2.5 Finite type invariants of $\mathbb{Q}$–spheres

We now consider the set $\mathcal{M}_\mathbb{Q}$ of $\mathbb{Q}$–spheres up to homeomorphism and their finite type invariant with respect to $\mathbb{Q}$LP–surgeries.

Like $\mathbb{Z}$LP–surgeries can be realized by borromean surgeries, $\mathbb{Q}$LP–surgeries can be reduced to some more specific moves. First, given a positive integer d, we define a *d–torus* as a $\mathbb{Q}$–torus T_d such that, for simple closed curves $\alpha, \beta \subset \partial T_d$ with $< \alpha, \beta >= 1$ and a simple closed curve $\gamma \subset T_d$, we have:

- $H_1(\partial T_d;\mathbb{Z}) = \mathbb{Z}[\alpha] \oplus \mathbb{Z}[\beta]$,
- $d[\alpha] = 0$ in $H_1(T_d;\mathbb{Z})$,

- $[\beta] = d[\gamma]$ in $H_1(T_d;\mathbb{Z})$,
- $H_1(T_d;\mathbb{Z}) = \frac{\mathbb{Z}}{d\mathbb{Z}}[\alpha] \oplus \mathbb{Z}[\gamma]$.

Then, we define an *elementary surgery* as a $\mathbb{Q}$LP–surgery among the following ones:

- connected sum with a $\mathbb{Q}$–sphere (genus 0),
- LP–replacement of a standard torus by a d–torus (genus 1),
- borromean surgery (genus 3).

Theorem 2.5 ([2, Theorem 1.15]). *If A and B are two $\mathbb{Q}$–handlebodies with LP–identified boundaries, then B can be obtained from A by a finite sequence of elementary surgeries and their inverses in the interior of the $\mathbb{Q}$–handlebodies.*

In terms of diagrams, the borromean surgeries will again correspond to Jacobi diagrams, while connected sums will correspond to isolated vertices. Although is does not seem possible to remove the genus–1 elementary surgeries, they don't have a diagrammatic counterpart.

We call *augmented diagram of degree n* the union of a Jacobi diagram of degree $k \leq n$ with $(n-k)$ weighted vertices, where the weights are prime integers, see Figure 9. Note that the degree of an augmented diagram is equal to its number of vertices. We denote $\mathcal{A}_n^{\text{aug}}$ the rational vector space generated by all augmented diagrams of degree n, quotiented out by the AS and IHX relations. Given an augmented diagram D of degree n, we define a bracket $[S^3; D] \in \mathcal{G}_n(\mathcal{M}_\mathbb{Q})$ as follows: to the Jacobi part of D we associate as previously a family of borromean surgeries in S^3, and to each isolated vertex with weight p, we associate the connected sum with a $\mathbb{Q}$–sphere M_p such that $H_1(M_p;\mathbb{Z}) \cong \mathbb{Z}/p\mathbb{Z}$. This provides a well-defined onto $\mathbb{Q}$–linear map $\varphi_n : \mathcal{A}_n^{\text{aug}} \to \mathcal{G}_n(\mathcal{M}_\mathbb{Q})$ [2], see also [8, Proof of Theorem 2.7].

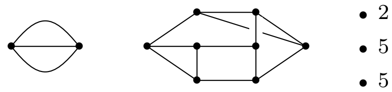

Figure 9: An augmented diagram of degree 13

At the level of invariants, the LMO invariant is defined for $\mathbb{Q}$–spheres and its degree n part is a finite type invariant of degree n with respect to $\mathbb{Q}$LP–surgeries, thanks to splitting formulas obtained by Massuyeau [Mas15]. There are also degree 1 invariants ρ_p for prime integers p, defined as follows: for a $\mathbb{Q}$–sphere M, $\rho_p(M) = -v_p(|H_1(M;\mathbb{Z})|) \bullet_p$ where v_p is the p–adic valuation [2, Proposition 1.9]. All these invariants can be merged into a universal finite type invariant of $\mathbb{Q}$–spheres by setting, for a $\mathbb{Q}$–sphere M:

$$Z^{\mathbb{Q}\text{S}}(M) = Z^{\text{LMO}}(M) \sqcup \exp_\sqcup\left(\sum_{p \text{ prime}} \rho_p(M)\right).$$

Theorem 2.6 ([2]). *The degree n part of the invariant $Z^{\mathbb{Q}S}$ induces the inverse of the map $\varphi_n : \mathcal{A}_n^{aug} \to \mathcal{G}_n(\mathcal{M}_\mathbb{Q})$. This defines a graded algebra isomorphism $\varphi : \mathcal{A}^{aug} \to \mathcal{G}(\mathcal{M}_\mathbb{Q})$.*

The proof of the above result given in [2] doesn't give an explicit universal finite type invariant, giving instead the family of Z and the ρ_p as globally universal. Using this trick, following the lines of a similar proof in [8] in the setting of invariants of knots in homology

3–spheres, provides a great simplification of that proof. Nevertheless, the version of [2] makes more explicit some algebraic structures on the involved graded spaces.

The Kontsevich–Kuperberg–Thurston invariant Z^{KKT} plays the same role in this finite type invariant theory as the LMO invariant, thanks to splitting formulas due to Lescop [Les04, Theorem 2.4]. It follows that Z^{KKT} is also a universal invariant of $\mathbb{Z}$–spheres with respect to borromean surgeries, and that it also provides, via the above construction, a universal invariant of $\mathbb{Q}$–spheres with respect to $\mathbb{Q}$LP–surgeries. This provides a comparison of these two invariants, both derived from the Kontsevich integral, following two different approaches.

Theorem 2.7 ([2])**.** *Let M and N be $\mathbb{Q}$–spheres such that $|H_1(M;\mathbb{Z})| = |H_1(N;\mathbb{Z})|$. For any $n \in \mathbb{N}$:*

$$\Big(Z_k^{LMO}(M) = Z_k^{LMO}(N) \text{ for all } k \leq n\Big) \Leftrightarrow \Big(Z_k^{KKT}(M) = Z_k^{KKT}(N) \text{ for all } k \leq n\Big).$$

3 Knots in homology 3–spheres

In this section, we study finite type invariants of pairs (M, K), where K is a knot in a $\mathbb{Z}$–sphere, in which case we call (M, K) a $\mathbb{Z}$*SK–pair*, or K is a null-homologous knot in a $\mathbb{Q}$–sphere, and we call (M, K) a $\mathbb{Q}$*SK–pair*. We denote $\mathcal{K}_{\mathbb{K}}$ the set of $\mathbb{K}$SK–pair up to homeomorphism of the pair.

3.1 Null surgeries and Blanchfield modules

Set $\mathbb{K} = \mathbb{Z}, \mathbb{Q}$. If (M, K) is a $\mathbb{K}$SK–pair, a Y–link $\Gamma \subset M \setminus K$ is *null* if, for each leaf γ of Γ, we have $\text{lk}(\gamma, K) = 0$. A *null borromean surgery* on (M, K) is a borromean surgery on a null Y–link. Similarly, given a $\mathbb{K}$SK–pair (M, K), a $\mathbb{K}$*–handlebody null in $M \setminus K$* is a $\mathbb{K}$–handlebody $A \subset M \setminus K$ such that the map $i_* : H_1(A;\mathbb{K}) \to H_1(M \setminus K;\mathbb{K})$ induced by the inclusion has a trivial image. A *null LP–surgery* on (M, K) is an LP–surgery $\left(\frac{B}{A}\right)$ such that A is null in $M \setminus K$. The $\mathbb{K}$SK–pair obtained by surgery is denoted by $(M, K)\left(\frac{B}{A}\right)$.

To study the filtration $\mathcal{F}_n(\mathcal{K}_{\mathbb{K}})$, the first step is to understand $\mathcal{G}_0(\mathcal{K}_{\mathbb{K}})$. In the previous cases, the considered operation was transitive on the set of objects; as a consequence, all degree 0 invariants were constant on the objects, and the space $\mathcal{G}_0$ was isomorphic to $\mathbb{Q}$. Here, null $\mathbb{K}$LP–surgeries define a nontrivial equivalence relation on the set of $\mathbb{K}$SK–pairs, whose classes turn out to be classified by the Blanchfield module, which we now introduce.

Let (M, K) be a $\mathbb{K}$SK–pair. Let $T(K)$ be a tubular neighborhood of K and denote $X = M \setminus Int\big(T(K)\big)$ the *exterior* of K. Consider the projection $\pi : \pi_1(X) \to \frac{H_1(X;\mathbb{Z})}{torsion} \cong \mathbb{Z}$ and the covering map $p : \tilde{X} \to X$ associated with its kernel. The covering $\tilde{X}$ is the *infinite cyclic covering* of X. The automorphism group $Aut(\tilde{X})$ of the covering is isomorphic to $\mathbb{Z}$ and acts on $H_1(\tilde{X};\mathbb{K})$. Denoting the action of a generator τ of $Aut(\tilde{X})$ as the multiplication by t, we get a structure of $\mathbb{K}[t^{\pm1}]$–module on $\mathfrak{A}(M, K) = H_1(\tilde{X};\mathbb{K})$. This $\mathbb{K}[t^{\pm1}]$–module is called the *Alexander module* of (M, K). It is known to be a finitely generated torsion $\mathbb{K}[t^{\pm1}]$–module.

On the Alexander module, we define the *Blanchfield form*, or *equivariant linking pairing*, $\mathfrak{b} : \mathfrak{A} \times \mathfrak{A} \to \frac{\mathbb{Q}(t)}{\mathbb{K}[t^{\pm1}]}$, as follows. We first define the equivariant linking number of two knots. Let J_1 and J_2 be two knots in $\tilde{X}$ such that $p(J_1) \cap p(J_2) = \emptyset$. Let $\delta \in \mathbb{K}[t]$ be the annihilator of $\mathfrak{A}$. There is a 2–chain S over $\mathbb{K}$ such that $\partial S = \delta(\tau)J_1$. The *equivariant linking number* of J_1 and J_2 is

$$\text{lk}_e(J_1, J_2) = \frac{1}{\delta(t)} \sum_{k\in\mathbb{Z}} \langle S, \tau^k(J_2)\rangle t^k,$$

where $\langle .,. \rangle$ stands for the algebraic intersection number. It is well-defined and we have $\mathrm{lk}_e(J_1, J_2) \in \frac{1}{\delta(t)}\mathbb{K}[t^{\pm 1}]$, $\mathrm{lk}_e(J_2, J_1)(t) = \mathrm{lk}_e(J_1, J_2)(t^{-1})$ and

$$\mathrm{lk}_e(P(\tau)J_1, Q(\tau)J_2)(t) = P(t)Q(t^{-1})\mathrm{lk}_e(J_1, J_2)(t).$$

Now, if γ (resp. η) is the homology class of J_1 (resp. J_2) in $\mathfrak{A}$, we define the Blanchfield form on γ and η by:

$$\mathfrak{b}(\gamma, \eta) = \mathrm{lk}_e(J_1, J_2) \ mod \ \mathbb{K}[t^{\pm 1}].$$

The Blanchfield form is *hermitian*: $\mathfrak{b}(\gamma, \eta)(t) = \mathfrak{b}(\eta, \gamma)(t^{-1})$ and

$$\mathfrak{b}(P(t)\gamma, Q(t)\eta)(t) = P(t)Q(t^{-1})\, \mathfrak{b}(\gamma, \eta)(t)$$

for all $\gamma, \eta \in \mathfrak{A}$ and all $P, Q \in \mathbb{K}[t^{\pm 1}]$. Moreover, as proven by Blanchfield [Bla57], it is *non degenerate*: $\mathfrak{b}(\gamma, \eta) = 0$ for all $\eta \in \mathfrak{A}$ implies $\gamma = 0$.

The *Blanchfield module* of a $\mathbb{K}$SK–pair (M, K) is the Alexander module of (M, K) endowed with its Blanchfield form; we denote it $(\mathfrak{A}, \mathfrak{b})(M, K)$. In the sequel, by *a Blanchfield module* $(\mathfrak{A}, \mathfrak{b})$, we mean a pair $(\mathfrak{A}, \mathfrak{b})$ that can be realized as the Blanchfield module of a $\mathbb{K}$SK–pair. An isomorphism between Blanchfield modules is an isomorphism between the underlying Alexander modules which preserves the Blanchfield form. Kearton [Kea75] proved that the realizable integral Blanchfield modules are exactly the pairs $(\mathfrak{A}, \mathfrak{b})$ satisfying:

- $\mathfrak{A}$ is $\mathbb{Z}$–torsion free,
- $\mathfrak{A}$ is a finitely generated torsion $\mathbb{Z}[t^{\pm 1}]$–module,
- $x \mapsto (1-t)x$ defines an isomorphism of $\mathfrak{A}$,
- $\mathfrak{b} : \mathfrak{A} \times \mathfrak{A} \to \mathbb{Q}(t)/_{\mathbb{Z}[t^{\pm 1}]}$ is a hermitian form.

In [1], we prove that the last three points, with $\mathbb{Q}$ instead of $\mathbb{Z}$, characterize the realizable rational Blanchfield modules. We further classify the rational Alexander modules and show that they split into two explicitly described groups: those admitting a single isomorphism class of Blanchfield forms and those admitting infinitely many non-isomorphic Blanchfield forms.

In [GR04], as a corollary of results of Matveev [Mat87], Naik and Stanford [NS03], and Trotter [Tro73], Garoufalidis and Rozansky established that two $\mathbb{Z}$SK–pairs can be obtained from one another by a finite sequence of null borromean surgeries (called null-moves in their paper) if and only if they have isomorphic integral Blanchfield modules. We prove the analogous result for $\mathbb{Q}$SK–pairs and null $\mathbb{Q}$LP–surgeries in [3]. It implies that the whole filtration defined on $\mathcal{F}_0(\mathcal{K}_\mathbb{K})$ by null $\mathbb{K}$LP–surgeries splits as a direct sum over all isomorphism classes of Blanchfield modules. As a consequence, we can fix an abstract Blanchfield module $(\mathfrak{A}, \mathfrak{b})$ and study our finite type invariants theory for $\mathbb{K}$SK–pairs whose Blanchfield module is isomorphic to $(\mathfrak{A}, \mathfrak{b})$; we denote $\mathcal{F}_0^\mathbb{K}(\mathfrak{A}, \mathfrak{b})$ the subspace of $\mathcal{F}_0(\mathcal{K}_\mathbb{K})$ generated by these pairs, and accordingly the associated filtration and graded space. For any $(\mathfrak{A}, \mathfrak{b})$, we have $\mathcal{G}_0^\mathbb{K}(\mathfrak{A}, \mathfrak{b}) \cong \mathbb{K}$.

The classification result of the classes of $\mathbb{K}$SK–pairs up to null $\mathbb{K}$LP–surgeries by their Blanchfield modules can be made more precise as follows. We will need this refinement in the study of the graded space $\mathcal{G}^\mathbb{K}(\mathfrak{A}, \mathfrak{b})$.

Theorem 3.1 ([3, Theorems 1.14 & 1.15]). *A null $\mathbb{K}$LP–surgery induces a canonical isomorphism between the Blanchfield modules of the involved $\mathbb{K}$SK–pairs. Conversely, for any isomorphism ζ from the Blanchfield module of a $\mathbb{K}$SK–pair (M, K) to the Blanchfield module of a $\mathbb{K}$SK–pair (M', K'), there is a finite sequence of null $\mathbb{K}$LP–surgeries from (M, K) to (M', K') that induces the composition of ζ with the multiplication by a power of t.*

3.2 Colored Jacobi diagrams and knots with trivial Alexander polynomial

Let $\delta \in \mathbb{Q}[t^{\pm 1}]$. A *$\delta$–colored diagram* is a trivalent graph whose vertices are oriented and whose edges are oriented and labeled by $\frac{1}{\delta(t)}\mathbb{Q}[t^{\pm 1}]$. The degree of a δ–colored diagram is the number of its vertices. Set:

$$\mathcal{A}_n(\delta) = \frac{\mathbb{Q}\langle \delta\text{–colored diagrams of degree } n\rangle}{\mathbb{Q}\langle \text{AS, IHX, LE, OR, Hol, Hol'}\rangle},$$

where the relations AS, IHX, LE (linearity for edges), OR (orientation reversal), Hol (Holonomy), Hol' are represented in Figures 5 and 10. Here the relation IHX holds with the central edge in each diagram labeled by 1. We have a graded algebra $\mathcal{A}(\delta) = \oplus_{n\in\mathbb{N}}\mathcal{A}_n(\delta)$. Once again, we have $\mathcal{A}_{2n+1}(\delta) = 0$ for all $n \geq 0$.

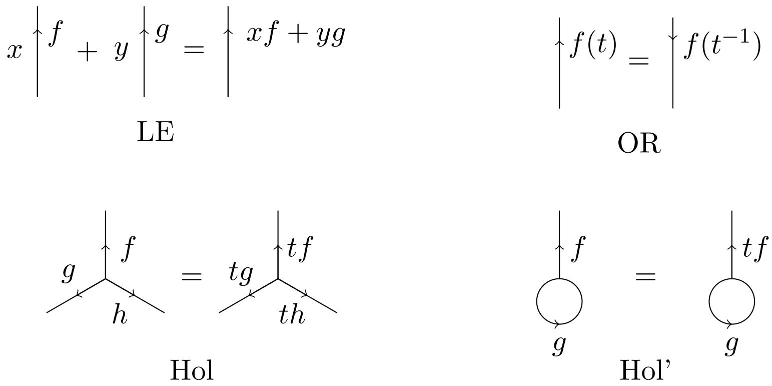

Figure 10: Relations, where $x, y \in \mathbb{Q}$, $f, g, h \in \frac{1}{\delta(t)}\mathbb{Q}[t^{\pm 1}]$.

The space $\mathcal{A}(\delta)$ was introduced by Garoufalidis, Kricker and Rozansky [GK04, GR04] as a target space for a rational lift of the Kontsevich integral. In the case of knots with trivial Alexander polynomial, it is also the good candidate to describe the space of finite type invariants. In [GR04], an onto $\mathbb{Q}$–linear graded map $\varphi : \mathcal{A}(1) \to \mathcal{G}^{\mathbb{Z}}(\mathfrak{A}_0)$ is constructed, where $\mathfrak{A}_0$ is the trivial Blanchfield module. It builds on the construction described in Subsection 2.4, with the following additive condition relative to the colors of the edges. We use the pair (S^3, U) defined by the unknot U in S^3. Given a colored diagram D whose edges labels are powers of t, we embed it in $S^3 \setminus U$ in such a way that, for each loop ℓ in D, the product of the edges labels along ℓ is $t^{\mathrm{lk}(\ell,U)}$. Since such diagrams generate $\mathcal{A}(1)$ over $\mathbb{Q}$, thanks to the LE relation, it suffices to define φ.

In [GK04], Garoufalidis and Kricker construct a rational lift for the Kontsevich integral, the Kricker invariant Z^{Kri}, and prove splitting formulas with respect to null borromean surgeries. In particular, they obtain a complete description of the graded space $\mathcal{G}^{\mathbb{Z}}(\mathfrak{A}_0)$.

Theorem 3.2 (Garoufalidis–Kricker)**.** *The Kricker invariant induces the inverse of the map $\varphi : \mathcal{A}(1) \to \mathcal{G}^{\mathbb{Z}}(\mathfrak{A}_0)$.*

Although the Kricker invariant is defined in [GK04] for $\mathbb{Z}$SK–pairs, the construction also works for $\mathbb{Q}$SK–pairs. Moreover, the invariants ρ_p of $\mathbb{Q}$–spheres introduced in Subsection 2.5 are also finite type invariants of $\mathbb{Q}$SK–pairs. As previously, we can merge these invariants:

$$Z^{\mathbb{Q}\mathrm{SK}} = Z^{\mathrm{Kri}} \sqcup \exp_{\sqcup}\left(\sum_{p \text{ prime}} \rho_p\right).$$

In the setting of $\mathbb{Q}$SK–pairs, we have to consider once again augmented diagrams, with isolated points. An *augmented δ–colored diagram of degree n* is the union of a δ–colored Jacobi diagram of degree $k \le n$ with $(n-k)$ vertices weighted by prime integers. We set:

$$\mathcal{A}_n^{\text{aug}}(\delta) = \frac{\mathbb{Q}\langle \text{Augmented } \delta\text{–colored diagrams of degree } n\rangle}{\mathbb{Q}\langle \text{AS, IHX, LE, OR, Hol, Hol'}\rangle}.$$

We define as previoulsy a graded map $\varphi : \mathcal{A}_n^{\text{aug}}(1) \to \mathcal{G}^{\mathbb{Q}}(\mathfrak{A}_0)$.

Theorem 3.3 ([8, Theorem 2.10])**.** *The map $\varphi : \mathcal{A}_n^{aug}(1) \to \mathcal{G}^{\mathbb{Q}}(\mathfrak{A}_0)$ is an algebra isomorphism whose inverse is induced by the Kricker invariant.*

Another universal invariant in this context was constructed by Lescop in [Les11]. Lescop proved in [Les13] that her invariant satisfies the same splitting formulas as the Kricker invariant. Hence, for $\mathbb{K} = \mathbb{Z}, \mathbb{Q}$, both the Lescop invariant and the Kricker invariant are universal finite type invariant of $\mathbb{K}$SK–pairs with trivial Blanchfield module with respect to null $\mathbb{K}$LP–surgeries. It implies in particular that the Lescop invariant and the Kricker invariant are equivalent for $\mathbb{K}$SK–pairs with trivial Blanchfield module.

We wish to get a combinatorial description of the graded space associated with finite type invariants of $\mathbb{K}$SK–pairs with respect to null $\mathbb{K}$LP–surgeries which holds for $\mathbb{K}$SK–pairs with any Blanchfield module. A natural candidate for this description is the graded space $\mathcal{A}(\delta)$ where the Kricker and Lescop invariants take values (or $\mathcal{A}^{\text{aug}}(\delta)$). However, the problem arises to give a topological meaning to the rational fractions labelling the edges of the diagrams. They can be interpreted as equivariant linkings in the infinite cyclic covering of the exterior of the knot, but this is not enough to construct a well-defined map onto the graded space. In the next section, we introduce diagrams carrying more precise information; we will use these diagrams to describe the graded space and finally construct a refined Kricker invariant, which turns out to be a universal finite type invariant of $\mathbb{K}$SK–pairs.

3.3 More colored diagrams and more general knots

Fix a Blanchfield module $(\mathfrak{A}, \mathfrak{b})$. Let $\delta \in \mathbb{K}[t^{\pm 1}]$ be the annihilator of $\mathfrak{A}$. An $(\mathfrak{A}, \mathfrak{b})$*–colored diagram D* is a unitrivalent graph without *strut*, *ie* isolated edge, with the following data:

- trivalent vertices are oriented;
- edges are oriented and labeled by $\mathbb{Q}[t^{\pm 1}]$;
- univalent vertices are labeled by $\mathfrak{A}$;
- for all $v \neq v'$ in the set V of univalent vertices of D, a rational fraction $f_{vv'}^D(t) \in \frac{1}{\delta(t)}\mathbb{Q}[t^{\pm 1}]$ is fixed such that $f_{vv'}^D(t)$ *mod* $\mathbb{K}[t^{\pm 1}] = \mathfrak{b}(\gamma, \gamma')$, where γ (resp. γ') is the coloring of v (resp. v'); we require that $f_{v'v}^D(t) = f_{vv'}^D(t^{-1})$.

When it does not seem to cause confusion, we write $f_{vv'}$ for $f_{vv'}^D$. The *degree* of a colored diagram is the number of trivalent vertices of its underlying graph. For $n \ge 0$, set:

$$\tilde{\mathcal{A}}_n(\mathfrak{A}, \mathfrak{b}) = \frac{\mathbb{Q}\langle (\mathfrak{A}, \mathfrak{b})\text{–colored diagrams of degree } n\rangle}{\mathbb{Q}\langle \text{AS, IHX, LE, OR, Hol, Hol', LV, EV, LD}\rangle},$$

where the relations AS, IHX, LE, OR, Hol, Hol', LV (linearity for vertices), EV (edge-vertex) and LD (linking difference) are described in Figures 5, 10 and 11. Here, the relation IHX holds with the central edge in each diagram labeled by 1 and the relations LE, OR, Hol, Hol' hold with $f, g, h \in \mathbb{Q}[t^{\pm 1}]$.

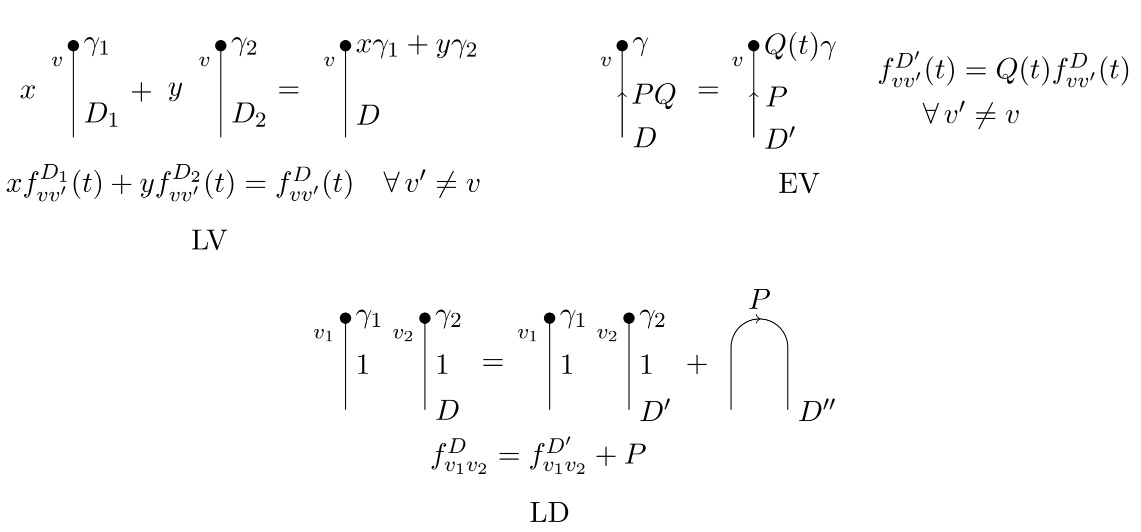

Figure 11: Relations, where $x, y \in \mathbb{Q}$, $P, Q \in \mathbb{Q}[t^{\pm 1}]$, $\gamma, \gamma_1, \gamma_2 \in \mathfrak{A}$.

The automorphism group $\mathrm{Aut}_{\mathbb{K}}(\mathfrak{A}, \mathfrak{b})$ of the Blanchfield module $(\mathfrak{A}, \mathfrak{b})$ acts on $\tilde{\mathcal{A}}_n(\mathfrak{A}, \mathfrak{b})$ by acting on the colorings of all the univalent vertices of a diagram simultaneously. Denote by Aut the relation which identifies two diagrams obtained from one another by the action of an element of $\mathrm{Aut}_{\mathbb{K}}(\mathfrak{A}, \mathfrak{b})$. Set:

$$\mathcal{A}^{\mathbb{K}}_n(\mathfrak{A}, \mathfrak{b}) = \tilde{\mathcal{A}}_n(\mathfrak{A}, \mathfrak{b})/\langle \mathrm{Aut}_{\mathbb{K}} \rangle \qquad \text{and} \qquad \mathcal{A}^{\mathbb{K}}(\mathfrak{A}, \mathfrak{b}) = \oplus_{n \in \mathbb{N}} \mathcal{A}^{\mathbb{K}}_n(\mathfrak{A}, \mathfrak{b}).$$

The integral Blanchfield module of a $\mathbb{Q}$SK–pair is a subgroup of its rational Blanchfield module, so that isomorphisms of the first induce isomorphisms of the second. Nevertheless, not all isomorphisms of the rational Blanchfield module are obtained in this way (see the remark following Proposition 7.9 in [8]), which makes a difference between the spaces $\mathcal{A}^{\mathbb{Z}}(\mathfrak{A}, \mathfrak{b})$ and $\mathcal{A}^{\mathbb{Q}}(\mathfrak{A}, \mathfrak{b})$. Note that the opposite of the identity is an automorphism of $(\mathfrak{A}, \mathfrak{b})$, so that, for all $n \geq 0$, $\mathcal{A}^{\mathbb{K}}_{2n+1}(\mathfrak{A}, \mathfrak{b}) = 0$.

As previously, there is an augmented version. An *augmented* $(\mathfrak{A}, \mathfrak{b})$*–colored diagram* is the union of an $(\mathfrak{A}, \mathfrak{b})$–colored diagram (its *Jacobi part*) and of finitely many isolated vertices weighted by prime integers. The *degree* of an $(\mathfrak{A}, \mathfrak{b})$–augmented diagram is the number of its vertices of valence 0 or 3. We set:

$$\mathcal{A}^{\mathrm{aug}}_n(\mathfrak{A}, \mathfrak{b}) = \frac{\mathbb{Q}\langle \text{augmented } (\mathfrak{A}, \mathfrak{b})\text{–colored diagrams of degree } n \rangle}{\mathbb{Q}\langle \text{AS, IHX, LE, OR, Hol, Hol', LV, EV, LD, Aut}_{\mathbb{Q}} \rangle} \quad \text{for } n \geq 0,$$

$$\mathcal{A}^{\mathrm{aug}}(\mathfrak{A}, \mathfrak{b}) = \oplus_{n \in \mathbb{N}} \mathcal{A}^{\mathrm{aug}}_n(\mathfrak{A}, \mathfrak{b}).$$

We now explain how $(\mathfrak{A}, \mathfrak{b})$–colored diagrams provide surgery data. Roughly speaking, the color of a univalent vertex, element of $\mathfrak{A}$, will represent the homology class of a lift of a leaf glued at this vertex, while the rational fractions $f_{vv'}$ will represent the equivariant linking between these lifted leaves.

Fix a Blanchfield module $(\mathfrak{A}, \mathfrak{b})$. An $(\mathfrak{A}, \mathfrak{b})$–colored diagram is *elementary* if its edges that connect two trivalent vertices are labeled by powers of t and if its edges adjacent to univalent vertices are labeled by 1. Below, we associate a null Y–link with some elementary diagrams that generate $\tilde{\mathcal{A}}_n(\mathfrak{A}, \mathfrak{b})$. Fix a $\mathbb{K}$SK–pair (M, K) and an isomorphism $\xi : (\mathfrak{A}, \mathfrak{b}) \to (\mathfrak{A}, \mathfrak{b})(M, K)$. Let $m(K)$ be a meridian of K.

Let D be an elementary diagram. An embedding of D in $M \setminus K$ is *admissible* if the following conditions are satisfied.

- The vertices of D are embedded in some ball $B \subset M \setminus K$.
- Consider an edge labeled by t^k. The homology class in $H_1(M \setminus K; \mathbb{Z})$ of the closed curve obtained by connecting the extremities of this edge by a path in B is $k\,[m(K)]$.

Such an embedding always exists. It suffices to embed the diagram in B, and to let each edge labeled by t^k turn around K, k times. With an admissible embedding of an elementary diagram, we wish to associate a null Y–link.

Let Γ be a Y–graph null in $M \setminus K$. Let p be the internal vertex of Γ. Let ℓ be a leaf of Γ. The curve $\hat{\ell}$ drawn in Figure 12 is the *extension of* ℓ *in* Γ.

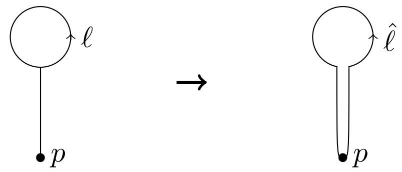

Figure 12: Extension of a leaf in a Y–graph

Let D be an elementary diagram, equipped with an admissible embedding in $M \setminus K$. Equip D with the framing induced by an immersion in the plane which induces the fixed orientation of the trivalent vertices. If an edge connects two trivalent vertices, then insert a little Hopf link in this edge, as shown in Figure 6. At each univalent vertex v, glue a leaf ℓ_v, trivial in $H_1(M \setminus K; \mathbb{Q})$, in order to obtain a null Y–link Γ. Let V be the set of all univalent vertices of D. Let B be the ball in the definition of the admissible embedding of D. Let $\tilde{B}$ be a lift of B in the infinite cyclic covering $\tilde{X}$ of the exterior of K in M. For $v \in V$, let γ_v be the coloring of v, let $\hat{\ell}_v$ be the extension of ℓ_v in Γ and let $\tilde{\ell}_v$ be the lift of $\hat{\ell}_v$ in $\tilde{X}$ defined by lifting the basepoint in $\tilde{B}$. The null Y–link Γ is a *realization of* D *in* (M, K) *with respect to* ξ if the following conditions are satisfied:

- for all $v \in V$, $\tilde{\ell}_v$ is homologous to $\xi(\gamma_v)$,
- for all $(v, v') \in V^2$, $\mathrm{lk}_e(\tilde{\ell}_v, \tilde{\ell}_{v'}) = f_{vv'}$.

If such a realization exists, the elementary diagram D is ξ*–realizable*.

Now, given a degree n (augmented) $(\mathfrak{A}, \mathfrak{b})$–colored diagram D whose Jacobi part is elementary and ξ–realizable, we can define a bracket $[(M, K); D] \in \mathcal{G}_n^{\mathbb{K}}(\mathfrak{A}, \mathfrak{b})$. In [8], we prove that such a bracket does not depend on the various choices. In particular, independence with respect to the pair (M, K) and the isomorphism ξ follows from Theorem 3.1. A suitable application of the edge-sliding and leaf-cutting methods in the infinite cyclic covering $\tilde{X}$ is also used. More precisely, we obtain the following.

Theorem 3.4 ([8, Theorems 2.7 & 2.17])**.** *Fix a Blanchfield module* $(\mathfrak{A}, \mathfrak{b})$ *over* $\mathbb{K}[t^{\pm 1}]$*. For all* $n \geq 0$*, there are canonical surjective* $\mathbb{Q}$*–linear maps* $\varphi_n^{\mathbb{Z}} : \mathcal{A}_n^{\mathbb{Z}}(\mathfrak{A}, \mathfrak{b}) \twoheadrightarrow \mathcal{G}_n^{\mathbb{Z}}(\mathfrak{A}, \mathfrak{b})$ *and* $\varphi_n^{aug} : \mathcal{A}_n^{\mathbb{Q}}(\mathfrak{A}, \mathfrak{b}) \twoheadrightarrow \mathcal{G}_n^{\mathbb{Q}}(\mathfrak{A}, \mathfrak{b})$*.*

A direct corollary is that $\mathcal{G}_{2n+1}^{\mathbb{Z}}(\mathfrak{A}, \mathfrak{b}) = 0$ for all $n \geq 0$.

Remark 3.5. The disjoint union of diagrams no longer defines a product on $\mathcal{A}^{\mathbb{K}}(\mathfrak{A},\mathfrak{b})$. The issue is that linkings $f_{vv'}$ have to be fixed for pairs of vertices v and v' from the initial two diagrams. There is no such canonical choice, and an arbitrary choice would hardly be coherent with the relations defining $\mathcal{A}^{\mathbb{K}}(\mathfrak{A},\mathfrak{b})$. In turn, the disjoint union of diagrams naturally defines a product from $\mathcal{A}^{\mathbb{K}}(\mathfrak{A}_1,\mathfrak{b}_1)\times\mathcal{A}^{\mathbb{K}}(\mathfrak{A}_2,\mathfrak{b}_2)$ to $\mathcal{A}^{\mathbb{K}}\big((\mathfrak{A}_1,\mathfrak{b}_1)\oplus(\mathfrak{A}_2,\mathfrak{b}_2)\big)$, with the new linkings chosen trivial.

3.4 The Kricker and Lescop invariants

The Kricker and Lescop invariants are equivariant versions of the LMO and KKT invariants; they are natural candidates to be universal finite type invariants of $\mathbb{K}$SK–pairs. However, for knots whose Blanchfield module is $(\mathfrak{A},\mathfrak{b})$, with annihilator δ, they take values in the graded space $\mathcal{A}(\delta)$, while in the description of the graded space $\mathcal{G}^{\mathbb{K}}(\mathfrak{A},\mathfrak{b})$, we intend to use $\mathcal{A}^{\mathbb{K}}(\mathfrak{A},\mathfrak{b})$. There is a natural "closing" map between these two diagram spaces.

With an $(\mathfrak{A},\mathfrak{b})$–colored diagram D of degree n, we associate a δ–colored diagram. Let V be the set of univalent vertices of D. A *pairing of* V is an involution of V with no fixed point. For such a pairing p, define a δ–colored diagram $p(D)$ in the following way. If $v\in V$ and $v'=p(v)$, replace in D the vertices v and v', and their adjacent edges, by a labeled edge, as indicated in Figure 13. Associating to D the sum over all pairings of V of the $p(D)$ provides a well-defined $\mathbb{Q}$–linear map $\psi_n:\mathcal{A}_n^{\mathbb{K}}(\mathfrak{A},\mathfrak{b})\to\mathcal{A}_n(\delta)$. This defines an algebra morphism $\psi:\mathcal{A}^{\mathbb{K}}(\mathfrak{A},\mathfrak{b})\to\mathcal{A}(\delta)$. It extends to an algebra morphism $\psi:\mathcal{A}^{\mathrm{aug}}(\mathfrak{A},\mathfrak{b})\to\mathcal{A}^{\mathrm{aug}}(\delta)$ sending a weighted isolated point to itself.

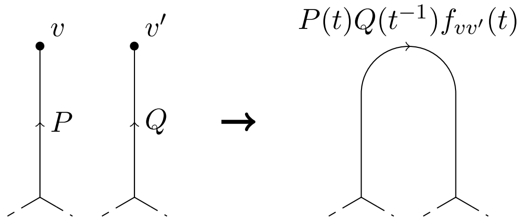

Figure 13: Pairing of vertices

These maps ψ fit into the following commutative diagrams.

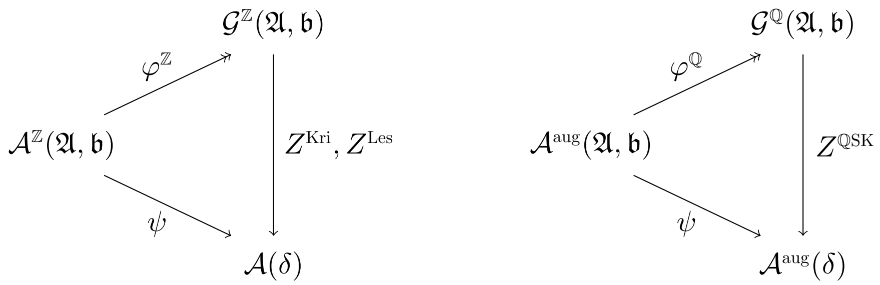

The fact that the diagrams commute follows from splitting formulas giving the behavior of the invariant with respect to null $\mathbb{K}$LP–surgeries. For the Lescop invariant, these formulas were obtained in [Les13]. For the Kricker invariant, they were proved in [GK04] for null borromean surgeries and extended in [7] to null $\mathbb{Q}$LP–surgeries, using a functorial extension of the Kricker invariant.

It appears that proving that ψ_n is an isomorphism would imply that φ_n is an isomorphism too. In [8], a partial result was obtained in this direction, focusing on $\mathbb{Q}$SK–pairs.

Theorem 3.6 ([8, Theorem 2.12])**.** *Let n be an even positive integer and $N \geq 3n/2$. Fix a Blanchfield module $(\mathfrak{A}, \mathfrak{b})$. Let δ be the annihilator of $\mathfrak{A}$. Define the Blanchfield module $(\overline{\mathfrak{A}}, \overline{\mathfrak{b}})$ as the direct sum of N copies of $(\mathfrak{A}, \mathfrak{b})$. Then the map $\overline{\psi}_n : \mathcal{A}_n^{aug}(\overline{\mathfrak{A}}, \overline{\mathfrak{b}}) \to \mathcal{A}_n^{aug}(\delta)$ is an isomorphism.*

To prove this theorem, an inverse is constructed for the map $\overline{\psi}$. Roughly, to associate an $(\overline{\mathfrak{A}}, \overline{\mathfrak{b}})$–colored diagram to a δ–colored diagram, the idea is to open each edge, inserting two univalent vertices with, as fixed linking, the label of the initial edge. However, the labels of the created univalent vertices have to be chosen to be coherent with the fixed linkings, which is not always possible. This explains why we need many copies of a given Blanchfield module, in fact one copy for each initial edge. The diagrams obtained in this way have at most two univalent vertices colored in each copy of $(\mathfrak{A}, \mathfrak{b})$, so that the proof of the theorem also involves showing that such diagrams generate $\mathcal{A}(\overline{\mathfrak{A}}, \overline{\mathfrak{b}})$. We may note that the method developed for that in [8] does not work when dealing with integral Blanchfield modules.

This result provides a rewritting of the map ψ_n in the general case. We have a natural map $\iota_n : \mathcal{A}_n(\mathfrak{A}, \mathfrak{b}) \to \mathcal{A}_n(\overline{\mathfrak{A}}, \overline{\mathfrak{b}})$ defined on a diagram by interpreting the labels of its univalent vertices as elements of the first copy of $(\mathfrak{A}, \mathfrak{b})$ in $(\overline{\mathfrak{A}}, \overline{\mathfrak{b}})$. The following diagram commutes.

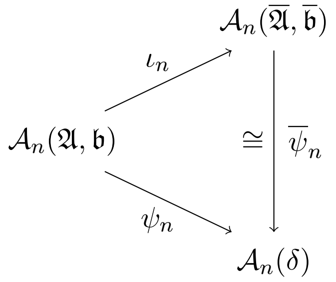

Nevertheless, in a joint work with Benjamin Audoux, we proved the following, which shows in particular that the map ψ_n is non injective in some cases.

Theorem 3.7 ([9, Theorem 1.1])**.** *If $(\mathfrak{A}, \mathfrak{b})$ is a Blanchfield module of $\mathbb{Q}$–dimension two, with annihilator δ, then:*

1. *the map $\psi_2 : \mathcal{A}_2^{\mathbb{Q}}(\mathfrak{A}, \mathfrak{b}) \to \mathcal{A}_2^{\mathbb{Q}}(\delta)$ is injective but not surjective;*
2. *the map $\psi_2 : \mathcal{A}_2^{\mathbb{Q}}(\mathfrak{A} \oplus \mathfrak{A}, \mathfrak{b} \oplus \mathfrak{b}) \to \mathcal{A}_2^{\mathbb{Q}}(\delta)$ is injective if and only if $\delta \neq t + 1 + t^{-1}$; in this case, it is an isomorphism.*

We will see in the sequel that the map φ is indeed an isomorphism, by constructing a refined Kricker invariant. Together with the above result, it shows that the Kricker and the Lescop invariant are not universal finite type invariants of $\mathbb{Q}$SK–pairs.

4 Refined Kricker invariant

We have introduced different invariants with universality properties, which play an important role in the finite type invariants theories we consider, but we didn't mention their construction so far. The key idea of these constructions is to apply the Kontsevich integral of links in S^3 to surgery presentations of the manifolds. The LMO invariant of $\mathbb{Q}$–spheres can be obtained by applying a formal Gaussian integral to the Kontsevich integral of a surgery link defining the $\mathbb{Q}$–sphere. The Kricker invariant is an adaptation of this idea to surgery presentations of $\mathbb{K}$SK–pairs, given by links in a solid torus. We shall now describe the refined Kricker invariant constructed in [15]. It is a lift of the Kricker invariant, also constructed from the Kontsevich integral of a surgery presentation, but replacing the formal Gaussian integral by another operation in order to get values in $\mathcal{A}(\mathfrak{A}, \mathfrak{b})$.

4.1 Surgery presentations and winding matrices

We fix a trivial knot $U \subset S^3$. A *surgery link* is a link $L = \sqcup_{i=1}^s L_i \subset (S^3 \setminus U)$ whose connected components L_i satisfy $\mathrm{lk}(L_i, U) = 0$ and whose linking matrix $(\mathrm{lk}(L_i, L_j))_{1 \le i,j \le n}$ is non-degenerate. This condition ensures that the pair (M, K) obtained from (S^3, U) by surgery on L is a $\mathbb{Q}$SK–pair. A *surgery presentation* of a $\mathbb{K}$SK–pair (M, K) is a surgery link L such that (M, K) is obtained from (S^3, U) by surgery on L. In turns out that any $\mathbb{K}$SK–pair admits such a surgery presentation. Our construction uses diagrams of these surgery links.

Let $L \subset S^3 \setminus U$ be a surgery link. An *admissible diagram* of L is a projection of $L \cup \mathcal{D}$ onto a square $[-1, 1]^2$ where:

- $\mathcal{D}$ is a disk bounded by U,
- the image of $\mathcal{D}$ is the segment line $[(0, 0), (1, 0)]$,
- the multiple points of the projection restricted to L are transverse double points disjoint from $\mathcal{D}$,
- the points of L that project onto $[(0, 0), (1, 0)]$ are the points of $L \cap \mathcal{D}$.

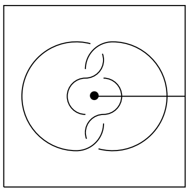

Figure 14: An admissible diagram of a surgery presentation

Let E be the exterior of U in S^3 and let $\tilde{E}$ be the infinite cyclic covering of X. Note that $\tilde{E}$ is homeomorphic to $\mathcal{D} \times \mathbb{R}$. In particular, the equivariant linking number of knots in $\tilde{E}$ takes values in $\mathbb{Z}[t^{\pm 1}]$.

Fix an admissible diagram of L and base points $\star_i$ of its components, far from the crossings and the disk $\mathcal{D}$. Let $\tilde{E}_0 \subset \tilde{E}$ be a copy of E. Define the lift $\tilde{L}_i$ of L_i in $\tilde{E}$ by lifting $\star_i$ in $\tilde{E}_0$. Consider the matrix of equivariant linkings $W_L = \Big(\mathrm{lk}_e(\tilde{L}_i, \tilde{L}_j)\Big)_{1 \le i,j \le n}$. If the link L is a surgery presentation for a $\mathbb{Q}$SK–pair (M, K), then the matrix ${}^tW_L$ is a presentation matrix of the Alexander module of (M, K) with generators the classes of meridians m_i of the components $\tilde{L}_i$ [1, Proposition 2.5]. Moreover, the Blanchfield form is given on these generators by the matrix $-W_L^{-1}$ [1, Corollary 3.2].

This matrix W_L can be computed diagrammatically as follows. Given an admissible diagram of L, define the *winding number* $w(L_i, L_j) \in \mathbb{Z}[t^{\pm 1}]$ of L_i and L_j in the following way. For a crossing c between L_i and L_j, denote $\varepsilon_{ij}(c)$ the algebraic intersection number of the disk

$\mathcal{D}$ with the path that goes from $\star_i$ to c along L_i and then from c to $\star_j$ along L_j. If $i = j$, change component at the first occurence of c. Set

$$w(L_i, L_j) = \begin{cases} \dfrac{1}{2} \displaystyle\sum_c \mathrm{sg}(c)\, t^{\varepsilon_{ij}(c)} & \text{if } i \neq j \\ \dfrac{1}{2} \displaystyle\sum_c \mathrm{sg}(c)\, (t^{\varepsilon_{ii}(c)} + t^{-\varepsilon_{ii}(c)}) & \text{if } i = j \end{cases}$$

where the sums are over all crossings between L_i and L_j. It turns out that

$$W_L = \big(w(L_i, L_j)\big)_{1 \leq i,j \leq n}.$$

In the sequel, we call W_L the *winding matrix* of L. We may note that $W_L(t^{-1}) = {}^tW_L(t)$.

4.2 Beaded Jacobi diagrams

We now introduce new diagram spaces needed in the construction of our invariant.

For a compact oriented 1–manifold X (resp. a finite set C), a *Jacobi diagram on* X (resp. a *Jacobi diagram on* C) is a unitrivalent graph whose trivalent vertices are oriented and whose univalent vertices are embedded in X (resp. labeled by C). When relevant, the manifold X is called the *skeleton* of the diagram. A *beaded Jacobi diagram on* X *or* C is a Jacobi diagram on X or C whose graph edges are oriented and labeled by $\mathbb{Q}[t^{\pm 1}]$ (see Figure 15. A *w–beaded Jacobi diagram on* X is a beaded Jacobi diagram on X whose skeleton is viewed as a union of edges —defined by the embedded vertices— that are labeled by powers of t, with the condition that the product of the labels on each component of X is 1. The *i–degree* of a unitrivalent diagram is its number of trivalent vertices. Set:

$$\widetilde{\mathcal{A}}(X) = \frac{\mathbb{Q}\langle \text{beaded Jacobi diagrams on } X\rangle}{\mathbb{Q}\langle \text{AS, IHX, STU, LE, OR, Hol, Hol'}\rangle},$$

$$\widetilde{\mathcal{A}}_{\mathrm{w}}(X) = \frac{\mathbb{Q}\langle \text{w–beaded Jacobi diagrams on } X\rangle}{\mathbb{Q}\langle \text{AS, IHX, STU, LE, OR, Hol, Hol', Hol}_{\mathrm{w}}\rangle},$$

$$\widetilde{\mathcal{A}}(*_C) = \frac{\mathbb{Q}\langle \text{beaded Jacobi diagrams on } C\rangle}{\mathbb{Q}\langle \text{AS, IHX, STU, LE, OR, Hol, Hol'}\rangle},$$

with the relations in Figures 5, 10 and 16, where the central edges in the relation IHX are labeled by 1 and $f, g, h \in \mathbb{Q}[t^{\pm 1}]$ in the relations LE, Hol, Hol', OR. In the pictures, the skeleton is represented with bold lines and the graph with thin lines. We indeed consider the i–degree completion of these vector spaces, keeping the same notation.

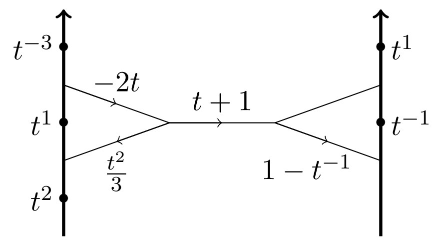

Figure 15: A w–beaded Jacobi diagram

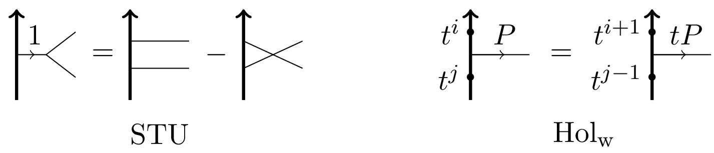

Figure 16: Relations STU and $\mathrm{Hol_w}$ on Jacobi diagrams.

Remark 4.1. For diagrams in $\widetilde{\mathcal{A}}_{\mathrm{w}}(X)$, the condition on the labels on the skeleton implies that all labels can be pushed off each component of the skeleton using the relation $\mathrm{Hol_w}$. When the component is an interval, there is a unique way to do so.

For a finite set C, denote by $\upharpoonleft_C$ (resp. $\circlearrowleft_C$) the manifold made of $|C|$ intervals (resp. circles) indexed by the elements of C. Remark 4.1 shows that there is a natural isomorphism $\widetilde{\mathcal{A}}_{\mathrm{w}}(\upharpoonleft_C) \cong \widetilde{\mathcal{A}}(\upharpoonleft_C)$. In the case of a squeleton with closed components, we need to add a relation to get such an isomorphism.

Given a beaded Jacobi diagram D on $\circlearrowleft_C$, a label $c \in C$ and an integer k, the associated *winding relation* identifies D with the diagram obtained from D by *pushing t^k at each vertex glued on $\circlearrowleft_c$, i.e.* by multiplying the label of each edge adjacent to a univalent vertex glued on $\circlearrowleft_c$ by t^k if the orientation of the edge goes backward the vertex and by t^{-k} otherwise, see Figure 17. Denote by $\sim_{\mathrm{w}}$ the induced equivalence relation. It provides an isomorphism $\widetilde{\mathcal{A}}_{\mathrm{w}}(\circlearrowleft_C) \cong \widetilde{\mathcal{A}}(\circlearrowleft_C)/_{\sim_{\mathrm{w}}}$. We want to relate this quotient to the space $\widetilde{\mathcal{A}}(\upharpoonleft_C)$. We define similarly as above a relation $\sim_{\mathrm{w}}$ on $\widetilde{\mathcal{A}}(\upharpoonleft_C)$. Following [BGRT02, Section 5.2] and [GK04], we also define a *link relation* on $\widetilde{\mathcal{A}}(\upharpoonleft_C)$ as follows. Given two beaded Jacobi diagrams D_1 and D_2 on C, we have $D_1 \sim_\ell D_2$ if, for an index $c \in C$ and two extra indices c_1 and c_2, there is a beaded Jacobi diagram D on $(C \setminus \{c\}) \cup \{c_1, c_2\}$ such that D_1 and D_2 are obtained from D by gluing together the squeleton components $\upharpoonleft_{c_1}$ and $\upharpoonleft_{c_2}$ in the two possible orders. It is easily checked that $\widetilde{\mathcal{A}}(\circlearrowleft_C)/_{\sim_{\mathrm{w}}} \cong \widetilde{\mathcal{A}}(\upharpoonleft_C)/_{\sim_{\mathrm{w}}, \sim_\ell}$.

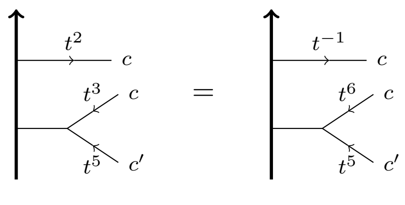

Figure 17: A winding relation pushing t^3 at c–labeled vertices

In [Bar95, Theorem 8], Bar-Natan defines a formal PBW isomorphism:

$$\chi_C : \widetilde{\mathcal{A}}(*_C) \xrightarrow{\cong} \widetilde{\mathcal{A}}(\upharpoonleft_C).$$

For a beaded Jacobi diagram D, the image $\chi_C(D)$ is the average of all possible ways to attach the c–labeled vertices of D on the corresponding c–indexed interval in $\upharpoonleft_C$ for each $c \in C$. To recover an isomorphism onto $\widetilde{\mathcal{A}}(\circlearrowleft_C)$, one needs to introduce again some relations.

Given a beaded Jacobi diagram D on C and elements $c, \bar{c} \in C$, we denote $\langle D \rangle_{c-\bar{c}}$ the sum of all diagrams obtained by gluing all c–labeled vertices to all $\bar{c}$–labeled vertices. We also denote $D_{|c \to ce^h}$ the diagram obtained from D by pushing e^h on each c–labeled vertex of D (see Figure 18. We define the link relation on $\widetilde{\mathcal{A}}(*_C)$ as follows: given two beaded Jacobi diagrams

D_1 and D_2 on C, we have $D_1 \sim_\ell D_2$ if, for some $c \in C$ and some extra vertices $h, \breve{h}$, there is a beaded Jacobi diagram D on $C \cup \{h, \breve{h}\}$ such that $D_1 = \langle D \rangle_{h-\breve{h}}$ and $D_2 = \langle D_{|c \to ce^h} \rangle_{h-\breve{h}}$.

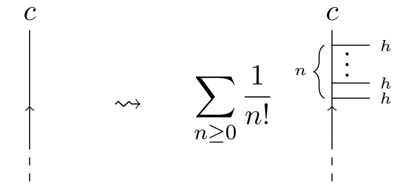

Figure 18: Pushing e^h on a c–labeled vertex

Proposition 4.2 (Garoufalidis–Kricker)**.** *For beaded Jacobi diagrams D_1 and D_2 on C, we have $D_1 \sim_\ell D_2$ if and only if $\chi_C(D_1) \sim_\ell \chi_C(D_2)$.*

We also have as above a winding relation $\sim_{\mathrm{w}}$ on $\widetilde{\mathcal{A}}(*_C)$ defined by pushing the t^k at the c–labeled vertices, see Figure 19. Set $\widetilde{\mathcal{A}}(\circledast_C) = \widetilde{\mathcal{A}}(*_C)/_{\sim_{\mathrm{w}}, \sim_\ell}$. The following is a corollary of Proposition 4.2.

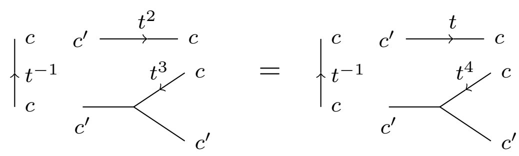

Figure 19: A winding relation pushing t at c–labeled vertices

Proposition 4.3. *The isomorphisms $\chi_C : \widetilde{\mathcal{A}}(*_C) \xrightarrow{\cong} \widetilde{\mathcal{A}}(\uparrow_C)$ descend to an isomorphisms $\chi_C : \widetilde{\mathcal{A}}(\circledast_C) \xrightarrow{\cong} \widetilde{\mathcal{A}}(\circlearrowleft_C)/_{\sim_w}$.*

We finally have the following commutative diagram of diagram spaces.

$$\begin{array}{ccccc}
\widetilde{\mathcal{A}}_{\mathrm{w}}(\uparrow_C) & \xrightarrow[\cong]{} & \widetilde{\mathcal{A}}(\uparrow_C) & \xrightarrow[\cong]{\chi_C^{-1}} & \widetilde{\mathcal{A}}(*C) \\
\downarrow & & \downarrow & & \downarrow \\
\widetilde{\mathcal{A}}_{\mathrm{w}}(\circlearrowleft_C) & \xrightarrow[\cong]{} & \widetilde{\mathcal{A}}(\circlearrowleft_C)/_{\sim_{\mathrm{w}}} & \xrightarrow[\cong]{\chi_C^{-1}} & \widetilde{\mathcal{A}}(\circledast_C)
\end{array}$$

4.3 Product and coproduct

We first define a coproduct on the diagram spaces of the previous subsection. Given a (w–)beaded Jacobi diagram D on X or C, denote by $\ddot{D}$ its graph part, and by $\ddot{D}_i$, $i \in I$, the connected components of $\ddot{D}$. Set $D_J = D \setminus (\sqcup_{i \in I \setminus J} \ddot{D}_i)$, multiplying the labels of the concatenated edges of the skeleton, when relevant. Define the coproduct of a diagram D by

$$\Delta(D) = \sum_{J \subset I} D_J \otimes D_{I \setminus J}.$$

Note that the different relations on beaded Jacobi diagrams respect the coproduct. This provides a notion of *group-like* elements, *i.e.* elements G such that $\Delta(G) = G \otimes G$. The isomorphisms χ of the previous subsection preserve the coproduct.

We now define a Hopf algebra structure on $\widetilde{\mathcal{A}}(*_C)$. Define the product of two diagrams as the disjoint union. The unit $\epsilon : \mathbb{Q} \to \widetilde{\mathcal{A}}(*_C)$ is defined by $\epsilon(1) = \varnothing$ and the counit $\varepsilon : \widetilde{\mathcal{A}}(*_C) \to \mathbb{Q}$ is given by $\varepsilon(D) = 0$ if $D \neq \varnothing$ and $\varepsilon(\varnothing) = 1$. The antipode is given by $D \mapsto (-1)^{|I|}D$. We finally have a structure of a graded Hopf algebra on $\widetilde{\mathcal{A}}(*_C)$, where the grading is given by the i–degree. It is known that an element in a graded Hopf algebra is group-like if and only if it is the exponential of a *primitive* element, *i.e.* an element G such that $\Delta(G) = 1 \otimes G + G \otimes 1$. Here, the primitive elements are the series of connected diagrams. We denote $\exp_\sqcup$, namely exponential with respect to the disjoint union, the exponential of diagrams.

4.4 Operation ω

This part aims at defining an operation on $\widetilde{\mathcal{A}}(*_{\{1,\dots,n\}})$ that will play the role of the formal Gaussian integration in our refinement of the Kricker invariant.

A hermitian matrix $W(t)$ with coefficients in $\mathbb{Q}[t^{\pm 1}]$ such that $\det(W(1)) \neq 0$ defines a Blanchfield module $(\mathfrak{A}, \mathfrak{b})$ by $\mathfrak{A} = \frac{\mathbb{Q}[t^{\pm1}]^n}{{}^tW\mathbb{Q}[t^{\pm1}]^n}$ and $\mathfrak{b}(e_i, e_j) = -(W^{-1})_{ij}(t)\ mod\ \mathbb{Q}[t^{\pm 1}]$, where the e_i are the generators associated with the presentation (see [1] for details). Given a beaded Jacobi diagram D on $\{1, \dots, n\}$, we define an $(\mathfrak{A}, \mathfrak{b})$–colored diagram $\omega_W(D)$ by replacing the label i on univalent vertices by e_i and fixing $f_{vv'}(t) = -(W^{-1})_{ij}(t)$ if the univalent vertices v and v' are labeled by i and j respectively.

A *strut* in a Jacobi diagram is an isolated thin edge. A beaded Jacobi diagram is *substantial* if it has no strut. To a square matrix W of size n, we associate $\sum_{1 \leq i,j \leq n}$ 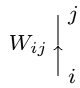 $\in \widetilde{\mathcal{A}}(*_{\{1,\dots,n\}})$.

Definition 4.4. An element $G \in \widetilde{\mathcal{A}}(*_{\{1,\dots,n\}})$ is *Gaussian* if $G = \exp_\sqcup\left(\frac{1}{2}W(t)\right) \sqcup H$ where $W(t)$ is a hermitian matrix of size n with coefficients in $\mathbb{Q}[t^{\pm1}]$ and H is substantial. If $\det(W(t)) \neq 0$, G is *non-degenerate* and we set $\omega(G) = \omega_{\frac{1}{2}W}(H)$.

The main technical difficulty in the construction of our refined Kricker invariant is the following proposition, based on a refinement of Proposition 4.2.

Proposition 4.5 ([15])**.** *Let* $G_1 = \exp_\sqcup\left(\frac{1}{2}W_1(t)\right) \sqcup H_1$ *and* $G_2 = \exp_\sqcup\left(\frac{1}{2}W_2(t)\right) \sqcup H_2$ *be non-degenerate Gaussians in* $\widetilde{\mathcal{A}}(*_{\{1,\dots,n\}})$*.*

- *If* $G_1 \sim_w G_2$*, then* $\omega(G_1) = \omega(G_2)$ *in* $\mathcal{A}^{\mathbb{K}}(\mathfrak{A}, \mathfrak{b})$*.*
- *If* $G_1 \sim_\ell G_2$*, then* $W_1(t) = W_2(t)$ *and* $\omega(G_1) = \omega(G_2)$ *in* $\mathcal{A}^{\mathbb{K}}(\mathfrak{A}, \mathfrak{b})$*.*

4.5 Invariant of a surgery presentation

We use the functor Z defined in [CHM08], which is a renormalization of the Le–Murakami functor [LM95, LM96]. The domain of this functor is the category $\mathcal{T}_q$ with objects the non-associative words in the letters $(+,-)$ and morphisms the q–tangles. Composition is given by vertical juxtaposition. We also define a tensor product by horizontal juxtaposition.

We define a category $\widetilde{\mathcal{A}}$ whose objects are associative words in the letters $(+,-)$ and whose sets of morphisms are $\widetilde{\mathcal{A}}(v,u) = \oplus_X \widetilde{\mathcal{A}}(X)$, where X runs over all compact oriented 1–manifolds with boundary identified with the set of letters of u and v, with the following sign convention: for u, a "+" when the orientation of X goes towards the boundary point and a "−" when it goes backward, and the converse for v. Figure 20 shows a q–tangle defining a morphism in $\widetilde{\mathcal{A}}(v,u)$ for $u = +(--)$ and $v = (-+)-$. Composition is given by vertical

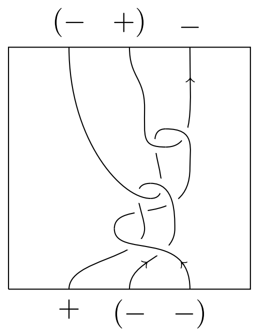

Figure 20: Diagram of a q–tangle

juxtaposition, where the label of a created edge is the product of the labels on the initial two edges. The tensor product given by disjoint union defines a strict monoidal structure on $\widetilde{\mathcal{A}}$.

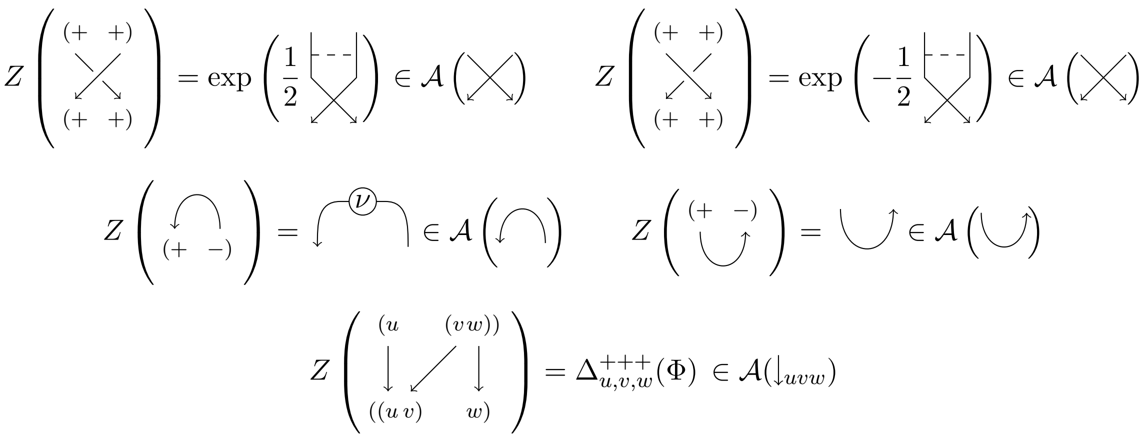

Figure 21: The functor $Z : \mathcal{T}_q \to \mathcal{A}$.

We recall in Figure 21 the definition of Z on the elementary q–tangles, where $\nu \in \mathcal{A}(\circlearrowright) \cong \mathcal{A}(\uparrow)$ is the value of the Kontsevich integral on the zero framed unknot, $\Phi \in \mathcal{A}(\downarrow\downarrow\downarrow)$ is a Drinfeld associator with rational coefficients and $\Delta^{+++}_{u_1,u_2,u_3} : \mathcal{A}(\downarrow\downarrow\downarrow) \to \mathcal{A}(\downarrow_{u_1u_2u_3})$ is obtained by applying $(|u_i| - 1)$ times the coproduct Δ on the i–th factor.

Let L be a surgery presentation for some $\mathbb{KSK}$–pair. Fixing an admissible diagram of L, one can view the surgery presentation as a q–tangle with empty top and bottom words and write it as the product of two q–tangles γ_t and γ_b, see Figure 22. The word at the top of γ_b and at the bottom of γ_t is a product $(v)(w)$, where w corresponds to the part of the tangle which meets the disk $\mathcal{D}$. Set:

$$Z^\bullet(L) = Z(\gamma_b) \circ (I_v \otimes G_w) \circ Z(\gamma_t) \ \in \widetilde{\mathcal{A}}(L),$$

where I_v is the identity on the word v and G_v is obtained from I_v by adding a label t (resp. t^{-1}) on skeleton components associated with a $-$ sign (resp. a $+$ sign), see Figure 23. It turns out that $Z^\bullet$ is invariant with respect to isotopy and to the cutting of γ. Moreover, $Z^\bullet(L)$ is group-like.

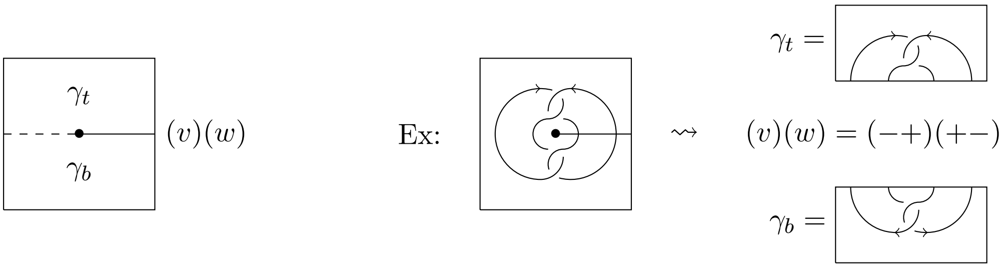

Figure 22: Cutting a surgery presentation into two q–tangles

Figure 23: The diagrams I_v and G_v.

4.6 Invariant of $\mathbb{K}$SK–pairs

Set:

$$Z^\circ(L) = \chi^{-1}\left(\nu^{\otimes \pi_0(L)} \sharp_{\pi_0(L)} Z^\bullet(L)\right) \in \widetilde{\mathcal{A}}\left(\circledast_{\pi_0(L)}\right)$$

where the connected sum means that a copy of ν is summed to each component of L. Note that $Z^\circ(L)$ is group-like since $Z^\bullet(L)$ and ν are group-like and χ preserves the coproduct.

Let $\overline{Z^\circ(L)} \in \widetilde{\mathcal{A}}\left(*_{\pi_0(L)}\right)$ be a lift of $Z^\circ(L)$. Such a lift can be constructed from an admissible diagram of L, with fixed base points $\star_i$ on each component L_i of L, following the above construction, with the skeleton components corresponding to the components of L defined as intervals by cutting each component L_i at the base point $\star_i$. We show in [15] that $\overline{Z^\circ(L)}$ is a non-degenerate Gaussian

$$\overline{Z^\circ(L)} = \exp_\sqcup\left(\frac{1}{2}W_L\right) \sqcup H,$$

where W_L is the equivariant linking matrix of L in the infinite cyclic covering of $(S^3, \mathcal{O})$. Moreover, Proposition 4.5 implies that the diagram $\omega\left(\overline{Z^\circ(L)}\right)$ does not depend on the chosen lift, which allows to set:

$$\omega\big(Z^\circ(L)\big) = \omega\left(\overline{Z^\circ(L)}\right) \quad \in \mathcal{A}^{\mathbb{K}}(\mathfrak{A}, \mathfrak{b}).$$

We can finally define our refined Kricker invariant.

Proposition 4.6 ([15])**.** *Let (M, K) be a $\mathbb{K}$SK–pair with an admissible surgery presentation L and Blanchfield module $(\mathfrak{A}, \mathfrak{b})$. Then*

$$\tilde{Z}^{\mathbb{K}}(M, K) = Z^\circ(U_+)^{-\sigma_+(L)} \sqcup Z^\circ(U_-)^{-\sigma_-(L)} \sqcup \omega\big(Z^\circ(L)\big) \quad \in \mathcal{A}^{\mathbb{K}}(\mathfrak{A}, \mathfrak{b}),$$

where $U_\pm$ is a trivial knot with framing ± 1 split from $\mathcal{O} \subset S^3$, defines an invariant $\tilde{Z}^{\mathbb{K}}$ of $\mathbb{K}$SK–pairs.

Remark 4.7. The construction of the original Kricker invariant is the same until the last step. Instead of applying the operation ω, Garoufalidis and Kricker apply a formal Gaussian integral which merges the strut part $\exp_\sqcup\left(\frac{1}{2}W_L\right)$ and the substantial part H by summing all possible ways to glue all vertices of one diagram with all vertices of the other diagram that have the same label. This defines an invariant with values in the space $\mathcal{A}(\delta)$ of trivalent diagrams. The formal Gaussion integration was initially introduced by Bar-Natan, Garoufalidis, Rozansky and Thurston to define the Aarhus integral, which recovers the LMO invariant. This version of the LMO invariant is constructed as the Kricker invariant, forgetting the knots in the 3–manifolds and the edge labels on the diagrams.

In view of this remark, the relation between the invariant $\tilde{Z}^{\mathbb{K}}$ and the Kricker invariant is easy to describe. Indeed, applying the operation ω first and the map $\psi : \mathcal{A}(\mathfrak{A}, \mathfrak{b}) \to \mathcal{A}(\delta)$ then has the same effect as applying the formal Gaussian integral.

Proposition 4.8 ([15])**.** *For any $\mathbb{K}$SK–pair (M, K), we have $Z^{Kri}(M, K) = \psi \circ \tilde{Z}^{\mathbb{K}}(M, K)$.*

In the case of $\mathbb{Q}$SK–pairs, we can once again merge the invariant $\tilde{Z}^{\mathbb{Q}}$ with the degree–1 invariants ρ_p, as follows.

$$\tilde{Z}^{\text{aug}} = \tilde{Z}^{\mathbb{Q}} \sqcup \exp_{\sqcup}\left(\sum_{p \text{ prime}} \rho_p\right)$$

In the sequel, we use the notation $\tilde{Z}$ for $\tilde{Z}^{\mathbb{Z}}$ if $\mathbb{K} = \mathbb{Z}$ and for $\tilde{Z}^{\text{aug}}$ if $\mathbb{K} = \mathbb{Q}$.

4.7 Universality

To prove that the invariant $\tilde{Z}^{\mathbb{Z}/\text{aug}}$ is a universal finite type invariant, we have to describe its behavior under null $\mathbb{K}$LP–surgeries. We fix an abstract Blanchfield module $(\mathfrak{A}, \mathfrak{b})$ and we restrict to $\mathbb{K}$SK–pairs whose Blanchfield module is isomorphic to $(\mathfrak{A}, \mathfrak{b})$. We need to show that $\tilde{Z}^{\mathbb{Z}/\text{aug}}$ induces a map on the graded space $\mathcal{G}^{\mathbb{K}}(\mathfrak{A}, \mathfrak{b})$ which is the inverse of the map $\varphi^{\mathbb{K}}$. For a $\mathbb{K}$SK–pair (M, K), in order to see $\tilde{Z}^{\mathbb{K}}(M, K)$ in the diagram space $\mathcal{A}^{\mathbb{K}}(\mathfrak{A}, \mathfrak{b})$, we a priori need to fix an isomorphism from the Blanchfield module of (M, K) to $(\mathfrak{A}, \mathfrak{b})$. However, the relation $\text{Aut}^{\mathbb{K}}$ implies that the value of $\tilde{Z}^{\mathbb{K}}(M, K) \in \mathcal{A}^{\mathbb{K}}(\mathfrak{A}, \mathfrak{b})$ does not depend on the chosen isomorphism, so that we will ignore it in the sequel.

To understand the behavior of our invariant under null LP–surgeries, we can focus on elementary surgeries, see Subsection 2.5; when $\mathbb{K} = \mathbb{Z}$, we only need to consider borromean surgeries. Hence, as a first step, we shall understand the behavior of $Z^{\bullet}$ with respect to borromean surgeries. In [Le97], Le studied the behavior of the LMO invariant with respect to borromean surgeries, in order to exhibit the universality property of this invariant. Since this can be regarded as a local problem, the same method applies here. To a Y–graph is associated a six-component surgery link, which can be turned to a trivial surgery link by separating the central three components, see Figure 24. The effect of such a difference on the invariant Z has been computed by Le in [Le97].

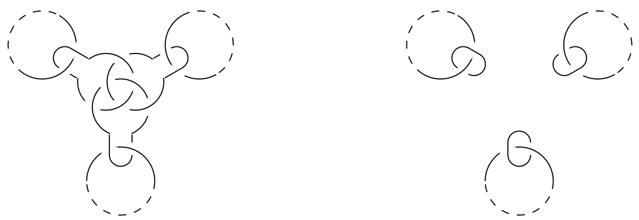

Figure 24: Surgery link associated to a Y–graph and corresponding trivial surgery

Theorem 4.9 (Le)**.**

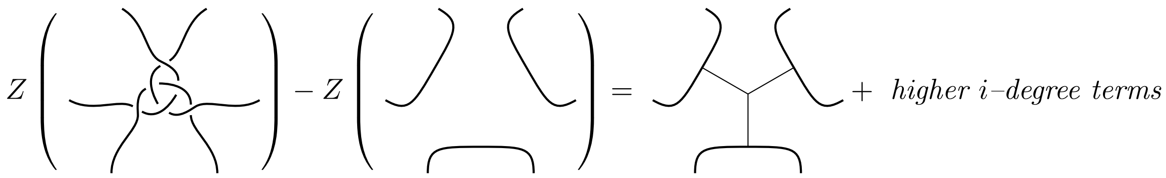

This provide us with finiteness properties for the invariant $\tilde{Z}^{\mathbb{K}}$ with respect to borromean surgeries.

Theorem 4.10 ([15])**.** *The degree–n part $\tilde{Z}_n^{\mathbb{K}}$ of the invariant $\tilde{Z}^k$ is a degree–n finite type invariant of $\mathbb{K}SK$–pairs with respect to null borromean surgeries.*

We now focus on $\mathbb{Q}$SK–pairs. Our second step is to describe the behavior of $\tilde{Z}^{\mathbb{Q}}$ under connected sum. Although it behaves well with respect to connected sums of $\mathbb{Q}$SK–pairs, what we consider here is the connected sum defining a genus 0 surgery, that is a connected sum performed on the $\mathbb{Q}$–sphere far from the knot. If (M, K) is a $\mathbb{Q}$SK–pair and N is a $\mathbb{Q}$–sphere, a surgery presentation for $(M\sharp N, K)$ is simply obtained by stacking surgery presentations for (M, K) and N (see Figure 25), giving the following.

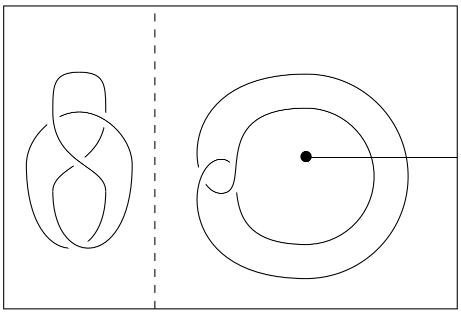

Figure 25: Stacking diagrams for a $\mathbb{Q}$–sphere and a $\mathbb{Q}$SK–pair.

Lemma 4.11. *Let (M, K) be a $\mathbb{Q}SK$–pair and let N be a $\mathbb{Q}$–sphere. Let $(\mathfrak{A}, \mathfrak{b})$ denote the Blanchfield module of (M, K). The invariant $\tilde{Z}^{aug}$ is given on the connected sum by:*

$$\tilde{Z}^{\mathbb{Q}}(M\sharp N, K) = \tilde{Z}^{\mathbb{Q}}(M, K) \sqcup Z^{LMO}(N) \ \in \mathcal{A}^{\mathbb{Q}}(\mathfrak{A}, \mathfrak{b}).$$

The last step is to deal with d–surgery. In Theorem 2.5, one can indeed restrict d–surgeries using a fixed d–torus for each integer d. Here we will use d–tori obtained from a standard torus by Dehn surgery on the link $J_1 \sqcup J_2$ in Figure 26. The corresponding d–surgery on a $\mathbb{Q}$SK–pair acts on the associated surgery link L by adding the surgery components J_1 and J_2, where the part involving J_2 is locally inserted as in Figure 26, while J_1 is embedded in a possibly complicated way. When $d = 1$, the knot J_2 is a meridian of J_1, so that the surgeries on L and on $L \cup J_1 \cup J_2$ are equivalent. Hence what we need to compute is the difference between the value of Z on $L \cup J_1 \cup J_2$ with the $2d$ crossings and the value of Z on $L \cup J_1 \cup J_2$ with only 2 crossings between J_1 and J_2.

Proposition 4.12 ([15])**.** *Let (M, K) be a $\mathbb{Q}SK$–pair. Fix a positive integer d. Consider a d–surgery $\left(\frac{T_d}{T_1}\right)$ on (M, K). Denote $J_1 \sqcup J_2^d$ the surgery link defined on Figure 26. Let*

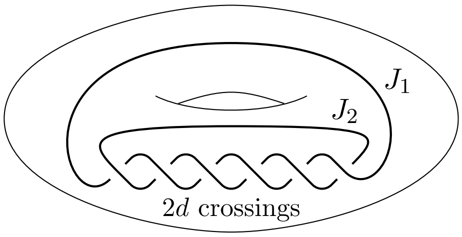

Figure 26: A d–torus constructed by Dehn surgery

L be an admissible surgery presentation of (M,K). Then $L_1 = L \sqcup J_1 \sqcup J_2^1$ and $L_d = L \sqcup J_1 \sqcup J_2^d$ are admissible surgery presentations of (M,K) and $(M,K)\left(\frac{T_d}{T_1}\right)$ respectively, and $\tilde{Z}^{\mathbb{Q}}\left((M,K)\left(\frac{T_d}{T_1}\right)\right) - \tilde{Z}^{\mathbb{Q}}(M,K)$ is a series of diagrams of degree at least 1 containing a univalent vertex associated to J_2.

This discussion shows that applying a null elementary surgery modifies the invariant $\tilde{Z}^{\mathbb{Q}}$ by terms with at least one trivalent vertex. These turn out to combine when looking at the image of the bracket defined by a family of null elementary surgeries. Hence, the evaluation of $\tilde{Z}^{\mathbb{Q}}$ on a bracket defined by k null elementary surgeries, and in turn, by any k null LP–surgeries, contains only diagrams with at least k trivalent vertices. It follows that, denoting $\tilde{Z}_n^{\mathbb{Q}}$ the degree–n part of the invariant $\tilde{Z}^{\mathbb{Q}}$ in the sense of the degree of the diagrams, $\tilde{Z}_n^{\mathbb{Q}}$ is a degree–n finite type invariant. Using that the ρ_p are degree–1 invariants, it is not difficult to deduce that the degree–n part $\tilde{Z}_n^{\mathrm{aug}}$ of $\tilde{Z}^{\mathrm{aug}}$ is also a degree–n finite type invariant. Thus $\tilde{Z}^{\mathrm{aug}}$ induces a map $\tilde{Z}^{\mathrm{aug}} : \mathcal{G}^{\mathbb{Q}}(\mathfrak{A},\mathfrak{b}) \to \mathcal{A}^{\mathrm{aug}}(\mathfrak{A},\mathfrak{b})$.

For $\mathbb{K} = \mathbb{Z},\mathbb{Q}$, a more precise analysis of the behavior of $\tilde{Z}^{\mathbb{Z}/\mathrm{aug}}$ with respect to connected sums and borromean surgeries allows to compute $\tilde{Z}_n^{\mathbb{Z}/\mathrm{aug}} \circ \varphi_n^{\mathbb{K}}(D)$ for a family of somehow simple diagrams D that generate $\mathcal{A}^{\mathbb{Z}/\mathrm{aug}}(\mathfrak{A},\mathfrak{b})$.

Theorem 4.13 ([15])**.** *The invariant $\tilde{Z}^{\mathbb{Z}/aug}$ realizes the inverse of $\varphi : \mathcal{A}^{\mathbb{Z}/aug}(\mathfrak{A},\mathfrak{b}) \to \mathcal{G}^{\mathbb{K}}(\mathfrak{A},\mathfrak{b})$. In particular, it is a universal finite type invariant of $\mathbb{K}SK$–pairs with respect to null $\mathbb{K}LP$–surgeries.*

Corollary 4.14. *The Kricker invariant and the Lescop invariant both induce on the graded space $\mathcal{G}^{\mathbb{K}}(\mathfrak{A},\mathfrak{b})$ the same map $\psi \circ \tilde{Z}^{\mathbb{Z}/aug}$.*

5 Perspectives

5.1 Refining the Lescop invariant

The Lescop invariant and the Kricker invariant are two powerful invariants of null-homologous knots in $\mathbb{Q}$–spheres, both derived from the Kontsevich integral, following two different approaches. Their status of universal finite type invariant for knots with trivial Alexander modules shows that they are equivalent for such knots. We have refined the Kricker invariant and obtained a universal finite type invariant for all $\mathbb{K}$SK–pairs.

Problem 5.1. *Construct a refinement of the Lescop invariant with values in $\mathcal{A}^{\mathbb{K}}(\mathfrak{A},\mathfrak{b})$ and prove that it provides a universal finite type invariant of $\mathbb{K}SK$–pairs.*

Such a refined Lescop invariant would be equivalent to the refined Kricker invariant. Moreover, the Kricker invariant can be recovered from the refined version, composing by the map ψ

of Subsection 3.4. Hence the equivalence of the original Kricker and Lescop invariants could be deduced from the equivalence of their refined versions.

5.2 Knots in $\mathbb{Z}$–spheres with respect to general $\mathbb{Z}$LP–surgeries

The finite type invariants we have considered are defined with respect to LP–surgeries satisfying a nullity condition. This is interesting in that it provides some structure on the graded space of finite type invariants. However, it obliges to work within each isomorphism class of Blanchfield modules. In order to consider the set of knots in $\mathbb{Z}$–spheres as a whole, one can work with general $\mathbb{Z}$LP–surgeries (or equivalently with general borromean surgeries) performed in the complement of the knot, removing the nullity condition. This move is in turn transitive on the set of knots in $\mathbb{Z}$–spheres.

Problem 5.2. *Describe the graded space $\mathcal{G}$ associated with knots in $\mathbb{Z}$–spheres with respect to general $\mathbb{Z}$LP–surgeries.*

First, one has to propose a graded space of diagrams adapted to this situation. In a first attempt, I plan to work with a space $\mathcal{A}$ of trivalent diagrams whose edges are labeled by rational fractions $\frac{P}{Q}$ where $Q(1) \neq 0$, quotiented out by the usual relations: AS, IHX, Hol, OR, LE.

Then, an onto map $\mathcal{A} \to \mathcal{G}$ has to be constructed. Given a diagram D defining a class in $\mathcal{A}$, one can choose a Blanchfield module $(\mathfrak{A}, \mathfrak{b})$ such that D defines a class in $\mathcal{A}(\mathfrak{A}, \mathfrak{b})$, take the image of this class via the isomorphism $\mathcal{A}(\mathfrak{A}, \mathfrak{b}) \cong \mathcal{G}(\mathfrak{A}, \mathfrak{b})$, and then via the natural map $\mathcal{G}(\mathfrak{A}, \mathfrak{b}) \to \mathcal{G}$.

$$\begin{array}{ccc} \mathcal{A} & \dashrightarrow\!\!\!\!\rightarrow & \mathcal{G} \\ \uparrow & & \uparrow \\ \mathcal{A}(\mathfrak{A}, \mathfrak{b}) & \xrightarrow{\cong} & \mathcal{G}(\mathfrak{A}, \mathfrak{b}) \end{array}$$

The point is to prove that this provides a well-defined onto map.

Finally, in order to get the inverse of this onto map, one has to provide a universal finite type invariant. A natural candidate is obtained by composing the refined Kricker invariant with the natural map $\mathcal{A}(\mathfrak{A}, \mathfrak{b}) \to \mathcal{A}$. The point to prove here is that this composed invariant satisfies splitting formulas with respect to general $\mathbb{Z}$LP–surgeries.

5.3 Knots in $\mathbb{Q}$–spheres with respect to general $\mathbb{Q}$LP–surgeries

The above problem has a natural counterpart for knots in $\mathbb{Q}$–spheres.

Problem 5.3. *Describe the graded space $\mathcal{G}$ associated with knots in $\mathbb{Q}$–spheres with respect to general $\mathbb{Q}$LP–surgeries.*

The ideas to tackle this problem are essentially the same as above, with one more difficulty. The general $\mathbb{Q}$LP–surgeries don't preserve the property for a knot to be null-homologous. It means that we need to work with all knots in $\mathbb{Q}$–spheres. Although it would be very interesting to deal with a theory involving all these knots, the construction of the (refined) Kricker invariant strongly makes use of the null-homologous property: it ensures the existence of an admissible surgery presentation, which is the starting point of the construction.

Problem 5.4. *Extend the refined Kricker invariant to all knots in $\mathbb{Q}$–spheres.*

Second part:
Trisections of 4–manifolds and further multisections

6 Introduction

The story starts in dimension 3. A connected, oriented 3–manifold can be decomposed as the union of two handlebodies glued along a compact surface; such a decomposition is called a Heegaard splitting. The notion of Heegaard splitting is a key notion in the study of 3–manifolds. Besides being a nice description of 3–manifolds, it provides a powerful tool to define or compute invariants. For instance, the construction of Heegaard Floer homology is based on Heegaard diagrams, which are combinatorial descriptions of Heegaard splittings.

Gay and Kirby [GK16] recently developed an analogous construction for smooth, connected, oriented 4–manifolds: such a manifold can be trisected as the union of three 4–dimensional 1–handlebodies with 3–dimensional handlebodies as pairwise intersections and a compact oriented surface as global intersection. Trisections provide 2–dimensional representations of smooth 4–manifolds *via* the datum of three families of curves on a closed surface —the central surface of the trisection. These so-called trisection diagrams, analogous to Heegaard diagrams, allow to use 2–dimensional and 3–dimensional techniques to study 4–manifolds. The theory of trisections has already proved useful in the study smooth 4–manifolds. For instance, it allowed Lambert-Cole [LC20] to reprove the Thom conjecture without using gauge theory. It also consitutes a new approach to important open problems, as the smooth Poincaré conjecture in dimension 4.

A trisection diagram determines a unique smooth 4–manifold up to diffeomorphism. In turn, the diagram determines the homotopy invariants of the manifold. In [FKSZ18], Feller, Klug, Schirmer and Zemke proposed a computation of the homology and intersection form of a manifold from a trisection diagram. With Vincent Florens [11], we generalized it to twisted homology, torsion and intersection form. Further, with Trenton Schirmer [14], we develop an efficient approach to recover and improve the previous results and generalize them to manifolds with boundary and multisections of 4–manifolds. This is described in Section 8.

Beyond dimensions 3 and 4, one may wonder if similar decompositions exist for smooth manifolds in general. In a joint work with Fathi Ben Aribi, Sylvain Courte and Marco Golla [16], we introduce multisections of smooth closed oriented manifolds, defined as decompositions into 1–handlebodies, where subcollections intersect along 1–handlebodies and the global intersection is a closed surface. We prove in [16] the existence of such decompositions for any smooth 5–manifold. In any dimension, we introduce stabilization moves and state a uniqueness conjecture. Further, multisections have a natural diagrammatic representation and we prove that a multisection diagram encodes a unique manifold up to PL homeomorphism. In [17], multisections are constructed for any surface bundle and any fiber bundle over the circle whose fiber is multisected. This allows to produce examples of multisected manifolds and their diagrams. This is described in Section 9. Further projects are exposed in Section 10.

Throughout this part, all manifolds are compact, connected and oriented. We call *n–dimensional handlebody* an n–manifold that admits a handle decomposition with one 0–handle and some 1–handles; the *genus* of a handlebody is the number of 1–handles.

7 Background

7.1 Heegaard splittings of 3–manifolds

A Heegaard splitting of a closed 3–manifold M is a decomposition $M = A \cup_\Sigma B$ where A and B are handlebodies with common boundary Σ. It is an important result that any closed 3–manifold admits such a Heegaard splitting. This can be proved using a triangulation of the manifold: one handlebody is given as a regular neighborhood of the 1–skeleton of the triangulation, the closure of its complement is a regular neighborhood of the 1–skeleton of the dual cellulation, so that it is also a handlebody. Another approach, dealing with the smooth structure of the manifold, makes use of Morse functions, namely smooth functions on the manifold with real values and no degenerate critical point. Any closed 3–manifold M admits a Morse function f with image $[0,3]$ whose critical points of index i are contained in the level $f^{-1}(\{i\})$. It follows that $f^{-1}(\{\frac{3}{2}\})$ is a closed surface that cuts M into two handlebodies.

Heegaard splittings appear to be unique up to a stabilization move. This move is defined as follows. Given a Heegaard splitting $M = A \cup_\Sigma B$ and a boundary-parallel arc γ properly embedded in B, one constructs another Heegaard splitting by adding to A a regular neighborhood of γ and removing its interior from B. Exchanging the roles of A and B gives the same result up to isotopy, so that there is a single stabilization move, well-defined on a given Heegaard splitting.

Theorem 7.1 (Reidemeister–Singer)**.** *Any two Heegaard splittings of a given closed 3–manifold can be made isotopic after some number of stabilizations.*

In higher dimensions, the first approach is adapted to PL topology and this has been investigated by Rubinstein and Tillmann (see Subsection 9.1). The second approach is more adapted to smooth manifolds and has been generalized by Gay and Kirby to deal with trisections in dimension 4. Our work in with higher-dimensional smooth manifolds lies in this framework.

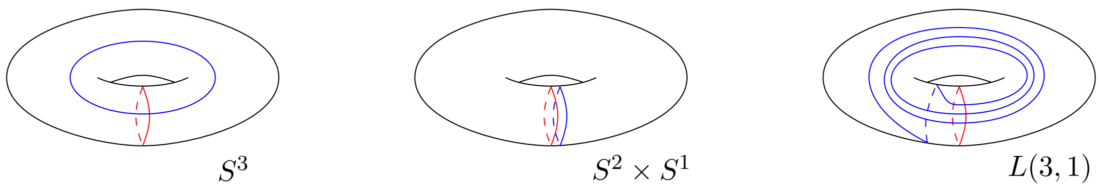

Figure 27: Heegaard diagrams

A Heegaard splitting of a 3–manifold can be represented by a Heegaard diagram. First define a *cut system* for a handlebody as a family of disjoint curves on its boundary that bound disjoint disks, such that cutting the handlebody along these disks gives a 3–ball. A Heegaard diagram for a given Heegaard splitting is given by two families of curves on the central surface that are cut systems for the two handlebodies of the splitting, see Figure 27. Given such a diagram, the 3–manifold can be easily reconstructed by thickening the surface, gluing disks along one family of curves on each side, and filling with two 3–balls. On a diagram, a stabilization appears as a connected sum with the diagram for S^3 represented in Figure 27. The Reidemeister–Singer theorem implies that any two Heegaard diagrams represent homeomorphic 3–manifolds if and only if they are handleslide-diffeomorphic (see Figure 28) after some stabilizations.

The notion of Heegaard splitting can be extended to 3–manifolds with non-empty boundary. If M is a 3–manifold with non-empty boundary, a *Heegaard splitting* of M is a decomposition $M = C_1 \cup_\Sigma C_2$ where Σ is a surface with non-empty boundary and each C_i is a *compression body*, namely a cobordism from its negative boundary $\partial_- C_i$ to its positive boundary $\partial_+ C_i = \Sigma$ which is constructed using only 1–handles. Diagrams for such Heegaard splittings are defined similarly as above.

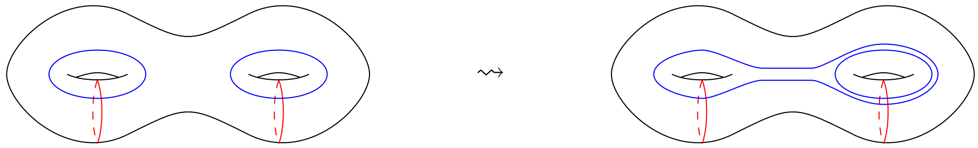

Figure 28: A curve can be slid along another curve in the same family

7.2 Trisections of 4–manifolds

We now define trisections of 4–manifolds, which generalize Heegaard splittings of 3–manifolds. Let X be a closed smooth 4–manifold. A $(g; k_1, k_2, k_3)$–*trisection of* X is a decomposition $X = X_1 \cup X_2 \cup X_3$ such that

- $X_i \cong \natural^{k_i}(S^1 \times B^3)$ is a 4–dimensional handlebody for each i,
- $X_{ij} = X_i \cap X_j \cong \natural^g(S^1 \times D^2)$ is a 3–dimensional handlebody for all $i \neq j$,
- $\Sigma = X_1 \cap X_2 \cap X_3$ is a closed surface of genus g.

Theorem 7.2 (Gay–Kirby)**.** *Any smooth 4–manifold admits a trisection.*

Like Heegaard splittings, trisections are unique up to some stabilization move, defined as follows. Fix a trisection of a 4–manifold X as above. For $\{i, j, k\} = \{1, 2, 3\}$, let γ be a boundary-parallel arc properly embedded in X_{jk}. Define X_i' from X_i by adding a regular neighborhood $\eta(\gamma)$ of γ. Set $X_j' = \overline{X_j \setminus \eta(\gamma)}$ and $X_k' = \overline{X_k \setminus \eta(\gamma)}$. Note that X_j' and X_k' are deformation retracts of X_j and X_k. Then (X_1', X_2', X_3') is a trisection of X, obtained from (X_1, X_2, X_3) by *stabilization*.

Theorem 7.3 (Gay–Kirby)**.** *Any two trisections of a given closed smooth 4–manifold are isotopic after stabilizations.*

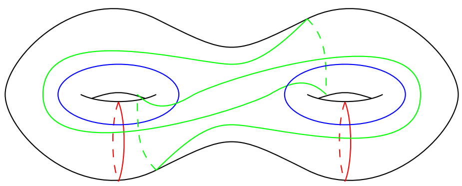

Figure 29: A trisection diagram for $S^2 \times S^2$

A *trisection diagram* for a given trisection consists of three cut systems $(\alpha_i)_{1\leq i\leq g}$, $(\beta_i)_{1\leq i\leq g}$ and $(\gamma_i)_{1\leq i\leq g}$ on the central surface Σ for the three 3–dimensional handlebodies of the trisection, namely $H_\alpha := X_{13}$, $H_\beta := X_{12}$ and $H_\gamma := X_{23}$.

Abstractly, a trisection diagram is a quadruplet $(\Sigma; \alpha, \beta, \gamma)$ where Σ is a closed genus–g surface and $(\alpha_i)_{1\leq i\leq g}$, $(\beta_i)_{1\leq i\leq g}$, $(\gamma_i)_{1\leq i\leq g}$ are three families of disjoint simple closed curves on Σ such that each pair of families is handleslide-diffeomorphic to the diagram in Figure 30. The latter condition is due to the fact that $\partial X_i = X_{ij} \cup_\Sigma X_{ik}$ is a Heegaard splitting of

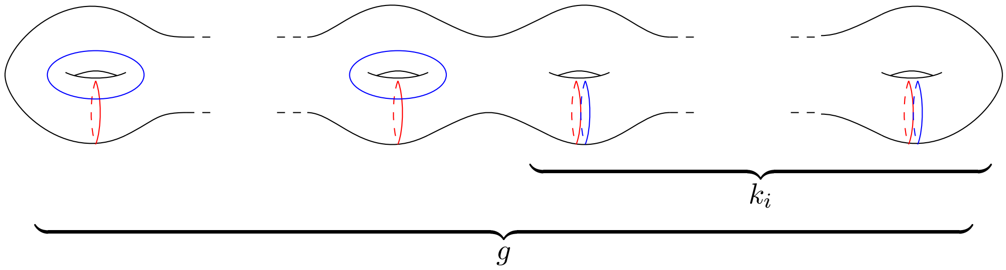

Figure 30: Genus–g Heegaard diagram for $\sharp^{k_i} S^1 \times S^2$

$\partial X_i \cong \sharp^{k_i}(S^1 \times S^2)$; it is known from Waldhausen [Wal68] that there is a unique Heegaard splitting of $\sharp^k(S^1 \times S^2)$ for a given genus $g \geq k$.

A trisection diagram determines a unique smooth 4–manifold, which can be reconstructed from the diagram as follows. Consider a disk D^2 with center p_0 and three distinct points p_α, p_β, p_γ on the boundary, see Figure 31. Take the product $D^2 \times \Sigma$ and add a 2–cell along $p_\nu \times \nu_i$ for all $\nu = \alpha, \beta, \gamma$ and all $1 \leq i \leq g$. It remains to add 3–cells and 4–cells to get a closed manifold; the result is well-defined up to diffeomorphism, thanks to a result of Laudenbach and Poénaru [LP72]. In this decomposition of X, H_ν is recovered as the union of $[p_0, p_\nu] \times \Sigma$ with the corresponding 2–cells and 3–cell.

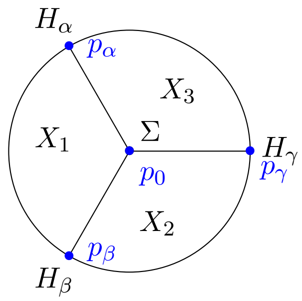

Figure 31: Schematic decomposition of X

There is obviously a single genus–0 trisection diagram, representing S^4. It is easy to check that any genus–1 trisection diagram is diffeomorphic to one in Figure 32.

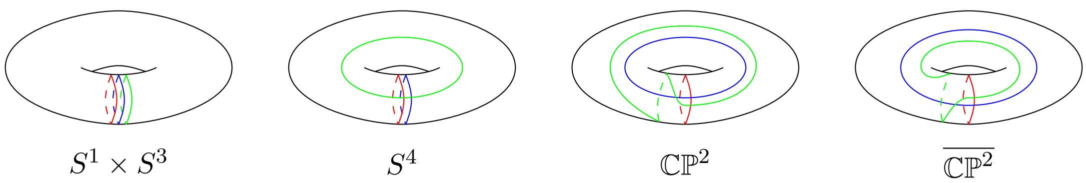

Figure 32: Genus–1 trisection diagrams

Like Heegaard splittings, trisections are defined for manifolds with boundary, as announced in [GK04] and developed by Castro, Gay and Pinzón-Caicedo in [Cas16, CGPC18a, CGPC18b]. This appears in the next section in the setting of Islambouli–Naylor multisections.

8 The algebraic topology of 4–manifolds multisections

8.1 Introduction

Since a trisection diagram determines a smooth 4–manifold up to diffeomorphism, one should be able to read topological invariants of the manifold on the diagram. In the setting of closed 4–manifolds, Feller, Klug, Schirmer and Zemke [FKSZ18] provided a computation of the homology and intersection form of the manifold from a trisection diagram, and we derived in [11] the twisted homology and torsion, and the twisted intersection form. Following these papers, Tanimoto [Tan21] computed the homology of 4–manifolds with connected boundary. In [14] we recover and generalize these results, computing from a diagram the twisted absolute and relative homology and torsion and the twisted intersection form for any trisected 4–manifold with boundary. Moreover, we work with "multisections" in the sense of Islambouli–Naylor [IN20], namely a cyclic decomposition of the manifold into any number of 4–dimensional handlebodies, where successive pieces meet along 3–dimensional handlebodies while non-successive ones meet along the central surface. While Feller–Klug–Schirmer–Zemke worked with a handle decomposition of the manifold underlying the trisection, we directly used in [11] the datum of the trisection. This last method reduced the homological computations, but the computation of torsion was quite intricate. In [14], we consider a deformation-retraction of the (possibly punctured) manifold onto a CW–complex associated with the multisection diagram. This approach is very efficient: it simplifies the computations and provides the torsion "for free". This retraction could be useful for further computations of homological or homotopical invariants.

Throughout this section, given a submanifold Z of a manifold X, $\eta(Z)$ denotes a regular neighborhood of Z in X.

We now define the precise setting. For 4–manifolds with boundary, the handlebodies of a multisection inherit (hyper) compression bodies structures related to the way they intersect the boundary of the manifold.

Definition 8.1. A *compression body* C is a cobordism from a compact orientable surface $\partial_- C$ to a connected compact orientable surface $\partial_+ C$ which is constructed using only 1–handles. Likewise a *hyper compression body* V is a cobordism from a compact orientable 3–manifold $\partial_- V$ to a connected compact orientable 3–manifold $\partial_+ V$ constructed using only 1–handles. A *lensed* (hyper) compression body is then obtained by collapsing the vertical boundary of the cobordism so that the boundary of $\partial_+ C$ ($\partial_+ V$) becomes identified with the boundary of $\partial_- C$ ($\partial_- V$).

In the case that $\partial_- C = \emptyset$, it is understood at C is built using only 1–handles attached to a single 0–handle. A (lensed) compression body is *trivial* if $\partial_- C \cong \partial_+ C$. This means it is just a thickened surface $S \times I$, or if lensed, it is obtained from $S \times I$ by collapsing the I–fibers of $\partial S \times I$.

Definition 8.2. A *multisection* of a compact orientable 4–manifold X is a decomposition $X = X_1 \cup \cdots \cup X_n$ into 4–dimensional handlebodies X_i with the following properties (all arithmetic involving indices is mod n):

1. each X_i has a lensed hyper compression body structure such that $\partial_- X_i = X_i \cap \partial X$ and if $\partial X \neq \emptyset$, there is a fixed surface Σ_∂ such that, for all $1 \leq i \leq n$, $\partial_- X_i$ is diffeomorphic to the trivial lensed compression body obtained by pinching the vertical boundary of $\Sigma_\partial \times I$,
2. $\Sigma = \bigcap_{i=1}^{n} X_i$ is a compact connected orientable surface,

3. $C_i = X_i \cap X_{i+1}$ is a 3–dimensional handlebody with a lensed compression body structure satisfying $\partial_+ C_i = \Sigma$ and $\partial_- C_i = C_i \cap \partial X \cong \Sigma_\partial$ for all i,
4. when $|i-j| > 1$, $X_i \cap X_j = \Sigma$.

A multisection is called a *trisection* when $n = 3$.

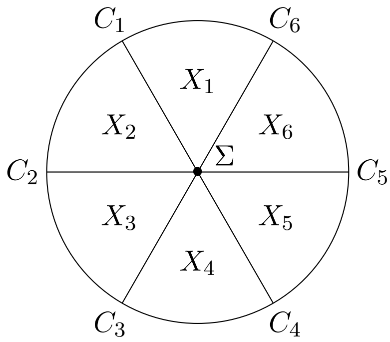

Figure 33: Schematic of a multisection

The condition that the C_i are handlebodies implies that Σ is closed if and only if X is closed, and Σ_∂ has no closed component.

In the case that $\partial X \neq \emptyset$, it is also to be understood that for all i mod n, $\partial_- X_i$ is parameterized as $\Sigma_\partial \times I / \sim$ in such a way that $\partial_- C_{i-1} = \Sigma_\partial \times \{0\}$ and $\partial_- C_i = \Sigma_\partial \times \{1\}$. Therefore, the multisection induces an open book decomposition on ∂X with page Σ_∂.

We fix once and for all a multisected 4–manifold $X = \cup_{1 \leq i \leq n} X_i$ and set $C_i = X_i \cap X_{i+1}$, $\Sigma = \cap_i X_i$. We also fix a homomorphism $\varphi : \mathbb{Z}[\pi_1(X)] \to R$ where R is a commutative ring.

Definition 8.3. Let C be a compression body. A *defining collection of disks* for C is a collection $\mathcal{D}$ of disks properly embedded in C such that $C \setminus \eta(\mathcal{D})$ is a thickening of $\partial_- C$ (for instance the co-core disks of the 1–handles in the definition). The boundary $\partial \mathcal{D} \subset \partial_+ C$ is a *defining collection of curves* for C.

Definition 8.4. A *diagram* of the multisection $X = \cup_{1 \leq i \leq n} X_i$ is a tuple $(\Sigma; c_1, \ldots, c_n)$ where c_i is a defining collection of curves for C_i.

A multisection diagram determines a unique smooth 4–manifold [CGPC18b]. The structure of the X_i gives some constraints on the curves of a multisection diagram. For each i, X_i is obtained from a thickened $\partial_- X_i$ by attaching 1–handles, so that $\partial_+ X_i \cong (S^2 \times S^1)^{\sharp k} \#(\# \partial_- X_i)$, where k is the number of 1–handles in excess of the minimum required to connect $\partial_- X_i$ and $\# \partial_- X_i$ is the connected sum of all components of $\partial_- X_i$. Now Definition 8.2 implies that $C_{i-1} \cup_\Sigma C_i$ is a sutured Heegaard splitting of $\partial_+ X_i$, so that the Heegaard diagram $(\Sigma; c_{i-1}, c_i)$ is always handleslide-diffeomorphic to a standard diagram as represented in Figure 34.

8.2 Twisted homology and torsion

8.2.1 Absolute homology and torsion of 4–manifolds with boundary

We shall derive chain complexes for the twisted homology groups $H_*^\varphi(X)$, assuming that $\partial X \neq \emptyset$. In particular, $\partial \Sigma \neq \emptyset$.

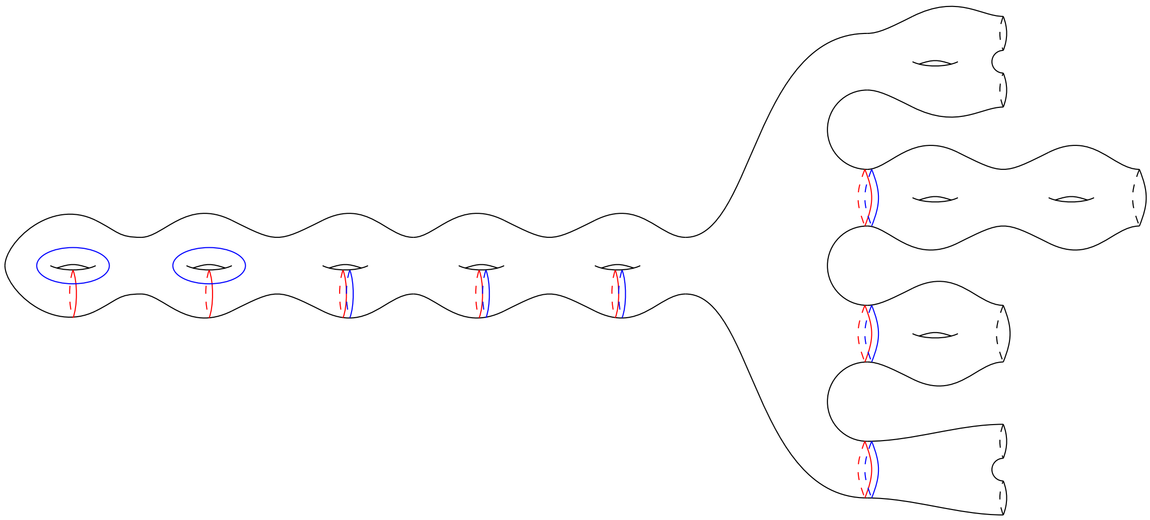

Figure 34: Heegaard diagram for $C_{i-1} \cup C_i$
In this example, C_{i-1} and C_i are constructed with eight 1–handles and X_i with six 1–handles. The manifold X has four boundary components. The components of the page Σ_∂ have a pair (genus, number of boundary components) equal to $(1,2)$, $(2,1)$, $(1,1)$ and $(0,2)$.

Given a hyper compression body V, a *defining collection of balls* for V is a collection $\mathcal{B}$ of 3–balls properly embedded in V such that $V \setminus \eta(\mathcal{B})$ is a thickening of $\partial_- V$. If defining collections $\mathcal{D}_i$ and $\mathcal{B}_i$ of disks and balls have been chosen for all $1 \leq i \leq n$, it turns out that the manifold X retracts onto $\Sigma \cup \mathcal{B} \cup \mathcal{D}$, where $\mathcal{D} = \cup_{i=1}^n \mathcal{D}_i$ and $\mathcal{B} = \cup_{i=1}^n \mathcal{B}_i$. It follows that the quad $(X, Y, \Sigma, *)$ deformation retracts on a CW–complex (Z_3, Z_2, Z_1, Z_0), where $Z_0 = *$, Z_1 is a bouquet of loops defining a basis of $H_1(\Sigma)$, $Z_2 = Z_1 \cup \mathcal{D}$, and $Z_3 = Z_2 \cup \mathcal{B}$. This provides a first complex giving the twisted homology and the torsion of X, as follows.

$$0 \to H_3^\varphi(X, Y) \to H_2^\varphi(Y, \Sigma) \to H_1^\varphi(\Sigma, *) \to H_0^\varphi(*) \qquad (\mathcal{C}')$$

Now, we let L_i^φ denote the submodule of $H_1^\varphi(\Sigma, *)$ generated by the twisted homology classes of the components of c_i. These allow to rewrite the above complex in terms of the homology of the surface Σ and these submodules. More precisely, we have $H_2^\varphi(C_i, \Sigma) \cong L_i^\varphi$ and $H_3^\varphi(X_i, C_{i-1} \cup C_i) \cong L_{i-1}^\varphi \cap L_i^\varphi$ for all i and we finally obtain the following result.

Theorem 8.5 ([14, Theorem 3.9]). *The twisted homology of X is given by the chain complex of free modules*

$$0 \to \bigoplus_{i=1}^n (L_{i-1}^\varphi \cap L_i^\varphi) \xrightarrow{\partial_2} \bigoplus_{i=1}^n L_i^\varphi \xrightarrow{\partial_1} H_1^\varphi(\Sigma, *) \xrightarrow{\partial_0} H_0^\varphi(*) \qquad (\mathcal{C})$$

where $\partial_2\big((x_i)_{1\leq i\leq n}\big) = (x_i - x_{i+1})_{1\leq i\leq n}$ and $\partial_1\big((x_i)_{1\leq i\leq n}\big) = \sum_{i=1}^n x_i$. Moreover, if R is a field, there is an explicit complex basis c of $\mathcal{C}$ such that $\tau^\varphi(X; h) = \tau(\mathcal{C}; c, h)$ for any homology basis h of X and $\mathcal{C}$.

8.2.2 Relative homology and torsion

The computation of the homology of $(X, \partial X)$ ends up being formally similar to that of X, except that minor complication arises from the fact that we need to puncture X.

We introduce a relative version of defining collections of disks and balls.

Definition 8.6. Let C be a lensed compression body. An *r–defining collection of disks* for C is a disjoint union $\mathcal{D}^r$ of disks, with boundary in $\partial_+ C$ or made of an arc in $\partial_+ C$ and an arc in $\partial_- C$, such that $C \setminus \eta(\mathcal{D}^r)$ is a 3–ball. The intersection with $\partial_+ C$ of an r–defining collection of disks for C is a *complete collection of arcs and curves* for C.

Likewise if V is a hyper compression body then an *r–defining collection of balls* for V is a union of 3–balls $\mathcal{B}^r$ such that $V \setminus \eta(\mathcal{B}^r)$ is a 4–ball.

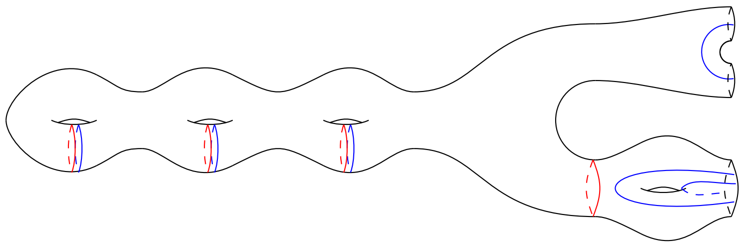

Figure 35: Curves on $\partial_+ C$ for a compression body C

A defining collection of curves for C is represented in red; this defines the compression body C.

A complete collection of arcs and curves for C is represented in blue.

For all $Z \subset X$, let $Z' = Z \setminus \eta(*)$. Fixing r–defining collections $\mathcal{D}_i^r$ and $\mathcal{B}_i^r$ of disks and balls for C_i and X_i respectively, we have a retraction of the manifold X' onto $\Sigma' \cup \mathcal{D}^r \cup \mathcal{B}^r \cup \partial X$, where $\mathcal{D}^r = \cup_{i=1}^n \mathcal{D}_i^r$ and $\mathcal{B}^r = \cup_{i=1}^n \mathcal{B}_i^r$. Further, the quad $(X', Y' \cup \partial X, \Sigma' \cup \partial X, \partial X)$ deformation retracts rel ∂X onto a CW–complex $(Z_3^\partial \cup \partial X, Z_2^\partial \cup \partial X, Z_1^\partial \cup \partial X, \partial X)$, where Z_1^∂ is a collection of arcs and loops on Σ' definind a basis of $H_1(\Sigma, \partial\Sigma)$, $Z_2^\partial = Z_1^\partial \cup \mathcal{D}^r$, $Z_3^\partial = Z_2^\partial \cup \mathcal{B}^r$. We deduce that the homology of $(X, \partial X)$ is given by the chain complex

$$H_4^\varphi(X, X') \to H_3^\varphi(X', Y' \cup \partial X) \to H_2^\varphi(Y', \Sigma' \cup \partial Y) \to H_1^\varphi(\Sigma', \partial\Sigma) \to 0. \qquad (\mathcal{C}'_\partial)$$

Let $\mathcal{J}_i^\varphi$ denote the subgroup of $H_1^\varphi(\Sigma', \partial\Sigma)$ generated by any complete collection of arcs and curves for C_i on Σ'. Using the above chain complex, we get the following.

Theorem 8.7 ([14, Theorem 4.9])**.** *The twisted homology of $(X, \partial X)$ is given by the chain complex of free modules*

$$H_2^\varphi(\Sigma, \Sigma') \xrightarrow{\partial_3} \bigoplus_i \mathcal{J}_{i-1}^\varphi \cap \mathcal{J}_i^\varphi \xrightarrow{\partial_2} \bigoplus_i \mathcal{J}_i^\varphi \xrightarrow{\partial_1} H_1^\varphi(\Sigma', \partial\Sigma) \to 0 \qquad (\mathcal{C}_\partial)$$

where $\partial_3\big([\Sigma]\big) = \big([\partial(\Sigma \setminus \Sigma')]\big)_{1 \le i \le n}$, $\partial_2\big((x_i)_{1\le i\le n}\big) = (x_i - x_{i+1})_{1 \le i \le n}$ and $\partial_1\big((x_i)_{1 \le i \le n}\big) = \sum_{i=1}^n x_i$. Moreover, if R is a field, there is an explicit complex basis c of $\mathcal{C}_\partial$ such that $\tau^\varphi(X, \partial X; h) = \tau(\mathcal{C}_\partial; c, h)$ for any homology basis h of $(X, \partial X)$ and $\mathcal{C}_\partial$.

8.2.3 Homology and torsion of closed 4–manifolds

When X is closed, the computation of the twisted homology and torsion mainly follows the lines of the computation of relative homology, since we need again to puncture X. However, it mixes some features of the absolute and relative cases. For instance, when X is closed, r–defining collections of disks and balls are the same as ordinary defining collections.

We fix $\star \in \Sigma$; for $Z \subset X$, we set $Z' = Z \setminus \eta(\star)$ and we fix $* \in \partial\Sigma'$. Let $\mathcal{D}$ and $\mathcal{B}$ be unions of defining collections of disks and balls for the C_i and the X_i respectively. It turns out that the quad $(X', Y', \Sigma', *)$ deformation retracts onto a CW–complex (Z_3, Z_2, Z_1, Z_0), where $Z_0 = *$, Z_1 is made of loops on Σ' defining a basis of $H_1(\Sigma)$, $Z_2 = Z_1 \cup \mathcal{D}$, $Z_3 = Z_2 \cup \mathcal{B}$. Subsequently, the homology of X is given by the chain complex

$$H_4^\varphi(X, X') \to H_3^\varphi(X', Y') \to H_2^\varphi(Y', \Sigma') \to H_1^\varphi(\Sigma', *) \to H_0^\varphi(*). \qquad (\overline{\mathcal{C}}')$$

Now, L_i^φ denotes the submodule of $H_1^\varphi(\Sigma', *)$ generated by the homology classes of the curves in c_i. The homology of X is finally given by the following.

Theorem 8.8 ([14, Theorem 6.4])**.** *If X is closed, the twisted homology of X is given by the chain complex*

$$H_2^\varphi(\Sigma, \Sigma') \xrightarrow{\partial_3} \bigoplus_i (L_{i-1}^\varphi \cap L_i^\varphi) \xrightarrow{\partial_2} \bigoplus_i L_i^\varphi \xrightarrow{\partial_1} H_1^\varphi(\Sigma', *) \to H_0^\varphi(*) \qquad (\overline{\mathcal{C}})$$

where $\partial_3\big([\Sigma]\big) = \big([\partial\Sigma']\big)_{1\le i\le n}$, $\partial_2\big((x_i)_{1\le i\le n}\big) = (x_i - x_{i+1})_{1\le i\le n}$ and $\partial_1\big((x_i)_{1\le i\le n}\big) = \sum_{i=1}^n x_i$. Moreover, if R is a field, there is an explicit complex basis c of $\overline{\mathcal{C}}$ such that $\tau^\varphi(X; h) = \tau(\overline{\mathcal{C}}; c, h)$ for any homology basis h of X and $\overline{\mathcal{C}}$.

8.3 Intersection forms

The expression of the homology of the 4–manifold X provided by the above complexes allows to realize the elements of the second homology groups by somehow explicit chains in the multisected manifold. These can be arranged to meet pairwise on copies of the central surface Σ, reducing their intersection to intersections of curves on Σ.

More precisely, we consider the manifold X with its multisection structure, as described in Section 7.2, see Figure 36. Given an element $h_1 = (x_1, \dots, x_n) \in \oplus_i L_i^\varphi$ in the kernel of ∂_1, construct a 2–chain in X with a copy of x_i at each point of a ray corresponding to the handlebody C_i, glued to surfaces in the C_i and a 2–chain on Σ whose boundary represents the sum of the x_i, see the left hand side of Figure 36. Given another element $h_2 = (y_1, \dots, y_n)$ in $\oplus_i L_i^\varphi$ or $\oplus_i \mathcal{J}_i^\varphi$, depending whether X is closed, perform a similar construction, slightly perturbing the rays as shown in Figure 36, right hand side. Now the intersections of our two 2–cycles occur along a finite number of copies of Σ, providing the expression in the theorem below. Here we a priori work with the non-twisted homology, but the construction lifts to the covering associated with φ, making the result general; this is mainly due to the fact that the diagram curves, which generate the L_i^φ, are homotopically trivial in X, so that they lie in the kernel of φ.

In [14], following [11] (see also [FKSZ18]), an expression for the intersection form on the second homology is obtained in terms of the intersection form on Σ. Stricly speaking, in the closed case, this latter intersection form is defined on $H_1^\varphi(\Sigma', *_1) \times H_1^\varphi(\Sigma', *_2)$ for two distinct basepoints $*_1$ and $*_2$ on $\partial\Sigma'$.

Theorem 8.9 ([14, Theorems 5.1 & 6.6])**.** *Assume X is closed (resp. $\partial X \neq \emptyset$). Suppose $h_1 = [(x_i)_{1\le i\le n}]$ and $h_2 = [(y_i)_{1\le i\le n}]$ in $H_2^\varphi(X)$ (resp. $h_2 \in H_2^\varphi(X, \partial X)$), where $(x_i)_{1\le i\le n}, (y_i)_{1\le i\le n} \in \oplus_i L_i^\varphi$ (resp. $(y_i)_{1\le i\le n} \in \oplus_i \mathcal{J}_i^\varphi$). Then*

$$\langle h_1, h_2 \rangle_X^\varphi = \sum_{1\le i<j\le n} \langle x_i, y_j \rangle_\Sigma^\varphi$$

where here $\langle\cdot,\cdot\rangle_X^\varphi$ and $\langle\cdot,\cdot\rangle_\Sigma^\varphi$ are the equivariant intersection forms on $H_2^\varphi(X)$ and $H_1^\varphi(\Sigma', *)$ (resp. on $H_2^\varphi(X) \times H_2^\varphi(X, \partial X)$ and $H_1^\varphi(\Sigma, *) \times H_1^\varphi(\Sigma', \partial\Sigma)$).

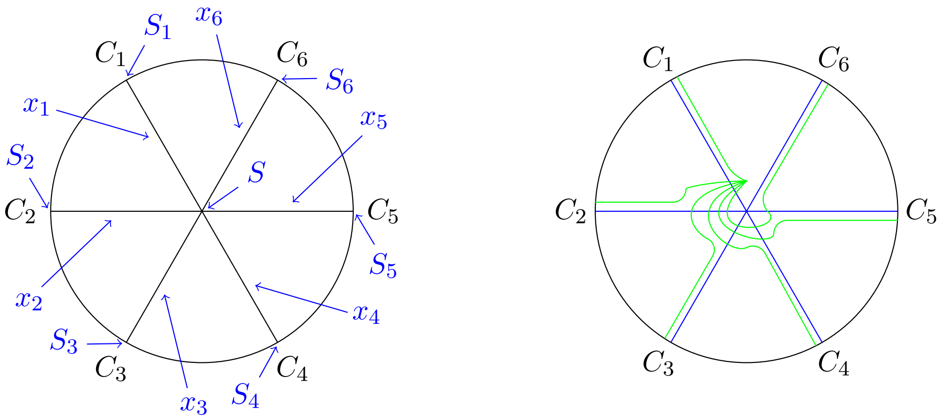

Figure 36: Representing and intersecting 2–cycles

The disks represent $\Sigma \times D^2$ with $2, 3, 4$–handles glued along $\Sigma \times S^1$ in order to complete the C_i and X.

The S_i are surfaces filling the x_i and S is a 2–chain filling the sum of the x_i.

On the right hand side, the blue lines represent x and the green lines represent y.

One may wonder if this expression of the intersection form, possibly restricting to trisections, can be used to reprove Donaldson's theorem on the intersection form of smooth simply-connected 4–manifolds via a combinatorial proof, using elementary tools.

Problem 8.10. *Use the expression of a smooth* 4*–manifold intersection form from a trisection diagram to reprove that any definite intersection form of a smooth simply-connected* 4*–manifold is diagonalizable.*

9 Multisections of higher-dimensional smooth manifolds

9.1 Definition

Beyond Heegaard splittings of 3–manifolds and trisections of smooth 4–manifolds, it is natural to ask whether a similar decomposition can be provided in higher dimensions. In [RT20], Rubinstein and Tillmann proposed an answer to this question in the case of closed PL manifolds. Working on triangulations, they proved that PL manifolds of any dimension $n \geq 2$ can be decomposed into $\lfloor \frac{n}{2} \rfloor + 1$ pieces that are n–dimensional handlebodies. In dimension 4, they recover for PL manifolds a similar decomposition as the Gay–Kirby trisections. Nevertheless, in higher dimensions, their construction does not present a structure as strong as the trisections one. The condition on the intersections of subcollections of the pieces is weaker: they do not need to be handlebodies and the central manifold is not a closed surface. In particular, there is a priori no hope to define 2–dimensional diagrams of such multisections.

We now propose a notion of n–section for higher-dimensional smooth manifolds which strengthens the analogy with Heegaard splittings and trisections.

Definition 9.1. An *n–section* or *multisection* of a closed smooth $(n+1)$–manifold W is a decomposition $W = \cup_{i=1}^{n} W_i$ such that:

- for $\emptyset \subsetneq I \subsetneq \{1, \dots, n\}$, $W_I = \cap_{i \in I} W_i$ is an $(n + 2 - |I|)$–dimensional handlebody,
- $\cap_{1 \leq i \leq n} W_i$ is a closed surface.

The k–*spine* of the multisection is the union $\cup_{|I|=n-k+2} W_I$ of the k–dimensional pieces.

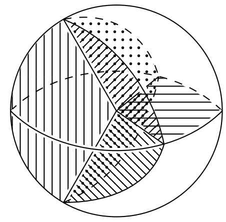

Figure 37: A schematic 4–section of a smooth 5–manifold
The four rays represent the 3–dimensional pieces intersecting along the central surface. They define six 2–dimensional sectors, corresponding to the 4–dimensional pieces, that divide the whole into four pieces.

Remark 9.2.

- It should be noted that the W_I cannot be all simultaneously diffeomorphic to a handlebody. We deal here with manifolds with corners, requiring that their canonical smoothing is diffeomorphic to a handlebody.
- The definition enjoys the following inductive property: for each I, the manifold ∂W_I has a natural $(n - |I|)$–section given by the W_J for $J = I \cup \{j\}$, $j \notin I$.
- A 1–section is a trivial decomposition. A 2–section is a Heegaard splitting and a 3–section is a trisection in the sense of Gay–Kirby.
- Definition 9.1 extends to the PL setting by replacing smooth submanifolds by PL submanifolds and diffeomorphisms by PL homeomorphisms everywhere.

Example 9.3. The sphere S^{n+1} admits a genus–0 multisection where each W_I has genus 0. The product $S^n \times S^1$ admits a genus–1 multisection where each W_I has genus 1.

9.2 Multisection diagrams

Given an n–section $\mathcal{M}$ of a smooth $(n+1)$–manifold W as above, denote $\Sigma = \cap_{1\leq i\leq n} W_i$ the central surface and choose for all $i \in \{1, \ldots, n\}$ a cut system $(\alpha^i_j)_{1\leq j\leq g}$ for the 3–dimensional handlebody $\cap_{k\neq i} W_k$. Then $(\Sigma; \alpha^1, \ldots, \alpha^n)$ is an n–*section diagram* for $(W, \mathcal{M})$. This is not unique, but it is well-known that each system of curves $(\alpha^i_1, \ldots, \alpha^i_g)$ is unique up to handleslides. Hence the n–section diagram associated to a multisected manifold is unique up to handleslides (performed independently in each family α^i).

Definition 9.4. An *abstract n–section diagram* is a genus–g closed surface Σ with n families of g disjoint simple closed curves, such that any subcollection of $k \in \{2, \ldots, n\}$ of these families is a k–section diagram for a multisection of a connected sum of copies of $S^1 \times S^k$.

The immediate questions about diagrams are those of realizability of a given abstract n–section diagram and uniqueness of the associated manifold. The collection of curves in an abstract n–section diagram tells us how to glue the 3–dimensional handlebodies $\cap_{k\neq i} W_k$ to the central surface $\Sigma = \cap_k W_k$. A priori, we have no information on how to glue the higher-dimensional pieces. However, Laudenbach–Poénaru [LP72] have shown that any diffeomorphism of the boundary of 4–dimensional handlebody H extends to a diffeomorphism of H. This shows that there is only one way to glue the 4–dimensional pieces. In [Mon79], Montesinos proved the analogous result for PL 4–manifolds. In higher dimension, the following result is due to Cavicchioli and Hegenbarth [CH93, Proposition 3.2] and relies on surgery theory.

Theorem 9.5 (Laudenbach–Poénaru, Montesinos, Cavicchioli–Hegenbarth)**.** *If H is an n–dimensional handlebody with $n \geq 4$, any PL homeomorphism of ∂H extends to a PL homeomorphism of H. This also holds for diffeomorphisms if $4 \leq n \leq 6$.*

Now, if an abstract n–section diagram is given on a surface Σ, we can prove by induction on the dimension that it defines a unique multisected $(n+1)$–manifold. First, we take the product $\Sigma \times D^{n-1}$. At n distinct points of ∂D^{n-1}, we glue tickened 3–dimensional handlebodies. Each pair of such handlebodies defines a connected sum of some $S^1 \times S^2$'s. We glue a thickened 4–dimensional handlebody to it and continue the process up to dimension $n+1$. At each step, the conditions of Definition 9.4 and the uniqueness of the manifold associated with a given diagram ensure that the $(k+1)$–manifolds appearing on the boundary are connected sums of $S^1 \times S^k$'s. Then the above result tells us that there is a unique way to glue the next pieces. We conclude as follows.

Theorem 9.6 ([16])**.**

- *For $n \leq 6$, any abstract n–section diagram is the diagram of some smooth multisected $(n+1)$–manifold, which is unique up to multisection preserving diffeomorphism if $n \leq 5$.*
- *For arbitrary n, any abstract n–section diagram is the diagram of some PL multisected $(n+1)$–manifold which is unique up to multisection preserving PL homeomorphism.*

The uniqueness part of the result is optimum. Indeed, for $n \geq 6$, exotic $(n+1)$–spheres are known to be twisted spheres, so that they admit genus–0 n–sections; hence they all admit the 2–sphere as an n–section diagram.

From dimension 8, it is known that there exist PL manifolds that do not admit any smooth structure. If such manifolds can be multisected, then their multisection diagrams cannot be realized by a smooth manifold.

9.3 Stabilizations and genus–1 multisections

The stabilization move along an arc that occurs for Heegaard splittings and trisections naturally generalizes to higher-dimensional multisections. In dimension 5 and higher, we need introduce higher order stabilization moves, not only along arcs, but also along higher-dimensional disks.

A *half-disk* is a disk Δ whose boundary $\partial\Delta$ is piecewise smooth and decomposed in two disks $\partial_-\Delta$ and $\partial_+\Delta$ which intersect precisely along their boundary. If Δ is one-dimensional, then $\partial_-\Delta = \emptyset$. A half-disk Δ in a manifold with boundary W is *standard* if $\Delta \cap \partial W = \partial_-\Delta$ and Δ is transverse to ∂W. Note that if $\partial W = \emptyset$, then Δ is necessarily one-dimensional. A half-disk $\Delta \subset W_I$ in a multisected manifold W is *standard* if for all $J \supset I$, $\Delta_J = \Delta \cap W_J$ is standard in W_J. A disk $D \subset W_I$ in a multisected manifold is *boundary parallel* if there is a standard half-disk $\Delta \subset W_I$ with $\partial_+\Delta = D$.

A tubular neighborhood N of a boundary parallel disk $D \subset W_I$ is in *good position* if it can be written $N = D \times D'$ where D' is a disk of dimension $|I|+1$ endowed with its standard $|I|$–section (with indexing set I) in such a way that for all non-empty $J \subset \{1, \dots, n\}$,

$$N \cap W_J = (D \cap W_{I \cup J}) \times D'_{I \cap J}.$$

Definition 9.7. Let I be a non-empty proper subset of $\{1,\dots,n\}$, $D \subset W_I$ a codimension 2 boundary parallel disk together with a tubular neighborhood $N = D \times D'$ in good position. The *I–stabilization* of the multisection is defined by removing the interior of $D \times D'_i$ from W_i if $i \in I$ and adding $D \times D'$ to W_i for some $i \notin I$.

The I–stabilization move is well-defined: any two boundary parallel disks in W_I are isotopic, any two tubular neighborhoods in good position are isotopic, and different choices of the W_i to which we add $D \times D'$ result in isotopic multisections. Moreover, there is the following duality: the results of an I–stabilization and of a $(\{1,\dots,n\} \setminus I)$–stabilization are isotopic.

Proposition 9.8 ([16])**.** *For a multisection $W = \cup_{i=1}^n W_i$, the result of an I–stabilization move is again a multisection. Furthermore, the genus of W_J is increased by 1 if $J \supset I$ or $J \supset I^c$, and else remains the same.*

Corollary 9.9. *The I–stabilization has the following effect on the induced multisection of ∂W_J:*

- *a connected sum with the genus–1 multisection of $S^1 \times S^{n-|J|}$ if $J \supset I$ or $J \supset I^c$,*
- *an $(I \cup J)$–stabilization on $W_{I \cup J}$ else.*

As can be expected, these moves correspond to the genus–1 multisections of the spheres. For $0 < k < n$, the $(n+1)$–sphere can be decomposed as

$$S^{n+1} = \partial\big(B^{k+1} \times B^{n-k+1}\big) = \big(S^k \times B^{n-k+1}\big) \cup \big(B^{k+1} \times S^{n-k}\big).$$

We further decompose S^k into disks as $S^k = \cup_{i=1}^k B_i$ so that each subcollection of the B_i intersects along a disk and $\cap_{i=1}^k B_i$ is a circle, and S^{n-k} similarly. This provides a multisection of S^{n+1} with a multisection diagram made of two groups of k and $(n-k)$ parallel curves respectively, where two curves from distinct groups meet at exactly one point, see the right hand side two diagrams in Figure 38 for $n = 4$ and $k = 1, 2$. Similarly, decomposing S^n into disks gives a genus–1 multisection of $S^1 \times S^n$ whose diagram is given by n parallel curves, as in the left hand side of Figure 38. For $n \geq 4$, in a genus–1 multisection diagram, the subdiagrams defined by three curves have to be diagrams for S^4 or $S^1 \times S^3$; it follows that these are the only possibilities.

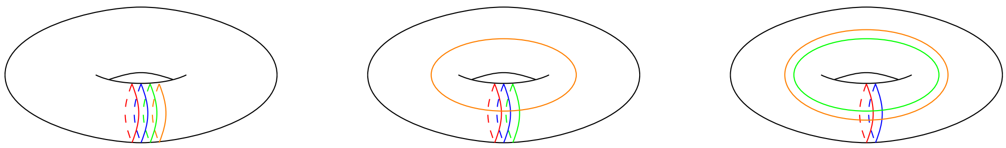

$S^1 \times S^4$ $\qquad$ S^5 $\qquad$ S^5

Figure 38: Genus–1 quadrisection diagrams

The I–stabilization move defined above can be performed by connect-summing with the genus–1 multisection of S^{n+1} defined here for $k = |I|$.

9.4 Existence in dimension five and perspectives

The study of existence and uniqueness of multisections for smooth manifolds relies on Morse functions and Cerf theory. On a closed smooth manifold, there exists an ordered Morse function, meaning that the critical points have distinct values and these values increase with the index of the critical point. Given such an ordered Morse function on a 3–manifold M, the preimage of a regular value separating the critical points of index 1 and 2 is a Heegaard surface.

In [LCM21], Lambert-Cole and Miller give a similar proof of existence in dimension 4, adapting the Gay–Kirby proof using handle decompositions. Given a 4–manifold X and an ordered Morse function f on X, let c_1 and c_2 be values separating the critical points of index 1 and 2, and 2 and 3 respectively. Let X_1 be the sublevel set defined by c_1, see Figure 39. Let $L \subset \partial X_1$ be the attaching link of the 2–handles defined by the critical points of index 2. A Heegaard splitting $\partial X_1 = X_{12} \cup X_{23}$ can be chosen such that L is contained in the core of X_{12}. Then define X_2 as X_{12} pushed along the flow between the values c_1 and c_2 and define X_3 accordingly. This provides a trisection of X.

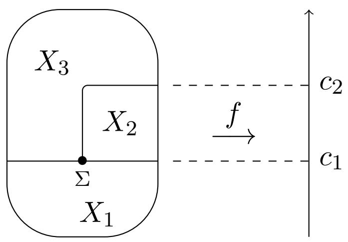

Figure 39: Trisecting a 4–manifold

In dimension 5, there are two approaches to prove the existence of a quadrisection from an ordered Morse function, namely “from the middle” or “from the bottom”. We start with the former. Let W be a 5–manifold and f an ordered Morse function of W. For $i = 1, 2, 3$, let c_i be a value separating the critical points of index i and $i+1$. In the middle level $f^{-1}(c_2)$, we have two links of 2–spheres L_2^+ and L_3^- defined as the intersection of $f^{-1}(c_2)$ with the ascending (resp. descending) manifolds of the critical points of index 2 (resp. index 3). Refining the above construction in dimension 4, one can construct a quadrisection of $f^{-1}(c_2)$, in the sense of Islambouli–Naylor, adapted to L_2^+ and L_3^- in the following sense. We build a quadrisection $f^{-1}(c_2) = W_{13} \cup W_{23} \cup W_{24} \cup W_{14}$ such that $W_{23} \cup W_{24}$ (resp. $W_{13} \cup W_{23}$) is obtained from a neighborhood of L_2^+ (resp. L_3^-) by adding $0, 1$–handles. Now define W_3 by pushing $W_{13} \cup W_{23}$ along the flow between c_2 and c_3, and similarly W_2 by pushing $W_{23} \cup W_{24}$ between c_2 and c_1. Finally let W_1 (resp. W_4) be “what remains below c_2” (resp. above c_2).

Alternatively, one can first trisect the bottom level $f^{-1}(c_1) = W_{12} \cup W_{13} \cup W_{14}$ in a way adapted to the descending links of the critical points of index 2 and 3, in particular such that the attaching link L_2^- is contained in the core of W_{12}. Then define W_2 as the trace of W_{12} from c_1 to c_2. This gives a decomposition of the level $f^{-1}(c_2)$ with two pieces isotopic to W_{13} and W_{14} and one obtained from W_{12} by surgery. The latter one has to be cut in two pieces in order to obtain a quadrisection of $f^{-1}(c_2)$ as described above (some stabilizations may be necessary here). We complete the quadrisection as above.

These two methods provide the following result.

Theorem 9.10 ([16])**.** *Any closed smooth 5–manifold admits a quadrisection.*

In dimension 5, the first construction might be simpler. Nevertheless, working in an arbitrary dimension, it seems that it does not help to start the process at a middle level. Our attempts to prove existence in higher dimensions follow the second construction.

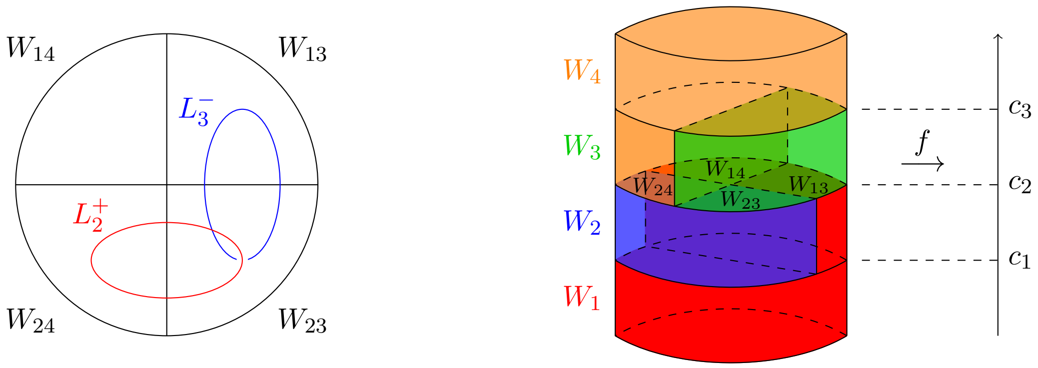

The middle level $f^{-1}(c_2)$ Morse function and quadrisection

Figure 40: Quadrisecting a 5–manifold

Problem 9.11. *Prove that any smooth manifold, of dimension* 3 *or more, admits a multisection.*

We also investigate an alternative approach, based on bridge multisections. A knot in a Heegaard splitting is in a *bridge position* if it intersects each handlebody along a boundary parallel tangle (a disjoint union of properly embedded arcs simultaneously boundary parallel). It is known that any knot in a 3–manifold with a given Heegaard splitting can be isotoped into a bridge position. In [MZ18], Meier and Zupan developed an analogous notion for surfaces in trisected 4–manifolds, called *bridge trisections*, and proved the analogous result. The notion naturally generalizes to higher dimensions. We shall say that an $(n-1)$–submanifold Z in a multisected $(n+1)$–manifold $W = \cup_{i=1}^{n} W_i$ is in a *bridge position* if, for each $\emptyset \subsetneq I \subsetneq \{1, \dots, n\}$, $Z \cap W_I$ is a disjoint union of properly embedded $(n-|I|)$–disks simultaneously boundary parallel.

Problem 9.12. *Prove that any codimension–*2 *submanifold in a multisected manifold can be isotoped into a bridge position, possibly after stabilization.*

To obtain a multisection of a manifold W, we can first construct a *pseudo-multisection*, namely a multisection where the W_I are not required to be handlebodies, but only to be connected and to have the right dimension. This is always possible. Then we want to manipulate the pseudo-multisection in order to remove the extra handles. For this, we may introduce *pseudo-stabilizations*, where we remove to some W_I, and add to some W_j with $j \notin I$, a properly embedded disk in W_I with a neighborhood in good position, but we do not require that the disk is boundary parallel. To perform such pseudo-stabilizations, we need to be able to put the boundary of the disk in good position, which can be reached by isotoping it into a bridge position in ∂W_I.

9.5 Multisecting surface bundles

Surface bundles turn out to admit multisections in any dimension. A multisection of a surface bundle can be obtained from a suitable decomposition of the basis into balls. This generalizes the work of Gay–Kirby [GK04] and Williams [Wil20] on trisections of 4–dimensional surface bundles.

Let M be a closed d–manifold. We call *good ball decomposition* of M a decomposition $M = \cup_{i=0}^d M_i$ where, for all $I \subset \{0, \ldots, d\}$, $\cap_{i\in I} M_i$ is a disjoint union of $(d - |I| + 1)$–balls and $\cup_{i\in I} \left(\cap_{j\in I\setminus\{i\}} M_i\right)$ is connected. Such decompositions do exist. For instance, from a CW–complex structure, define M_0 as a neighborhood of the vertices, M_1 as a neighborhood of the 1–faces in the complement of M_0, and so on.

Let $p : W \to M$ be a surface bundle. Taking the preimage of a good ball decomposition of M, we get a decomposition of W into pieces that are products of a surface, the fibre, with balls. To obtain a multisection from this, we dig some "disk tunnels" into the different pieces, which we add to other pieces. If $Z \subset M$ is a disjoint union of contractible subspaces of M, a *disk section of p over Z* is a neighborhood N of a section of p over Z such that $p^{-1}(z) \cap N$ is a disk for all $z \in Z$.

Proposition 9.13 ([17])**.** *Fix $n > 1$. Let $p : W \to M$ be a surface bundle, where W is a closed $(n+1)$–manifold. Assume we are given a good ball decomposition $M = \cup_{i=1}^n M_i$. For $1 \leq i \neq j \leq n$, fix a disk section N_{ij} of p over M_i, so that the N_{ij} are pairwise disjoint. Set*

$$W_i = \left(\overline{p^{-1}(M_i) \setminus \cup_{j\neq i} N_{ij}}\right) \cup \left(\cup_{j\neq i} N_{ji}\right).$$

Then $W = \cup_{i=1}^n W_i$ is a multisection.

Remark 9.14. It is necessary to dig at least one disk section in each $p^{-1}(M_i)$, but the construction may work in specific examples with less disk sections. The point to check is that each W_I is connected.

We now present some examples, in which we use only one disk section N_i over each M_i and we set $W_i = \left(\overline{p^{-1}(B_i) \setminus N_i}\right) \cup (N_{i+1})$. When the bundle is simply a product, we define the disk sections as $N_i = D_i \times M_i$, where the D_i are disjoint disks on the fiber.

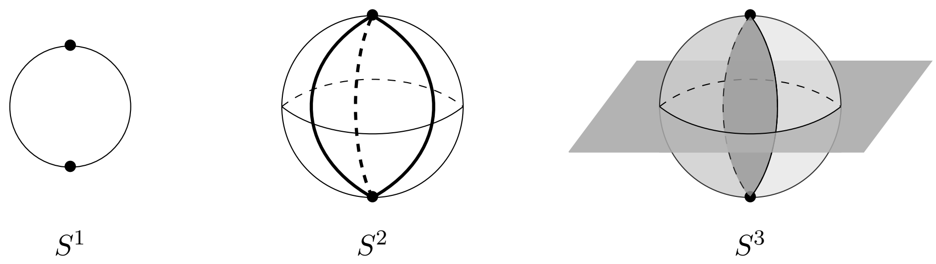

Figure 41: Good ball decomposition of S^k for small k

We start with bundles over spheres. The $n-1$–sphere admits a good ball decomposition $S^{n-1} = \cup_{i=0}^{n-1} B_i$ where $\cap_{i\in I} M_i$ is a single ball for $\emptyset \neq I \subsetneq \{0, \ldots, n-1\}$ and $\cap_{i=0}^{n-1} M_i$ is made of two points, see Figure 41. It can be obtained by projecting S^{n-1} on $\mathbb{R}^{n-1}$, viewing the image B^{n-1} as an $(n-1)$–simplex cut into the cones with vertex its center and bases its faces, and pulling-back this decomposition. If W is a surface bundle over S^{n-1}, the associated multisection has a central surface is given by two copies of the fiber (the preimages of $\cap_{i=0}^{n-1} M_i$) joined by a tube for each edge in the $\cap_{j\neq i} M_j$.

Lemma 9.15. *A surface bundle over S^{n-1} with fiber a closed surface of genus g admits a multisection of genus $2g + n - 1$.*

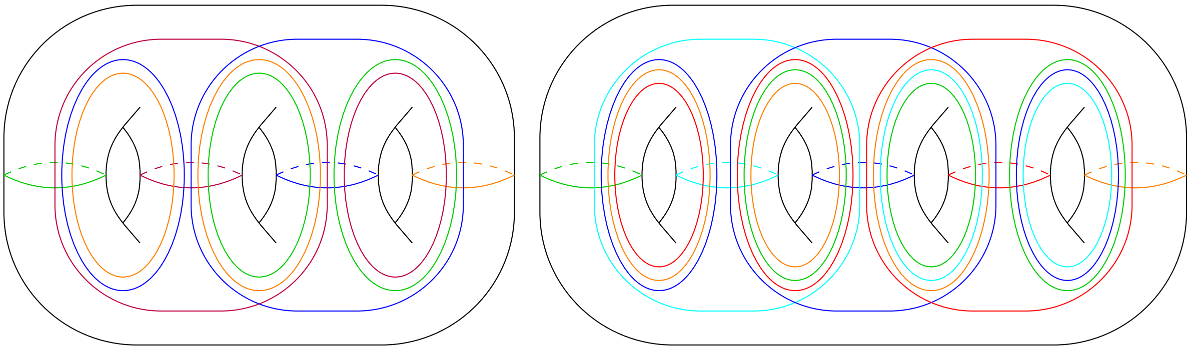

Figure 42: Multisection diagrams for $S^2 \times S^3$ and $S^2 \times S^4$

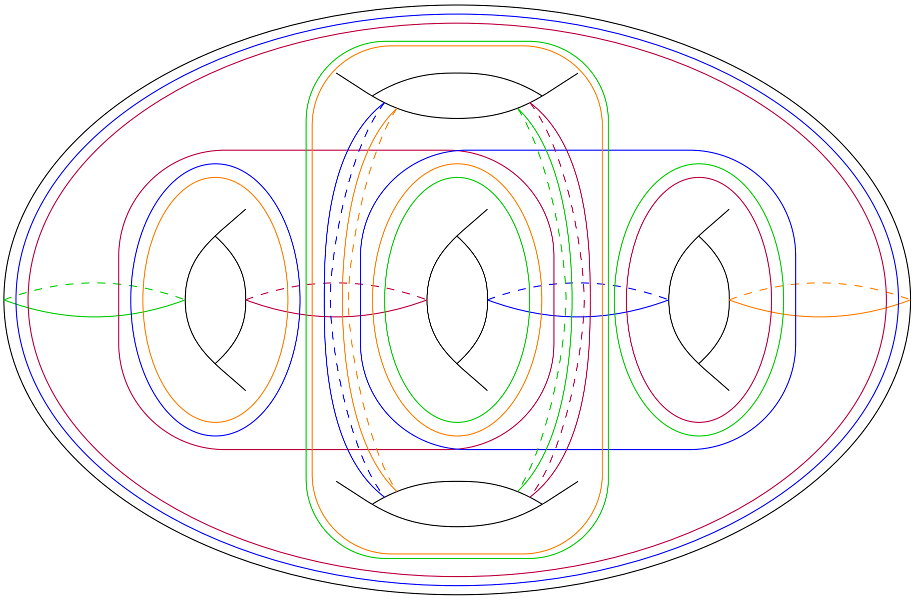

Figure 43: Quadrisection diagram for $S^1 \times S^1 \times S^3$

Examples of the associated diagram are given in Figures 42 and 43.

In dimension 6, we get infinitely many 6–manifolds admitting a 5–section of genus 4, namely the S^2–bundles over S^4. Such a bundle can be constructed by gluing two copies of $S^2 \times B^4$ via a map $\varphi : S^3 \to S0(3)$. Writing S^3 as the quotient of $S^2 \times [0, 2\pi]$ by the shrinking of $S^2 \times \{0\}$ and $S^2 \times \{2\pi\}$, we define a map φ_m that sends (x, t) onto the rotation of axis given by x and angle mt. This defines an S^2–bundle $W(m)$. While $W(-m)$ is diffeomorphic to $W(m)$, the group $\pi_3\big(W(m)\big)$ is finite of order m. To get a simple multisection diagram of $W(m)$, it appears helpful to modify the map φ_m by a homotopy. We write S^3 as $S^2 \times [-1, 2\pi]$ with $S^2 \times \{-1\}$ and $S^2 \times \{2\pi\}$ shrunk, and we define φ_m as previously on $S^2 \times [0, 2\pi]$ and constant equal to the identity on $S^2 \times [-1, 0]$. Taking a good ball decomposition $S^4 = \cup_{1 \le i \le 5} B_i$ as above, we set $B_a = B_1 \cup B_2$ and $B_b = B_3 \cup B_4 \cup B_5$ and we assume that the parametrizations of S^3 as boundary of B_a and B_b are such that:

$$S^3 \cap \partial B_1 = \big(S^2 \times [-1, 0]\big)/\sim \qquad S^3 \cap \partial B_3 = \big(\Delta_3 \times [-1, 2\pi]\big)/\sim$$
$$S^3 \cap \partial B_2 = \big(S^2 \times [0, 2\pi]\big)/\sim \qquad S^3 \cap \partial B_4 = \big(\Delta_4 \times [-1, 2\pi]\big)/\sim$$
$$S^3 \cap \partial B_5 = \big(\Delta_5 \times [-1, 2\pi]\big)/\sim$$

where $S^2 = \Delta_3 \cup \Delta_4 \cup \Delta_5$ is a good ball decomposition of S^2. Now the bundle $W(m)$ is given by the gluing of $S^2 \times B_a$ and $S^2 \times B_b$ via the map $\varphi_m : S^2 \times \partial B_a \to S^2 \times \partial B_b$. We choose D_1 and D_2 as small neighborhoods of the two points in $\Delta_3 \cap \Delta_4 \cap \Delta_5$, and $D_3 \subset \Delta_4$, $D_4 \subset \Delta_5$, $D_5 \subset \Delta_3$ disjoint from $\varphi_m(D_1 \cup D_2)$. This gives explicit disks sections, and a careful analysis of the gluing locus, where all the 3–dimensional handlebodies of the multisection lie, provides the diagram in Figure 44. The only 3–dimensional piece where the gluing is non-trivial is W_{2345}, represented in green.

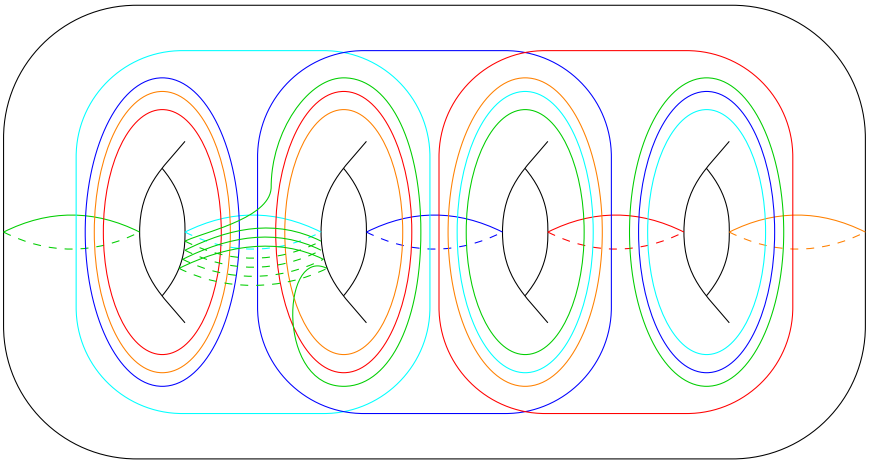

Figure 44: Multisection diagram for the S^2–bundle $W(2)$ over S^4

For a diagram of $W(m)$, the green curve that differs from the diagram of $S^2 \times S^4$ has to turn $2m$ times.

We now give a good ball decomposition of $S^2 \times S^1$. The factor S^2 is cut into two disks; each of these disks product S^1 is then cut into two balls, see Figure 45. In this decomposition $S^2 \times S^1 = \cup_{1 \le i \le 4} M_i$, each M_i is a 3–ball, each M_{ij} is made of two 2–disks, each M_{ijk} is made of four intervals and M_{1234} contains exactly eight points. In the associated quadrisection of a surface bundle over $S^2 \times S^1$, the central surface is made of 8 copies of the fiber joined by 16 tubes.

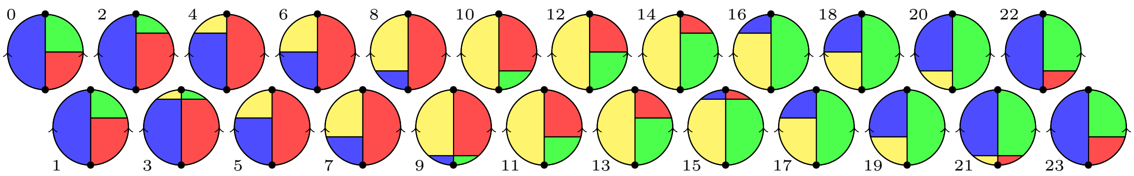

Figure 45: Good ball decomposition of $S^2 \times S^1$: the S^2–slices

Here, S^1 is regarded as $[0, 24]/(0 = 24)$. We represent M_1 in blue, M_2 in yellow, M_3 in red and M_4 in green.

Lemma 9.16. *A surface bundle over $S^2 \times S^1$ admits a quadrisection of genus $8g + 9$, where g is the genus of the fiber.*

In Figure 46, we give a quadrisection diagram for $S^2 \times S^2 \times S^1$. To draw the diagram curves on the genus–9 surface, we need to determine, for each 3–dimensional handlebody of the quadrisection, a family of 9 properly embedded disks that cut the handlebody into a 3–ball. We have

$$W_{123} = \Big((S^2 \setminus (D_1 \cup D_2 \cup D_3)) \times M_{123}\Big) \cup \Big(\partial D_2 \times M_{23}\Big) \cup \Big(\partial D_3 \times M_{13}\Big) \cup \Big(D_4 \times M_{412}\Big).$$

From Figure 45, it can be read that M_{23} (resp. M_{13}) is made of two disks, viewed as one bigon and one hexagon regarding the repartition of their boundaries along M_{123} and M_{234} (resp. M_{123} and M_{341}). Our 9 disks in W_{123} are as follows:

- 4 meridional disks in the four solid tubes composing $D_4 \times M_{412}$,
- the union of:
  - a point in ∂D_2 product with the bigon in M_{23},
  - an arc joining ∂D_1 to ∂D_2 on S^2 product with the relevant interval in M_{123} (the one on the boundary of the bigon in M_{23}),
- the union of:
  - a point in ∂D_2 product with the hexagon in M_{23},
  - an arc joining ∂D_1 to ∂D_2 on S^2 product with the relevant three intervals in M_{123},
- disks analogous to the previous two with ∂D_3 instead of ∂D_2 and M_{13} instead of M_{23},
- an arc joining ∂D_1 to itself around ∂D_2 product with an interval in M_{123} (different from the ones corresponding to the bigons).

The other cut systems are obtained similarly.

We finally present good ball decompositions of the real projective spaces. Using homogeneous coordinates $[x_0 : \cdots : x_n]$ for $\mathbb{RP}^n$, we set $M_i = \{|x_i| \geq |x_j| \mid \forall j\}$. This defines a good ball decomposition of $\mathbb{RP}^n$ where $\cap_i M_i$ is contains 2^n points and each $\cap_{j \neq i} M_i$ is made of 2^{n-1} intervals.

Lemma 9.17. *A surface bundle over $\mathbb{RP}^n$ admits a multisection of genus $2^n g + 2^{n-1}(n-1)+1$, where g is the genus of the fiber.*

This construction may generalized to *relative surface bundles*. Given a k–dimensional submanifold B in a manifold W, the pair (W, B) is a *relative fiber bundle* over M if:

- $W \setminus B$ fibers over M,
- each fiber is the interior of a $(k+1)$–dimensional submanifold $F \subset W$ such that $\partial F = B$.

For instance, relative fiber bundles over S^1 are called open book decompositions.

Problem 9.18. *Adapt the above construction to get multisections of relative surface bundles.*

If M is a sphere, taking the preimage of the good ball decomposition described above (see Figure 41) gives a multisection of W; this works well because there are exactly two vertices and the other pieces are connected.

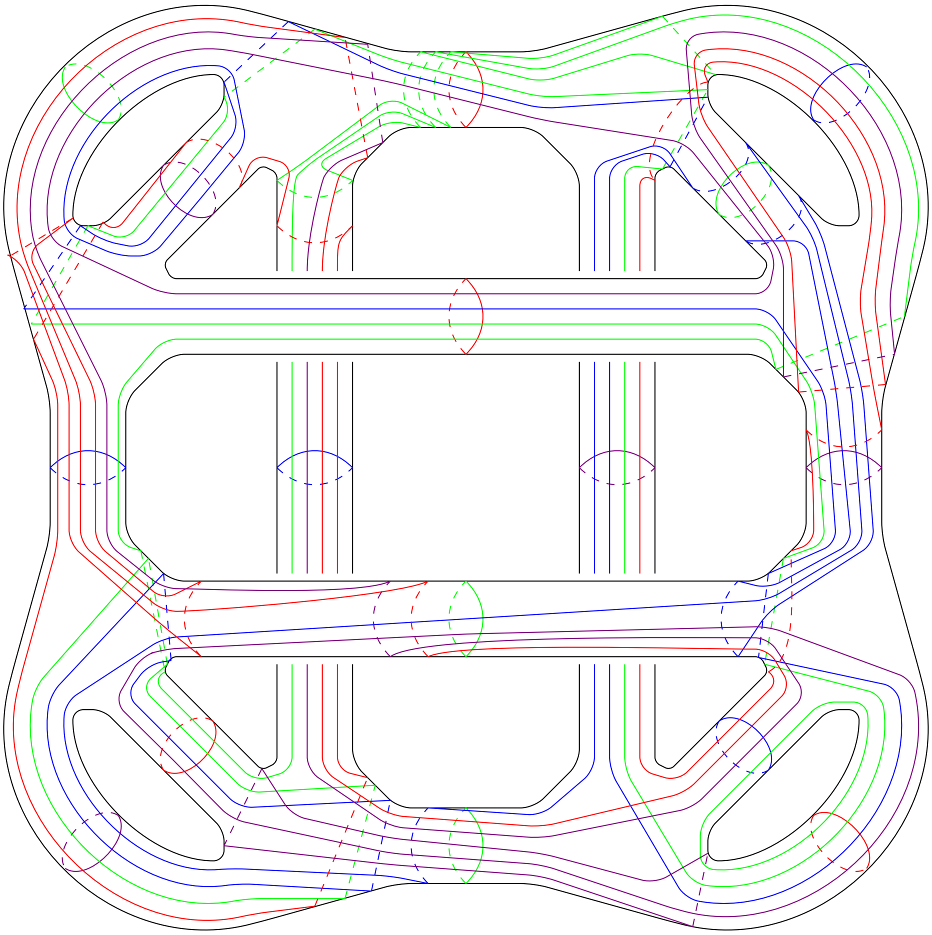

Figure 46: Quadrisection diagram for $S^2 \times S^2 \times S^1$

9.6 Multisecting fiber bundles over the circle

For a closed 3–manifold that fibers over the circle, there is a simple construction of a Heegaard splitting, which is the one described in the previous subsection. It has been generalized to dimension 4 by Gay and Kirby [GK16] and Koenig [Koe21]. A similar construction can indeed be performed in any dimension.

Proposition 9.19 ([17]). *Any fiber bundle over the circle whose fiber admits a multisection globally preserved by the monodromy can be multisected.*

The construction goes as follows. Suppose an $(n+1)$–manifold W fibers over S^1 with fiber a closed n–manifold X and monodromy φ. Assume X admits a multisection $X = \cup_{i=1}^{n-1} X_i$ preserved by φ and denote σ the permutation such that $\varphi(X_i) = X_{\sigma(i)}$. We shall construct a multisection of W using the multisection of X and a decomposition of S^1 into intervals. Via a diffeomorphism $W \cong X \times I/_{(x,0) \sim (\varphi(x),1)}$, we define the W_i in the product $X \times I$.

Assume for simplicity that $n = 4$. There are three cases, depending of the type of σ: identity, transposition or 3–cycle. These are schematized in Figure 47. For instance, when

$\sigma = (123)$, we first set:

$$W_1' = \left(X_1 \times \left[\frac{4}{5}, 1\right]\right) \cup_\varphi \left(X_2 \times \left[0, \frac{3}{5}\right]\right) \qquad W_2' = \left(X_2 \times \left[\frac{3}{5}, 1\right]\right) \cup_\varphi \left(X_3 \times \left[0, \frac{2}{5}\right]\right)$$

$$W_3' = \left(X_3 \times \left[\frac{2}{5}, 1\right]\right) \cup_\varphi \left(X_1 \times \left[0, \frac{1}{5}\right]\right) \qquad W_4' = X_1 \times \left[\frac{1}{5}, \frac{4}{5}\right]$$

At this stage, the W_i' are handlebodies, but their intersections are not. We shall again arrange this by tubing. We say that a 4–ball in X is in *good position* if it is transverse to the X_i, the X_{ij} and the central surface S, and if it intersects each of these pieces along a ball of the corresponding dimension. For each interval in our construction, namely $\left[\frac{i}{5}, \frac{i+1}{5}\right]$ for $i = 1, 2, 3$ and $\left[\frac{4}{5}, 0\right] \cup \left[0, \frac{1}{5}\right]$, we take a tube $B^4 \times I$ made of a 4–ball in good position above each point of the interval, and we add it to the W_i' which doesn't appear above this interval. For instance, a tube above $\left[\frac{2}{5}, \frac{3}{5}\right]$ is removed to $W_1 \cup W_3 \cup W_4$ and added to W_2' to form W_2. This finally defines a quadrisection of W. The central surface Σ is given by four copies of S, above $\frac{i}{5}$ for $i = 1, .., 4$, joined by tubes. The genera of the surfaces are related by $g(\Sigma) = 4g + 1$, where $g = g(S)$. The schemes of Figure 47 show how to apply this construction for other permutations of the trisection of X. The genus of Σ is then given by $5g + 1$ and $6g + 1$ respectively.

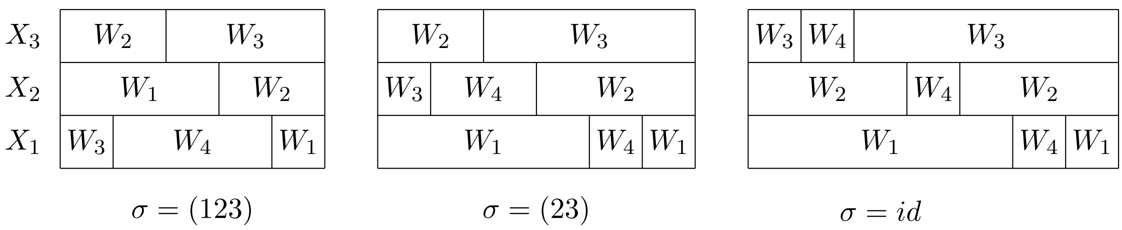

Figure 47: Scheme of the quadrisection of W for different permutations σ

In higher dimensions, the same construction works, as long as we can determine the right scheme. The idea is to use the decomposition of σ into disjoint cycles. Figures 47 and 48 give a model for cycles. Then different cycles can be stacked together as examplified in Figures 47 and 49.

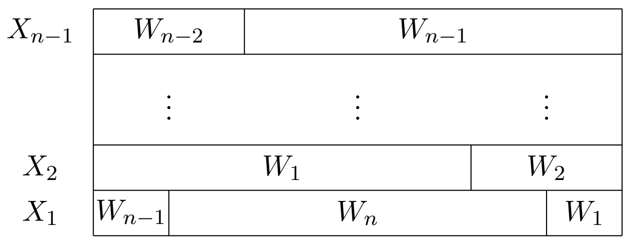

Figure 48: Scheme of the multisection of W for a monodromy inducing a cycle

The genus we obtain for given n and σ is $Ng+1$, where g is the genus of S and N equals the number of cycles in the decomposition of σ (including fixed points as order–1 cycles) plus the sum of the orders of these cycles. In dimension 4, it gives $3g+1$ for the identity and $4g+1$ for the transposition (12). In the latter case, Koenig proved that the obtained trisection can be destabilized to get a genus–$(3g+1)$ trisection. In higher dimensions, some destabilizations can be performed, but the global picture is more intricate. It would be interesting to determine whether it is possible to reach the genus $ng+1$ in all cases.

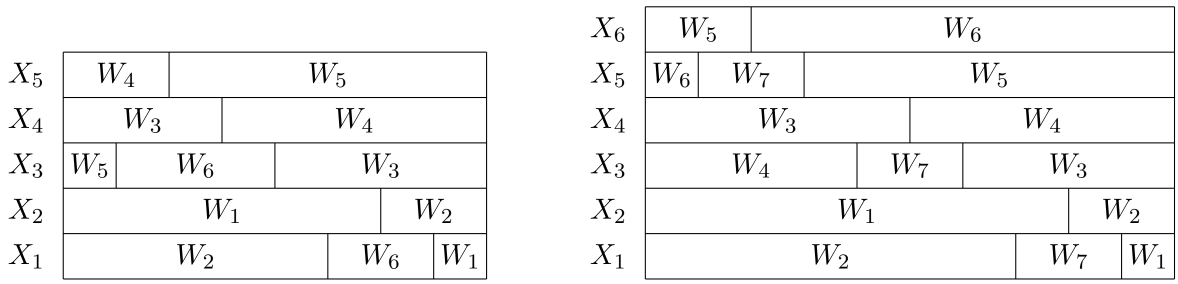

$n=6$ $\sigma=(12)(345)$ $n=7$ $\sigma=(12)(34)(56)$

Figure 49: Other schemes of multisections

We shall explain on the example of $\mathbb{CP}^2\times S^1$ how to draw a diagram of the multisection we have constructed. We start with the diagram of $\mathbb{CP}^2$ given in Figure 32, whose surface is denoted by S, where the red curve represents X_{12}, the blue curve represents X_{23} and the green curve represents X_{13}. We use the alternative scheme given in Figure 50. We draw the surface Σ as $N=6$ copies S_i of S set along a cycle and joined by tubes creating the hole in the middle, see Figure 51. The 3–dimensional handlebodies of the quadrisection are made of copies of the 3–dimensional handlebodies of the trisection of $\mathbb{CP}^2$ and copies of the punctured surface S product an interval, joined by tubes. For instance, in our example, the handlebody W_{124} is made of:

- copies of X_{13} represented by the purple curves on S_1 and S_6,
- the product of a puncture S with an interval running from S_2 to S_3, where the purple curves represent arcs on the punctured S that define disks in the product,
- the same thing between S_4 and S_5,
- the tubes joining the above pieces, to which corresponds a meridian purple curve which could be draw between S_i and S_{i+1} for any $i\neq 2,4$.

The other families of curves are obtained accordingly. If the monodromy φ were non-trivial, then the green curves on S_1/S_6 would have to join arcs on S_6 to their images by φ on S_1. Note that we have to represent the successive copies of S with alternating orientation. The monodromy φ reverses the orientation of S precisely when n is odd.

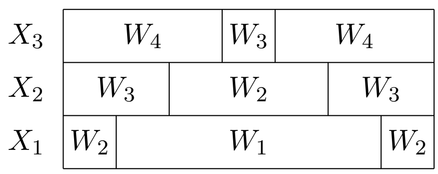

Figure 50: Scheme of a quadrisection of $\mathbb{CP}^2\times S^1$

On this diagram, two destabilizations can be performed. Sliding the orange curve on S_2 along the orange curve on S_1 and the green curve on S_2 along the green curve on S_3, we get parallel green and purple curves dual to parallel blue and orange curves. This allows to destabilize once. The second destabilization is symmetric with respect to a vertical axis.

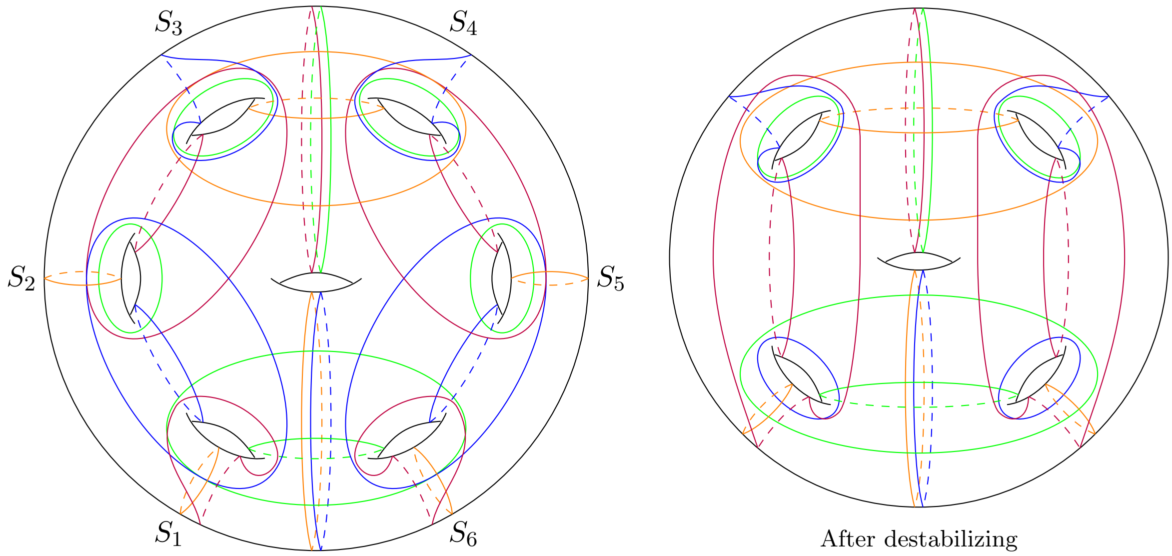

Figure 51: Quadrisection diagrams of $\mathbb{CP}^2 \times S^1$

10 Further projects

10.1 Low genus multisections

The *n–section genus* or *multisection genus* of an $(n+1)$–manifold W is the smallest genus of an n–section of W. In any dimension, the sphere is the only genus–0 manifold up to PL homeomorphism. In dimension 3, there are infinitely many genus–1 manifolds, namely $S^1 \times S^2$ and the lens spaces. In dimension 4, the genus–1 manifolds are $S^1 \times S^3$, $\mathbb{CP}^2$ and $\overline{\mathbb{CP}^2}$, and the genus–2 manifolds are $S^2 \times S^2$ and connected sums of genus–1 manifolds, as proved by Meier and Zupan [MZ17]. In dimension $n+1 \geq 4$, up to PL homeomorphism, $S^1 \times S^n$ is the only genus–1 manifold.

Question 10.1. *For $n \geq 2$, what is the smallest integer k_n such that there are infinitely many manifolds of n–section genus k_n up to PL homeomorphism?*

We know that $k_2 = 1$, $k_3 = 3$ and $k_n > 1$ for $n > 2$. Since the constraints on the subdiagrams of a multisection diagram get stronger when the number of families of curves increases, it is tempting to conjecture that k_n increases with n. Also, it turns out that there is no irreducible 5–manifold with quadrisection genus 2, so that $k_4 > 2$. It seems likely that this remains true in higher dimensions.

Conjecture 10.2. *For $n > 3$, there is no irreducible manifold of n–section genus 2; in particular $k_n > 2$.*

The discussion below shows that $k_n \leq n$. We may also note that $k_5 \leq 4$, since any manifold in the infinite family of S^2–bundles over S^4 admits a 5–section of genus 4.

Figure 52 shows an n–section diagram of genus n such that associated manifolds have a fundamental group of order p for a given $p > 0$. It implies that there are infinitely many $(n+1)$–manifolds of multisection genus at most n. These diagrams are a generalization of the trisection diagrams of spun lens spaces obtained by Meier in [Mei18]. It may be noted that, for $n = 2$, this is a diagram for a connected sum of two copies of the lens space $L(p, 1)$.

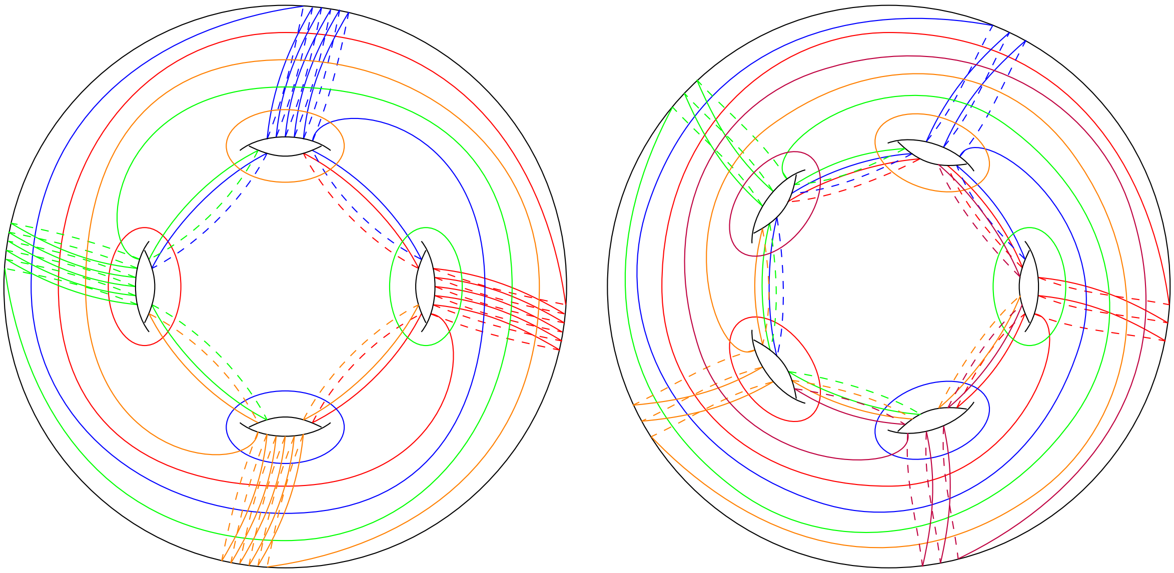

$n = 4$ and $p = 6$ $\qquad$ $n = 5$ and $p = 3$

Figure 52: Diagrams of n–sections with fundamental group of order p

Question 10.3. *What manifolds correspond to the diagrams in Figure 52?*

These diagrams represent connected sums of lens spaces when $n = 2$ and spun lens spaces when $n = 3$, which suggests to consider manifolds obtained from lens spaces. Given a 3–manifold M, construct an $(n+1)$ manifold as follows:

$$\left((M \setminus B^3) \times S^{n-2}\right) \cup \left(S^2 \times D^{n-1}\right).$$

When M is a lens space, this might be a good candidate for a manifold represented by the diagrams in Figure 52. My student Rudy Dissler (co-advised with Benjamin Audoux) works on the multisections of such higher-dimensional spun manifolds; his attempts to generalize Meier's method to higher dimensions seems promising.

10.2 PL multisections

We have seen in Subsection 9.2 that, from dimension 7, a multisection diagram determines the manifold only up to PL homeomorphism, and, from dimension 8, the existence of a manifold associated to a given abstract diagram is ensured only in the PL category. It suggest that the notion of multisection might be intrinsically a PL notion. Beyond the diagrammatic representation of multisections, which works perfectly for PL manifolds, questions of existence and uniqueness could be studied in this setting.

Problem 10.4. *Study the existence and uniqueness up to stabilization of multisections for PL manifolds.*

Although it might be natural to approach this problem using triangulations, there is a risk to be led to Rubinstein–Tillmann multisections, which is not what we seek. Maybe working with handle decompositions or discrete Morse theory would be more fruitful.

10.3 Multisection diagrams and homotopy invariants

The computation of homotopy invariants from a trisection diagram can most probably be generalized to higher dimensions, with similar results expected. For instance, for a closed smooth $(n+1)$–manifold W, given a multisection diagram $\big(\Sigma;(\alpha^i)\big)$, the homology of W is given by the following complex of free groups.

$$\mathbb{Z} \xrightarrow{0} \bigoplus_{i=1}^{n} (\cap_{j\neq i} L_j) \to \cdots \to \bigoplus_{|I|=\ell} (\cap_{i\in I} L_i) \to \cdots \to \bigoplus_{i=1}^{n} L_i \to H_1(\Sigma) \xrightarrow{0} \mathbb{Z}$$

Generalization of the homology and torsion computation are more or less direct. Further investigation could provide a description of the middle dimension homology group and its intersection form.

Problem 10.5. *Find an explicit expression for the intersection form of an even-dimensional smooth manifold from a multisection diagram.*

It should also be possible to derive the homotopy groups from a multisection diagram. The fundamental group is indeed easy to compute from a diagram. In dimension 4, my student Anthony Saint-Criq (co-advised with Thomas Fiedler) participates to a working group with other young researchers on the computation of the π_2 from a trisection diagram.

10.4 Morse n–functions

In dimension 4, Gay and Kirby mainly introduced trisections from a Morse 2–function viewpoint. Morse 2–functions are maps on smooth manifolds with values in $\mathbb{R}^2$, which behave locally as homotopies between Morse functions. When the image of the singular locus of such a Morse 2–function is as represented in Figure 53, where the boxes only contain crossings, the Morse 2–function is *trisecting*, meaning that the preimage of the cutting of the disk along the red arcs is a trisection. This viewpoint is somehow natural and helps understanding certain aspects of trisections. For instance, in the case of 4–manifolds with boundary, the open book structure on the boundary is very natural from this picture. In higher dimension, it would be interesting to have such a viewpoint. Although it may be very difficult to define generic Morse n–functions, one can work first in dimension 5, or start with a notion of "multisecting" Morse n–functions.

Problem 10.6. *Define a notion of multisecting Morse n–function. Prove that any multisection can be obtained from such an n–function, at least after stabilization.*

In [GK16], Gay and Kriby prove the existence of trisections by constructing a trisecting Morse 2–function on a given 4–manifold. In [BS17, BS18], Baykur and Saeki reprove the existence in a different way: they start with a generic Morse 2–function and manipulate it in order to obtain a trisecting Morse 2–function. For the uniqueness result, Gay and Kirby use handle decompositions, but suggest that a Morse theoretic proof of uniqueness should be possible.

Problem 10.7. *Prove the uniqueness of trisections up to stabilization using homotopies of Morse 2–functions. Further, prove existence of quadrisections of 5–manifolds via Morse 3–functions.*

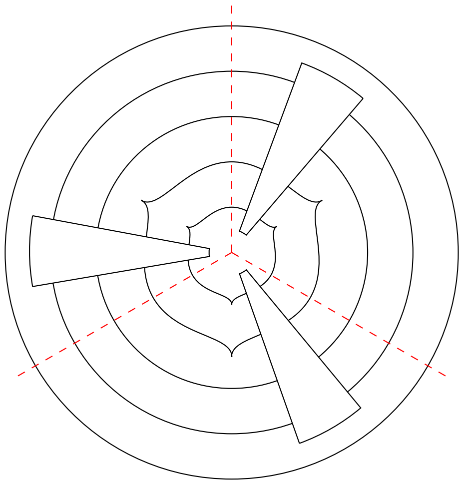

Figure 53: The singular locus of a trisecting Morse 2–function

10.5 Multisections of manifolds with boundary

The notions of Heegaard splittings and trisections have been extended to manifolds with boundary. We shall introduce a similar extension in higher dimensions.

For $k \geq 2$, we define a *k–dimensional trivial compression body* as a thickened surface $S \times D^{k-2}$. Then, for $k \geq 3$, a *k–dimensional compression body* is a k–manifold C obtained from a $(k-1)$–dimensional trivial compression body $\partial_- C$, its *negative boundary*, by thickening and adding 1–handles; the *positive boundary* of C is $\partial_+ C = \overline{\partial C \setminus \partial_- C}$. Now a multisection of a compact $(n+1)$–manifold W is defined as a decomposition $W = \cup_{i=1}^n W_i$ where:

- for $\emptyset \subsetneq I \subsetneq \{1, \dots, n\}$, $W_I = \cap_{i \in I} W_i$ is an $(n + 2 - |I|)$–dimensional compression body such that $\partial_- W_I = W_I \cap \partial W$,
- $\Sigma = \cap_{i=1}^n W_i$ is a compact surface.

Such a multisection induces a relative surface bundle over S^{n-2} on the boundary, where the fiber is the compact surface S appearing in the trivial compression bodies structures of the $\partial_- W_I$.

A general existence result turns out to be hopeless. It is not hard to see that a smooth 4–manifold of Euler characteristic 2 that admits a relative surface bundle structure over S^2 is diffeomorphic to S^4. Since there are many bounding 4–manifolds of Euler characteristic 2, not all compact 5–manifolds can be multisected in the above sense.

Problem 10.8. *Study existence and uniqueness of multisections for compact manifolds whose boundary endows a relative surface bundle structure.*

The rough idea would be to construct a function on the boundary related to the relative bundle structure, and extend it to an ordered Morse function on the whole manifold in order to apply similar methods as in the closed case.

The above definition intends to provide a somehow symmetric decomposition of the manifold. Nevertheless, other notions of multisections for compact manifolds can be studied. In particular, one can ask that all W_i are handlebodies except one that is a compression body. In other terms, we can put all the boundary into one piece of the decomposition. The study of existence and uniqueness for this notion turns out to be very similar to the closed case. In particular, such decompositions do exist in dimension 3, 4 and 5.

10.6 Generalized multisections

Multisections provide decompositions into very simple pieces with a good diagrammatic description. More general decompositions into handlebodies can be imagined. We call *n–dimensional k–handlebody* an n–manifold constructed with handles of order at most k. We define a *k–handlebodies n–section*, or *multisection*, of an $(n+2k-1)$–manifold W as a decomposition $W = \cup_{i=1}^n W_i$ where:

- for $\emptyset \subsetneq I \subsetneq \{1,\dots,n\}$, $W_I = \cap_{i\in I} W_i$ is an $(n+2k-|I|)$–dimensional k–handlebody,
- $\Sigma = \cap_{i=1}^n W_i$ is a $2k$–manifold.

It is easy to check the existence of a k–handlebodies 2–section for a $(2k+1)$–manifold W: as for Heegaard splittings, take an ordered Morse function on W and cut W along a regular level separating the critical points of order k and $k+1$. It is also not very hard to generalize the proof of existence of trisections to get existence of k–handlebodies 3–section for $(2k+2)$–manifolds. Things get more intricate for higher values of n.

Problem 10.9. *Study existence and uniqueness up to some set of stabilization moves of k–handlebodies n–sections for $(n+2k-1)$–manifolds.*

It seems that the stabilization moves to be considered here are the same moves used for standard n–sections, restricting to stabilization moves of order at least k for a k–handlebody multisection.

Although we cannot hope for diagrams of such generalized multisections, we can ask what information is necessary to encode them.

Question 10.10. *What information in the central $2k$–manifold, a priori given by some submanifolds, do we need to encode a k–handlebodies multisected manifold? Can any two such data for a given manifold be related by some handleslides and stabilizations?*

10.7 Relative bundles over spheres and bounding manifolds

We have seen that multisections can be defined for manifolds with boundary, and we have proposed a notion of k–handlebodies multisection. Merging these two generalizations provides a notion of k–handlebodies n–section for $(n+2k-1)$–manifolds with boundary. Again, questions of existence and uniqueness up to stabilization are raised. Further, such a k–handlebodies n–section induces on the boundary a relative fiber bundle structure over S^{n-2}.

Problem 10.11. *Study existence and uniqueness of k–handlebodies n–sections for compact $(n+2k-1)$–manifolds whose boundary endows a relative fiber bundle structure over S^{n-2}.*

An interesting feature of these relative bundle structures over spheres is that they provide a filtration on the set of smooth manifolds of a given dimension. Indeed, the p–sphere S^p admits an obvious relative bundle structure over S^{p-1}, where the binding is made of two points. We can compose it with a given relative bundle (X,B) over the sphere S^p to obtain a relative bundle over S^{p-1}. The new binding is made of two copies of the original fiber, glued along B.

We have seen that not all bounding 4–manifolds are relative surface bundles. However, we can wonder if a bounding manifold admits a relative bundle structure over a sphere of some dimension. Conversely, not all relative fiber bundles are boundaries: all odd-dimensional manifolds admit open book decompositions while some do not bound. It would be interesting to identify those relative fiber bundles that are bounding manifolds. Understanding what is needed to extend a relative bundle on a boundary into a generalized multisection of the manifold could give a hint. It might be possible then to deduce a geometric condition characterizing bounding manifolds.

Third part:
T–genus and generalized ribbon-slice problem

11 Introduction

A knot in the 3–sphere is *slice* if it bounds a disk properly embedded in the 4–ball. A knot is *ribbon* if it bounds a disk immersed in the 3–sphere with only so-called ribbon intersections. It is easy to see that any ribbon knot is slice, but the converse, raised by Fox in 1962 [Fox62], is still an open problem, now known as the ribbon-slice conjecture. The first attempts to prove this conjecture led to a 3–dimensional characterization of slice knots. Following Hosokawa and Yanagawa [HY65], Kawauchi, Shibuya and Suzuki [KSS83] proved that the slice knots are exactly those that bound a normal singular disk in the 3–sphere with no clasp and no triple point of a certain type, called here borromean. In [13], we generalize this result to give a 3–dimensional characterization of the slice genus, proving that the slice genus of a knot is the minimal genus of a normal singular surface in the 3–sphere, with no clasp and no borromean triple point, bounded by the knot.

It was proved by Kaplan [Kap79] that any knot bounds a normal singular disk with no clasp. This allowed Murakami and Sugishita [MS84] to define the T–genus of a knot as the minimal number of borromean triple points on such a disk. They proved that the T–genus is a concordance invariant and an upper bound for the slice genus. Further, they showed that the mod–2 reduction of the T–genus coincides with the Arf invariant. From these properties, they deduced the value of the T–genus for several knots for which the difference between the T–genus and the slice genus is 0 or 1. This raises the question of whether this difference can be greater than one; we prove in [13] that it can be arbitrarily large. For this, we show that the T–genus is an upper bound for the 4–dimensional positive clasp number and we use a recent result of Daemi and Scaduto [DS20] that says that the difference between the 4–dimensional positive clasp number and the slice genus can be arbitrarily large.

In [13], we also introduce the ribbon T–genus of a knot, defined as the minimal number of borromean triple points on an immersed disk bounded by the knot with no clasp and no non-borromean triple point. In [KMS83], Kawauchi, Murakami and Sugishita proved that the T–genus of a knot equals its Δ–distance to the set of slice knots. We prove the ribbon counterpart of it, namely that the ribbon T–genus of a knot equals its Δ–distance to the set of ribbon knots. As a consequence, the ribbon-slice conjecture is equivalent to the coincidence of the T–genus and the ribbon T–genus for all knots in the 3–sphere.

For higher-dimensional knots, *ie* embeddings of an n–sphere in an $(n+2)$–sphere up to isotopy, called n–knots, we still have notions of ribbon and slice knots and the easy fact that ribbon implies slice. Moreover, it was proved by Yajima [Yaj64] and Yanagawa [Yan69] for $n = 2$ and by Hitt [Hit79] for $n > 2$ that there are slice n–knots that are not ribbon. However, one can consider that the problem is not completely solved in higher dimensions. Indeed, the usual notion of a ribbon n–knot imposes a somehow restrictive condition. Relaxing this condition, one gets larger generalizations of ribbon knots in higher dimensions; this relaunches the debate about the ribbon-slice problem.

With Emmanuel Wagner [10], we introduced a notion of A–ribbon 2–knots in the 4–sphere. This allowed us to give a criterion on a 2–knot which ensures to recover the factorization property of the Alexander polynomial that holds for standard knots. Along the way, we determined a type of geometric position of an A–ribbon 2–knot which provides a presentation of its Alexander polynomial. This could be useful is the study of higher-dimensional ribbon-slice questions.

12 Slice genus, T–genus and 4D clasp number

12.1 Characterization of the slice genus

If Σ is a compact surface immersed in S^3, the self-intersections of Σ are lines of double points, which possibly intersect along triple points. The lines of double points are circles or intervals; the latter are of two kinds: ribbons and clasps (see Figure 54). A *ribbon* is a line of double points whose preimages by the immersion are a *b–line* properly immersed in Σ and an *i–line* immersed in the interior of Σ. A *clasp* is a line of double points that is not a ribbon. When three ribbons meet at a triple point, there are again two possibilities. We say that the triple point is *borromean* if its three preimages are intersections of a b–line and an i–line (see Figures 55 and 56). We will also consider surfaces with *branch points*, namely points that have a neighborhood as represented in Figure 57.

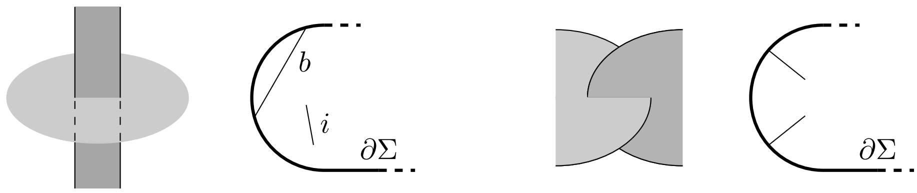

ribbon clasp

Figure 54: Lines of double points and their preimages

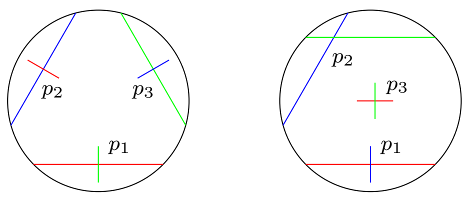

borromean non borromean

Figure 55: Triple points on a disk

The picture represents the singular set of the disk on its preimage.

The points p_1, p_2 and p_3 are the three preimages of a triple point p.

A compact surface is:

- *normal singular* if it is immersed in S^3 except at a finite number of branch points,
- *ribbon* if it is immersed in S^3 with no clasp and no triple point,
- *T–ribbon* if it is immersed in S^3 with no clasp and no non-borromean triple point,
- *slice* if it is smoothly properly embedded in B^4.

Beyond ribbons and clasps, the different types of double point lines that appear on a normal singular surface are closed lines, namely *circles*, or intervals, called *branched ribbons* if one endpoint is branched and *branched circles* if the two endpoints are branched, see Figure 58, where the preimages are drawn. Like for a ribbon, the two preimages of a branched ribbon are naturally divided into a *b–line* that contains a boundary point and an *i–line* that doesn't. For

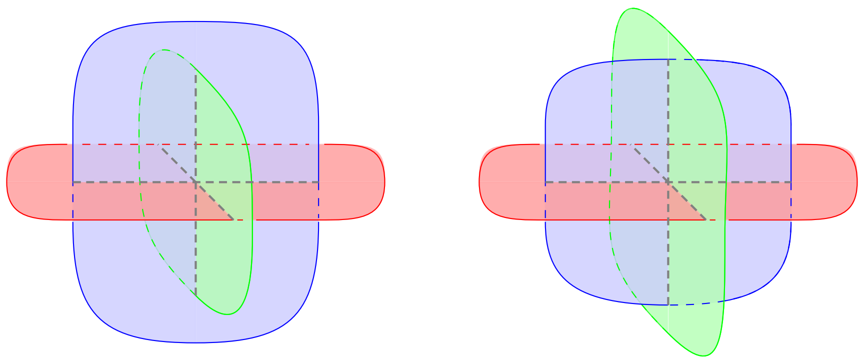

Figure 56: Borromean and non borromean triple points

On the left hand side (resp. right hand side), a borromean link (resp. a trivial link) bounds a disks complex with three ribbons and one borromean (resp. non borromean) triple point.

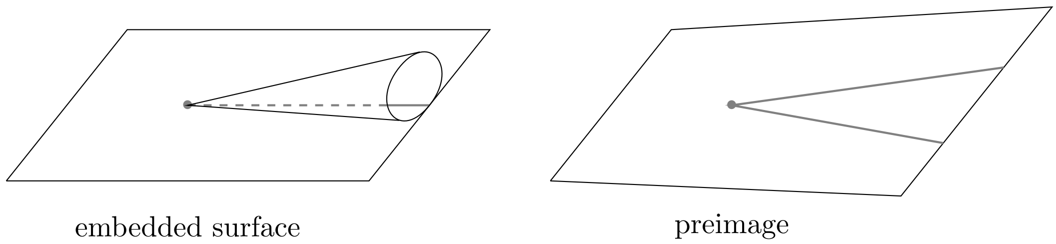

Figure 57: A branched point

a (branched) circle, one may call b–line one preimage and i–line the other. A normal singular surface with such namings assigned to the preimages of each (branched) circle is said to be *marked*. A triple point on a normal singular surface is *borromean* if its three preimages are intersections of a b–line and an i–line.

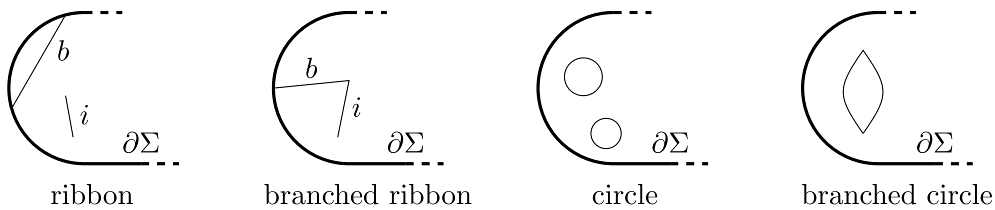

Figure 58: Double points lines on a normal singular surface (preimages)

The following result generalizes the characterization of slice knots by Kawauchi–Shibuya–Suzuki [KSS83, Corollary 6.7].

Theorem 12.1 ([13])**.** *The slice genus of a knot K equals the minimal genus of a marked normal singular surface bounded by K with no clasp and no borromean triple point.*

The proof is based on manipulation of surfaces. Given a marked normal singular surface bounded by K with no clasp and no borromean triple point, one can desingularize the surface as usual by pushing its interior into B^4 in order to get a slice surface. The other direction requires more work. Start with a slice surface for K, isotope it in a good position —essentially invariant with respect to the radius except at three levels where minima, saddle points and maxima arise— and project it radially on S^3. A careful analysis shows that the projection is a normal singular surface admitting a marking with no clasp and no borromean triple point.

12.2 Slice and ribbon *T*–genera

The *T–genus* $T_s(K)$ (resp. *ribbon T–genus* $T_r(K)$) is the minimal number of borromean triple points on a marked normal singular disk (resp. T–ribbon disk) with no clasp bounded by K; obviously $T_s(K) \leq T_r(K)$. Note that these numbers are well-defined: Kaplan [Kap79] proved that any knot bounds a T–ribbon disks complex.

In [MS84], Murakami and Sugishita proved that the T–genus is an upper bound for the slice genus: $g_s(K) \leq T_s(K)$ for any knot K. In [13], we prove the ribbon counterpart of it.

Theorem 12.2. *For any knot K, $g_r(K) \leq T_r(K)$.*

The proof relies on the expression of the T–genus in terms of Δ–distance, which is the distance on the set of knots defined by the Δ–move (see Figure 59). The *Δ–slicing number* $s_\Delta(K)$ (resp. *Δ–ribonning number* $r_\Delta(K)$) is the minimal number of Δ–moves necessary to change K into a slice (resp. ribbon) knot. Murakami and Nakanishi [MN89] proved that the Δ–move is an unknotting operation, so that these numbers are well-defined. Kawauchi, Murakami and Sugishita [KMS83] proved that the T–genus of a knot equals its slicing number: $T_s(K) = s_\Delta(K)$ for any knot K. The ribbon version of this also holds.

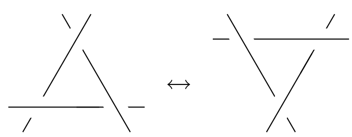

Figure 59: Δ–move

Theorem 12.3 ([13])**.** *For any knot K, $T_r(K) = r_\Delta(K)$.*

The proof goes as follows. The knot K can be obtained from a ribbon knot by $r_\Delta(K)$ Δ–moves. This ribbon knot bounds a ribbon disk and each Δ–move can be performed by gluing a borromean link to the knot, see Figure 60, while gluing to the T–ribbon disk the three disks on the left hand side of Figure 56. Hence we add a borromean triple point for each Δ–move. Conversely, starting with a T–ribbon disk for K, one can isotope the disk so that each ribbon contains at most one triple point, and then observe that a borromean triple point can be removed by cutting three disks behaved like in the left hand side of Figure 56, which amounts to perform a Δ–move on the knot.

In order to perform a Δ–move on a knot K bounding a T–ribbon disk, instead of gluing three disks as above, one can glue the three surfaces represented in Figure 61. This allows to deduce Theorem 12.2 from Theorem 12.3.

It is a natural generalization of the ribbon-slice question to ask whether the T–genus and the ribbon T–genus always coincide. The expressions of the T–genera in terms of Δ–distance show that it is indeed equivalent.

Corollary 12.4. *The slice knots are all ribbon if and only if $T_s(K) = T_r(K)$ for any knot K.*

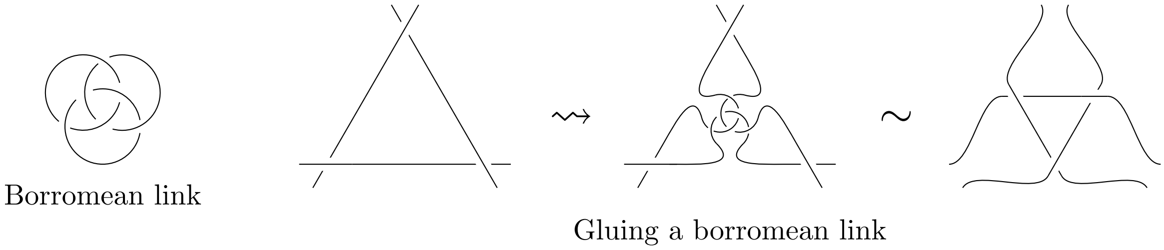

Figure 60: Borromean link and Δ–move

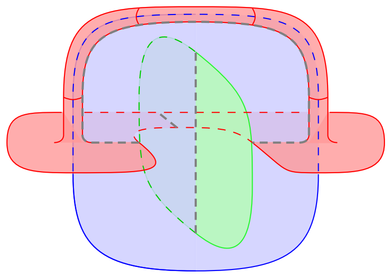

Figure 61: Ribbon complex for the borromean link

Two components of the link (green and blue) bound disks, while the red component bounds a punctured torus. These surfaces intersect pairwise along a ribbon and have no triple intersection. This produces three ribbons, represented as gray dashed curves.

12.3 Comparing invariants

In [MS84], Murakami and Sugishita proved that the T–genus of knots is a concordance invariant whose mod–2 reduction is the Arf invariant. They deduced the value of the T–genus for several knots satisfying $T_s(K) - g_s(K) = 0, 1$. The question arises then to know if this difference can be arbitrarily large. To answer this question, we compare the T–genus with the 4–dimensional positive clasp number. The *4–dimensional clasp number* $c_4(K)$ of a knot K is the smallest number of transverse double points on an immersed disk in B^4 bounded by K. We define similarly the *4–dimensional positive/negative clasp number* $c_4^+(K)/c_4^-(K)$ by counting the positive/negative double points. We also consider a balanced version of this invariant, which is the most natural in the comparison with the T–genus. The *balanced 4–dimensional clasp number* $c_4^b(K)$ of a knot K is the smallest number of positive transverse double points on an immersed disk in B^4, bounded by K, with trivial self-intersection number (*ie* the disk has the same number of positive and negative transverse double points). We have the following immediate inequalities (note that a positive or negative transverse double point can be added to an immersed surface in B^4 without modifying its boundary).

$$c_4^{\pm}(K) \leq c_4^b(K) \leq c_4(K) \leq 2c_4^b(K)$$

It is well known that the 4–dimensional clasp number is an upper bound for the slice genus —a transverse double point can be smoothed at the cost of adding one to the genus of the surface. Further, on a connected surface, a pair of transverse double points of opposite signs can be removed by tubing, thus adding only one to the genus. This gives the following inequality.

Lemma 12.5. *For any knot K, $g_s(K) \leq c_4^b(K)$.*

Moreover, the balanced 4–dimensional clasp number is related to the T–genus.

Theorem 12.6 ([13])**.** *For any algebraically split knot K, $c_4^b(K) \leq T_s(K)$.*

Once again, this can be shown by pushing into B^4 the interior of a marked normal singular surface bounded by K, with $T_s(K)$ borromean triple points. The i–lines are pushed the farther and the b–lines the closer, while the points lying at the intersection of a b–line and an i–line are pushed at a medium level. This provides an immersed surface in B^4 with $T_s(K)$ triple points, that can further be pertubed so that each triple point gives rise to a pair of tranverse double points of opposite signs.

In [DS20], Daemi and Scaduto minored the difference $c_4^+(K) - g_s(K)$ for the connected sums of copies of the knot 7_4.

Theorem 12.7 (Daemi–Scaduto)**.** *For any positive integer n, $c_4^+(\sharp^n 7_4) - g_s(\sharp^n 7_4) \geq n/5$.*

Corollary 12.8. *The difference between the T–genus and the slice genus can be arbitrarily large.*

This raises the question of what can be the difference between the T–genus and the balanced 4–dimensional clasp number. In [Mil22], Miller proves the existence of knots with arbitrarily large slice genus and trivial positive and negative 4–dimensional clasp number, which implies that the difference $T_s - c_4^{\pm}$ can be arbitrarily large.

Question 12.9. *Can the difference $T_s - c_4^b$ be arbitrarily large?*

Figure 62 shows a family of knots that could realize such an unbounded difference, namely the family of twist knots. The 4–dimensional clasp number equals 1 for all non-slice twist knots; I would conjecture that their T–genus raises linearly with the number of twists.

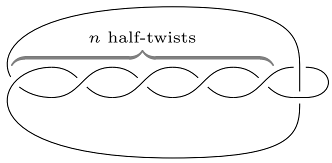

Figure 62: The n–th twist knot

13 Refined ribbon-slice question in higher dimensions

13.1 Higher-dimensional ribbon and slice knots

We start with some definitions. Given an immersed $(n+1)$–ball B in S^{n+2}, a self-intersection of B is *ribbon* if its preimages by the immersion are one embedded in the interior of the $(n+1)$–ball, and the other properly embedded. An n–knot is called *ribbon* if it bounds a *ribbon ball*, *ie* an immersed $(n+1)$–ball in S^{n+2} whose self-intersections are n–disks and are ribbon. An n–knot is called *slice* if, when S^{n+2} is considered as the boundary of B^{n+3}, it bounds an $(n+1)$–ball embedded in B^{n+3} —a *slice ball*. One proves that ribbon implies slice by pushing the interior of the ribbon ball into B^{n+3} in such a way that the self-intersecting leaves are separated, which is possible thanks to the ribbon condition.

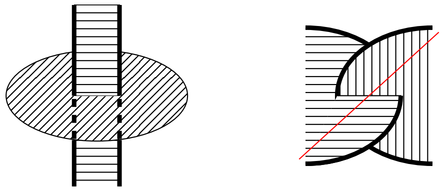

Figure 63: Ribbon self-intersection for $n = 1$

Theorem 13.1 (Yajima, Yanagawa, Hitt). *For any $n \geq 2$, there exists a slice n–knot which is not ribbon.*

Given a slice n–knot K in S^{n+2}, it is always possible to find a slice ball B in $B^{n+3} \setminus \{0\}$ bounded by K such that the function "distance from origin" in B^{n+3} induces a Morse function d on B. For $1 \leq k \leq n+1$, we call *k–slice* an n–knot that bounds a slice ball B for which the function d has only critical points of indices at most k. It is known that the 1-slice n–knots are exactly the ribbon n–knots. Hence, when $n = 1$, the ribbon-slice question for classical knots asks whether it is always possible to avoid local maxima on the slice ball. In higher dimensions, more values of indices of critical points have to be avoided, so that the gap between ribbon and slice knots seems to increase with the dimension.

For classical knots, we have the Kawauchi–Shibuya–Suzuki "ribbon-type" characterization of slice knots: a knot is slice if and only if it bounds a marked normal singular disk with no clasp and no borromean triple point. In order to get a similar characterization of k–slice n–knots, we consider generalized notions of ribbon n–knots.

For $1 \leq k \leq n+1$, define a *k–ribbon n–knot* as an n–knot that bounds a *k–ribbon ball*, *ie* an immersed $(n+1)$–ball B in S^{n+2} whose self-intersections are ribbon and are $(k-1)$–handlebodies (*ie* can be built with handles of order at most $k-1$). Note that 1–ribbon n–knots are standard ribbon n–knots. As previously, one can push the k–ribbon ball into B^{n+3}. The definition of the k–ribbon self-intersections is designed in order to control the indices of the Morse function d on the obtained slice ball. We have the following consequence.

Proposition 13.2. *For any $1 \leq k \leq n+1$, any k–ribbon n–knot is k–slice.*

The reciprocal assertion can be though of as a higher-dimensional version of the ribbon-slice conjecture. Like for standard slice knots, we can consider a weak version of it.

Conjecture 13.3. *An n–knot is k–slice if and only if it bounds an immersed $(n+1)$–ball in S^{n+2}, with double point set made of ribbon $(k-1)$–handlebodies, whose multiple points have order at most $k+1$ and a well-defined type. If $k = n+1$, branch points have to be allowed.*

Beyond this conjecture, it would be interesting to understand the global picture of the ribbon-slice question in higher dimensions. It means in particular determining for an n–knot if $(k+1)$–ribbon implies k–ribbon or if $(k+1)$–slice implies k–slice for some value of k. For instance, it is true for all n that $(n+1)$–ribbon implies n–ribbon; this can be seen using some kind of finger move to puncture the ribbon intersections.

A somehow combinatorial approach could be possible via bridge multisections of n–knots.

Problem 13.4. *Determine a characterization of ribbon and slice 2–knots in terms of bridge position in the trisected 4–sphere. Further, develop a diagrammatic of embedded codimension–2 submanifolds in S^{n+2} and characterize k–ribbon and k–slice n–knots.*

13.2 A–ribbon 2–knots

In a joint work with Emmanuel Wagner [10], we studied the topological properties of 2–knots whose Alexander polynomial has a certain factorization property. An alternative notion of ribbon 2–knots naturally arose in this study.

Like for standard knots, one defines the Alexander module of an n–knot K as the first homology group of the infinite cyclic covering of the exterior of K, with its natural structure of $\mathbb{Z}[t^{\pm 1}]$–module. The Alexander module is a finitely generated torsion module over $\mathbb{Z}[t^{\pm 1}]$, so that one can consider its order $\Delta_K \in \mathbb{Z}[t^{\pm 1}]/\mathbb{Z}[t^{\pm 1}]^\times$, called the Alexander polynomial of K. Fox and Milnor [FM66] proved that the Alexander polynomial of a slice 1–knot writes $\Delta_K(t) = f(t)f(t^{-1})$ for some polynomial $f \in \mathbb{Z}[t^{\pm 1}]$; this is the factorization property. Conversely, for 2–knots, Kinoshita [Kin61] showed that any polynomial $f \in \mathbb{Z}[t^{\pm 1}]$ such that $f(1) = 1$ is the Alexander polynomial of a ribbon 2–knot. The starting point of my work with Emmanuel Wagner was the following question: which topological condition on a 2–knot implies the factorization property for its Alexander polynomial?

To answer this question, we introduced the notion of A–ribbon 2–knot. A 2–knot is A–ribbon if it bounds an A–ribbon 3–ball, which is defined as a ribbon 3–ball, except that the self-intersections are no longer 2–disks but annuli. This notion encompasses two classes of 2–knots whose Alexander polynomial has the factorization property, namely the connected sums of a ribbon 2–knot with its mirror image and the so-called spuns of ribbon 1–knots. The A–ribbon property provides a kind of duality in the computation of the Alexander polynomial, but it is not enough to get the factorization property. We even proved that all ribbon 2–knots are A–ribbon, so that the mentioned result of Kinoshita applies to A–ribbon 2–knots. Nevertheless, adding a condition on the relative positions of the self-intersections of the A–ribbon 3–ball, we obtained in [10] an intrinsic criterion on a 2–knot that ensures the factorization of its Alexander polynomial.

Obviously, an A–ribbon 2–knot is 2–ribbon, so that we are interested in the relation with ribbon and slice 2–knots. We have the following implications:

$$\text{ribbon} \quad \Longrightarrow \quad \text{A–ribbon} \quad \Longrightarrow \quad \text{slice.}$$

The first one is explained by Figure 64 and the second one is obtained as usual by pushing the interior of an A–ribbon 3–ball into B^5. We may consider the reciprocal assertions. My conjecture is that both are false, so that I am seeking obstructions. A candidate to be such an obstruction is the Alexander module. For a ribbon 2–knot, this module has no $\mathbb{Z}$-torsion, while there exists slice 2–knots whose Alexander module has a non-trivial $\mathbb{Z}$–torsion submodule. Hence, determining if the Alexander module of an A–ribbon 2–knot can contain non-trivial $\mathbb{Z}$–torsion elements will allow to invalidate one of the above reciprocals.

Question 13.5. *Does there exist an A–ribbon* 2*–knot whose Alexander module contains non-trivial* $\mathbb{Z}$*–torsion?*

In [10], we introduced the *fusion presentation* of an A–ribbon 2–knot, defined as follows. Let $C_0, \dots, C_k$ be disjoint 3–dimensional handlebodies trivially embedded in a 3–dimensional hyperplane in S^4. Let $E_1, \dots, E_k$ be disjoint copies of $S^1 \times [0,1] \times [0,1]$ embedded in S^4 in such a way that:

- $S^1 \times [0,1] \times \{0\}$ and $S^1 \times [0,1] \times \{1\}$ are embedded in the boundaries of the C_i's,
- $S^1 \times [0,1] \times (0,1)$ is disjoint from the boundaries of the C_i's and meets transversely the interiors of the C_i's along annuli $S^1 \times [0,1] \times \{*\}$,

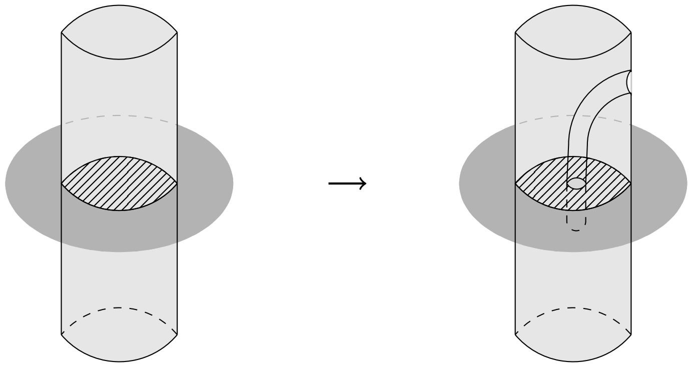

Figure 64: A finger move on a ribbon singularity

The picture represent a piece of the ribbon ball at a time t_0. The dark gray disk is locally invariant with respect to the time direction. This dark gray leaf meets the light gray one along a ribbon singularity, which is initially a disk (left hand side) and becomes an annulus after the finger move (right hand side).

- $B = (\sqcup_{i=0}^k C_i) \cup (\sqcup_{i=1}^k E_i)$ is an immersed ball.

Such an immersed ball B is called an *A–fusion 3–ball*. It is immediate that the boundary of an A–fusion 3–ball is an A–ribbon 2–knot.

Proposition 13.6 ([10, Proposition 2.4])**.** *Any A–ribbon 2–knot bounds an A–fusion 3–ball.*

A presentation of the Alexander module can be computed from a fusion presentation of an A–ribbon 2–knot. Hence explicit 2–knot answering Question 13.5 could be produced via fusion presentations.

AUTHOR'S BIBLIOGRAPHY

[1] D. MOUSSARD – "On Alexander modules and Blanchfield forms of null-homologous knots in rational homology spheres", *Journal of Knot Theory and its Ramifications* **21** (2012), no. 5, p. 1250042, 21.

[2] — , "Finite type invariants of rational homology 3–spheres", *Algebraic & Geometric Topology* **12** (2012), no. 4, p. 2389–2428.

[3] — , "Rational Blanchfield forms, S–equivalence, and null LP–surgeries", *Bulletin de la Société Mathématique de France* **143** (2015), no. 2, p. 403–431.

[4] — , "Equivariant triple intersections", *Annales de la Faculté des Sciences de Toulouse. Mathématiques. Série 6.* **26** (2017), no. 3, p. 601–644.

[5] — , "Realizing isomorphisms between first homology groups of closed 3–manifolds by borromean surgeries", *Journal of Knot Theory and its Ramifications* **24** (2015), no. 4, p. 1550024, 17.

[6] G. COUSIN & D. MOUSSARD – "Finite braid group orbits in Aff($\mathbb{C}$)–character varieties of the punctured sphere", *International Mathematics Research Notices* **2018** (2018), no. 11, p. 3388–3442.

[7] D. MOUSSARD – "Splitting formulas for the rational lift of the Kontsevich integral", *Algebraic & Geometric Topology* **20** (2020), no. 1, p. 303–342.

[8] — , "Finite type invariants of knots in homology 3–spheres with respect to null LP–surgeries", *Geometry* & *Topology* **23** (2019), no. 4, p. 2005–2050.

[9] B. AUDOUX & D. MOUSSARD – "Toward universality in degree 2 of the Kricker lift of the Kontsevich integral and the Lescop equivariant invariant", *International Journal of Mathematics* **30** (2019), no. 5, p. 1950021, 37.

[10] D. MOUSSARD & E. WAGNER – "A Fox–Milnor theorem for the Alexander polynomial of knotted 2–spheres in S^4", *Journal of the Mathematical Society of Japan* **72** (2020), no. 3, p. 891–907.

[11] V. FLORENS & D. MOUSSARD – "Torsions and intersection forms of 4–manifolds from trisection diagrams", *Canadian Journal of Mathematics* **74** (2022), no. 2, p. 527–549.

[12] G. MASSUYEAU & D. MOUSSARD – "A splicing formula for the LMO invariant", *Canadian Journal of Mathematics* **73** (2021), no. 6, p. 1743–1770.

[13] D. MOUSSARD – "Slice genus, T–genus and 4–dimensional clasp number", arXiv: 2101.01553, to appear in *Communications in Analysis and Geometry*, 2021.

[14] D. MOUSSARD & T. SCHIRMER – "The algebraic topology of 4–manifolds multisections", arXiv:2111.09071, 2021.

[15] B. AUDOUX & D. MOUSSARD – "A universal finite type invariant for knots in homology 3–spheres", arXiv:2209.00473, 2022.

[16] F. BEN ARIBI, S. COURTE, M. GOLLA & D. MOUSSARD – "Multisecting smooth manifolds", in preparation, 2022.

[17] D. MOUSSARD – "Multisections of surface bundles and bundles over the circle", in preparation, 2022.

Other references

[AL05] E. Auclair & C. Lescop – "Clover calculus for homology 3–spheres via basic algebraic topology", *Algebraic & Geometric Topology* **5** (2005), p. 71–106.

[Bar95] D. Bar-Natan – "On the Vassiliev knot invariants", *Topology* **34** (1995), no. 2, p. 423–472.

[BGRT02] D. Bar-Natan, S. Garoufalidis, L. Rozansky & D. P. Thurston – "The Århus integral of rational homology 3–spheres II: Invariance and universality", *Selecta Mathematica* **8** (2002), no. 3, p. 341–371.

[BGRT04] D. Bar-Natan, S. Garoufalidis, L. Rozansky & D. P. Thurston – "The Århus integral of rational homology 3–spheres. III. Relation with the Le–Murakami–Ohtsuki invariant", *Selecta Mathematica* **10** (2004), no. 3, p. 305–324.

[Bla57] R. C. Blanchfield – "Intersection theory of manifolds with operators with applications to knot theory", *Annals of Mathematics (2)* **65** (1957), p. 340–356.

[BS17] R. İ. Baykur & O. Saeki – "Simplifying indefinite fibrations on 4–manifolds", arXiv:1705.11169, 2017.

[BS18] — , "Simplified broken Lefschetz fibrations and trisections of 4–manifolds", *Proceedings of the National Academy of Sciences* **115** (2018), no. 43, p. 10894–10900.

[Cas16] N. A. Castro – "Relative trisections of smooth 4–manifolds with boundary", PhD Thesis, University of Georgia, 2016.

[CGPC18a] N. Castro, D. Gay & J. Pinzón-Caicedo – "Diagrams for relative trisections", *Pacific Journal of Mathematics* **294** (2018), no. 2, p. 275–305.

[CGPC18b] N. A. Castro, D. T. Gay & J. Pinzón-Caicedo – "Trisections of 4–manifolds with boundary", *Proceedings of the National Academy of Sciences* **115** (2018), no. 43, p. 10861–10868.

[CH93] A. Cavicchioli & F. Hegenbarth – "On the determination of PL manifolds by handles of lower dimension", *Topology and its Applications* **53** (1993), no. 2, p. 111–118.

[CHM08] D. Cheptea, K. Habiro & G. Massuyeau – "A functorial LMO invariant for Lagrangian cobordisms", *Geometry & Topology* **12** (2008), no. 2, p. 1091–1170.

[DS20] A. Daemi & C. Scaduto – "Chern–Simons functional, singular instantons, and the four-dimensional clasp number", arXiv:2007.13160, 2020.

[FKSZ18] P. Feller, M. Klug, T. Schirmer & D. Zemke – "Calculating the homology and intersection form of a 4-manifold from a trisection diagram", *Proceedings of the National Academy of Sciences* **115** (2018), no. 43, p. 10869–10874.

[FM66] R. H. Fox & J. W. Milnor – "Singularities of 2–spheres in 4–space and cobordism of knots", *Osaka Journal of Mathematics* **3** (1966), p. 257–267.

[Fox62] R. H. Fox – "Some problems in knot theory", in *Topology of 3–manifolds and related topics (Proc. The Univ. of Georgia Institute, 1961)*, Prentice-Hall, Englewood Cliffs, N.J., 1962, p. 168–176.

[GGP01] S. Garoufalidis, M. Goussarov & M. Polyak – "Calculus of clovers and finite type invariants of 3–manifolds", *Geometry & Topology* **5** (2001), p. 75–108.

[GK04] S. Garoufalidis & A. Kricker – "A rational noncommutative invariant of boundary links", *Geometry & Topology* **8** (2004), p. 115–204.

[GK16] D. T. Gay & R. Kirby – "Trisecting 4–manifolds", *Geometry & Topology* **20** (2016), no. 6, p. 3097–3132.

[GR04] S. Garoufalidis & L. Rozansky – "The loop expansion of the Kontsevich integral, the null-move and S–equivalence", *Topology* **43** (2004), no. 5, p. 1183–1210.

[Hab00] N. Habegger – "Milnor, Johnson, and tree level perturbative invariants", preprint, 2000.

[Hit79] L. R. Hitt – "Examples of higher-dimensional slice knots which are not ribbon knots", *Proceedings of the American Mathematical Society* **77** (1979), no. 2, p. 291–297.

[HY65] F. Hosokawa & T. Yanagawa – "Is every slice knot a ribbon knot?", *Osaka Journal of Mathematics* **2** (1965), no. 2, p. 373–384.

[IN20] G. Islambouli & P. Naylor – "Multisections of 4–manifolds", arXiv: 2010.03057, 2020.

[Kap79] S. J. Kaplan – "Constructing framed 4–manifolds with given almost framed boundaries", *Transactions of the American Mathematical Society* **254** (1979), p. 237–263.

[Kea75] C. Kearton – "Blanchfield duality and simple knots", *Transactions of the American Mathematical Society* **202** (1975), p. 141–160.

[Kin61] S. Kinoshita – "On the Alexander polynomials of 2–spheres in a 4–sphere", *Annals of Mathematics (2)* **74** (1961), p. 518–531.

[KMS83] A. Kawauchi, H. Murakami & K. Sugishita – "On the T–genus of knot cobordism", *Proceedings of the Japan Academy, Series A, Mathematical Sciences* **59** (1983), no. 3, p. 91–93.

[Koe21] D. Koenig – "Trisections of 3–manifold bundles over S^1", *Algebraic & Geometric Topology* **21** (2021), no. 6, p. 2677–2702.

[Kon93] M. Kontsevich – "Vassiliev's knot invariants", *Advances in Soviet Mathematics* **16** (1993), no. 2, p. 137–150.

[Kri00] A. Kricker – "The lines of the Kontsevich integral and Rozansky's rationality conjecture", arXiv:math/0005284, 2000.

[KSS83] A. Kawauchi, T. Shibuya & S. Suzuki – "Descriptions on surfaces in four-space. II. Singularities and cross-sectional links", *Kobe University. Mathematics Seminar Notes* **11** (1983), no. 1, p. 31–69.

[KT99] G. Kuperberg & D. Thurston – "Perturbative 3–manifold invariants by cut-and-paste topology", arXiv:math.GT/9912167, 1999.

[LC20] P. Lambert-Cole – "Bridge trisections in $\mathbb{CP}^2$ and the Thom conjecture", *Geometry & Topology* **24** (2020), no. 3, p. 1571–1614.

[LCM21] P. Lambert-Cole & M. Miller – "Trisections of 5-manifolds", *MATRIX Annals* (2021), p. 117–134.

[Le97] T. T. Q. Le – "An invariant of integral homology 3–spheres which is universal for all finite type invariants", in *Solitons, geometry, and topology: on the crossroad*, Amer. Math. Soc. Transl. Ser. 2, vol. 179, Amer. Math. Soc., Providence, RI, 1997, p. 75–100.

[Les04] C. Lescop – "Splitting formulae for the Kontsevich–Kuperberg–Thurston invariant of rational homology 3–spheres", arXiv:math.GT/0411431, 2004.

[Les11] — , "Invariants of knots and 3–manifolds derived from the equivariant linking pairing", in *Chern–Simons gauge theory: 20 years after*, AMS/IP Stud. Adv. Math., vol. 50, AMS, Providence, RI, 2011, p. 217–242.

[Les13] — , "A universal equivariant finite type knot invariant defined from configuration space integrals", arXiv:1306.1705, 2013.

[LM95] T. Q. T. Le & J. Murakami – "Representation of the category of tangles by Kontsevich's iterated integral", *Communications in mathematical physics* **168** (1995), no. 3, p. 535–562.

[LM96] — , "The universal Vassiliev–Kontsevich invariant for framed oriented links", *Compositio Mathematica* **102** (1996), no. 1, p. 41–64.

[LMO98] T. T. Q. Le, J. Murakami & T. Ohtsuki – "On a universal perturbative invariant of 3–manifolds", *Topology* **37** (1998), no. 3, p. 539–574.

[LP72] F. Laudenbach & V. Poénaru – "A note on 4–dimensional handlebodies", *Bulletin de la Société Mathématique de France* **100** (1972), p. 337–344.

[Mas15] G. Massuyeau – "Splitting formulas for the LMO invariant of rational homology three-spheres", *Algebraic & Geometric Topology* **14** (2015), no. 6, p. 3553–3588.

[Mat87] S. V. Matveev – "Generalized surgery of three-dimensional manifolds and representations of homology spheres", *Mathematical notes of the Academy of Sciences of the USSR* **42** (1987), no. 2, p. 651–656.

[Mei18] J. Meier – "Trisections and spun four-manifolds", *Mathematical Research Letters* **25** (2018), no. 5, p. 1497–1524.

[Mil22] A. N. Miller – "Amphichiral knots with large 4–genus", *Bulletin of the London Mathematical Society* **54** (2022), no. 2, p. 624–634.

[MN89] H. Murakami & Y. Nakanishi – "On a certain move generating link-homology", *Mathematische Annalen* **284** (1989), no. 1, p. 75–89.

[Mon79] J. M. Montesinos – "Heegaard diagrams for closed 4–manifolds", in *Geometric Topology*, 1979, p. 219–237.

[MS84] H. Murakami & K. Sugishita – "Triple points and knot cobordism", *Kobe Journal of Mathematics* **1** (1984), p. 1–16.

[MZ17] J. Meier & A. Zupan – "Genus-two trisections are standard", *Geometry & Topology* **21** (2017), no. 3, p. 1583–1630.

[MZ18] — , "Bridge trisections of knotted surfaces in 4–manifolds", *Proceedings of the National Academy of Sciences of the United States of America* **115** (2018), no. 43, p. 10880–10886.

[NS03] S. Naik & T. Stanford – "A move on diagrams that generates S–equivalence of knots", *Journal of Knot Theory and its Ramifications* **12** (2003), no. 5, p. 717–724.

[RT20] J. H. Rubinstein & S. Tillmann – "Multisections of piecewise linear manifolds", *Indiana University Mathematics Journal* **69** (2020), no. 6, p. 2208–2238.

[Tan21] H. Tanimoto – "Homology of relative trisection and its application", arXiv: 2101.11493, 2021.

[Tro73] H. F. Trotter – "On S–equivalence of Seifert matrices", *Inventiones Mathematicae* **20** (1973), p. 173–207.

[Wal68] F. Waldhausen – "Heegaard-Zerlegungen der 3–sphäre", *Topology* **7** (1968), no. 195–203, p. 78.

[Wil20] M. Williams – "Trisections of flat surface bundles over surfaces", PhD Thesis, The University of Nebraska–Lincoln, 2020.

[Yaj64] T. Yajima – "On simply knotted spheres in $\mathbb{R}^4$", *Osaka Journal of Mathematics* **1** (1964), p. 133–152.

[Yan69] T. Yanagawa – "On ribbon 2–knots. The 3–manifold bounded by the 2–knots", *Osaka Journal of Mathematics* **6** (1969), p. 447–464.